MODULATING MEMBRANE TRAFFIC REGULATORS TO IMPAIR BREAST CANCER PROGRESSION

ANDREIA TEIXEIRA FERREIRA

Tese para obtenção do grau de Doutor em Ciências da Saúde

na Especialidade em Biomedicina

na Faculdade de Ciências Médicas | NOVA Medical School da Universidade NOVA de Lisboa

Setembro, 2022

Campo Mártires da Pátria, 130
1169-056 Lisboa · Portugal

www.nms.unl.pt

MODULATING MEMBRANE TRAFFIC REGULATORS TO IMPAIR BREAST CANCER PROGRESSION

Andreia Teixeira Ferreira

Prof. Doutor Duarte Barral, Investigador Principal da NOVA Medical School NMS/UNL

Doutora Cristina Casalou, Investigadora Sénior da UCD School of Medicine, Charles Institute of Dermatology University College Dublin

Prof. Doutora Teresa Barona, Investigador Principal da NOVA Medical School NMS/UNL

Tese para obtenção do grau de Doutor em Ciências da Saúde

na Especialidade em Biomedicina

Acknowledgments

Quero começar por agradecer ao meu orientador, Duarte Barral, pela oportunidade de realizar o meu projeto no seu laboratório. Não teria conseguido chegar até aqui se não fosse pelo seu apoio, olhar crítico e ajuda nas alturas em que mais precisei. Obrigada pela confiança que sempre depositou em mim e nas minhas capacidades, e por me ter dado autonomia para fazer o meu percurso, podendo contar sempre com o seu auxílio. Fazer parte de um laboratório como o seu e aprender com alguém tão experiente na área do tráfego de membranas, foi para mim uma experiência muito enriquecedora, onde saí completamente da minha "zona de conforto" e aprendi a ter uma visão muito diferente do processo científico. Finalmente, queria agradecer-lhe por promover um espírito de grupo e por ser o principal impulsionador das nossas atividades de lazer, que foram muito importantes para fortalecer a equipa.

Quero também deixar um agradecimento especial à minha co-orientadora Cristina Casalou, por tudo aquilo que me ensinou na área da biologia do cancro, pelas sugestões e pelas críticas construtivas que inúmeras vezes me ajudaram a encontrar um rumo para as minhas experiências. Obrigada também pela tua "boa onda", pelas longas horas de conversa e por nunca desistires de mim. És sem dúvida uma inspiração e um exemplo a seguir pelo teu espírito de sacrifício, a tua dedicação e o gosto que demonstras pela ciência.

Agradeço também à minha co-orientadora Teresa Barona, pelo apoio e por uma visão mais "patológica" do meu trabalho. Obrigada por estar sempre disponível quando mais precisei e por me tentar sempre tranquilizar nos momentos em que mais duvidei de mim e das minhas capacidades. Obrigada também pela boa disposição e pelos momentos bons que partilhei consigo ao longo destes 4 anos.

Um agradecimento muito especial à Cristina Escrevente. Agradeço pelo apoio a nível científico e pelas críticas sempre muito construtivas e pertinentes que ajudaram a melhorar, e muito, este trabalho. Obrigada pelos momentos de maior descontração e gargalhadas, por me deixares desabafar, sempre que precisei de um ombro amigo e por seres a melhor vizinha de bancada que poderia desejar.

Agradeço também ao Pedro Castanheira por ter sido o meu companheiro do grupo do cancro. Obrigada pela amizade, pelo feedback que deste ao meu trabalho e por teres sido sempre uma ajuda valiosa nesta caminhada.

Quero agradecer à minha Dianinha, que foi a minha primeira "filha". Contigo tive a minha primeira experiência de orientação e não podia ter pedido melhor aluna e companheira para começar. Obrigada por seres um "furacão", sempre animada, determinada e organizada (nível extremo). Agradeço também pelo teu empenho e curiosidade, e por teres sido uma ajuda preciosa neste projeto. Gosto muito de ti e espero continuar na tua vida por muito tempo.

Um obrigado do tamanho do mundo à minha Madalena. És sem dúvida uma das melhores pessoas que já conheci! Obrigada pela tua dedicação a este projeto e por seres o meu braço direito e a minha companhia durante uma parte significativa deste percurso. És uma miúda incrível, sempre bem-disposta e sempre pronta ajudar. Foram muitos momentos de frustração que, com a tua palavra amiga e espírito positivo, se tornaram momentos de superação e de novas ideias. Tens com certeza um futuro risonho pela frente e espero continuar a fazer parte dele.

À minha terceira "filha", a super Melissa. Foi um gosto enorme ter contribuído para a realização do teu trabalho de mestrado. Obrigada por teres entrado no nosso grupo e por trazeres uma alegria e uma determinação difíceis de superar. Se há coisa que este doutoramento me deu, foi a possibilidade de conhecer pessoas inspiradoras e tu, és sem dúvida, uma delas!

Quero também agradecer à minha Lykes. És e serás sempre um exemplo a seguir como cientista, e, principalmente, como pessoa. Obrigada pelos "brainstorms" informais no laboratório, pelas críticas sempre pertinentes ao meu trabalho e por estares disponível para me ouvir e ajudar. Agradeço-te também por me inspirares e motivares a ser melhor. Conhecer-te foi uma das melhores coisas desta fase da minha vida e espero que continues a fazer parte dela durante muitos anos!

Ao meu alentejano. Luigi, o meu muito obrigada por teres sido das pessoas que mais me marcou ao longo destes 4 anos. Tens um coração de ouro és também uma inspiração como cientista. Obrigada pelas discussões produtivas, por me ajudares sempre que precisei, por teres sido, muitas vezes, aquela "voz" amiga que veio mesmo a calhar e por me fazeres rir, muito!

Uma palavra especial de agradecimento à Matilde, a minha beta favorita. Foste das pessoas que mais acreditou em mim e nas minhas capacidades. As tuas palavras de apoio foram muito importantes nos momentos de maior pressão e ajudaram-me a encontrar motivação e força para não desistir. Obrigada também pela tua amizade e companheirismo e por seres a melhor parceira de planeamento das atividades de grupo!

Ao Charneca, o meu outro alentejano, pela amizade e por todas as gargalhadas que partilhamos no laboratório e fora dele. Obrigada pelo teu apoio e até te agradeço pelas piadas

rebuscadas que, por vezes, não atingi! Espero que continuemos a partilhar bons momentos e umas boas cervejinhas, por muito tempo.

Quero também agradecer ao Michael e escrevo em português porque precisas de treinar. Obrigada pelas críticas construtivas e pela tua contribuição a nível científico para o meu trabalho. Obrigada também pelas tuas cervejas maravilhosas e a par com o Charneca, pelas "más" piadas que tanto insistes em contar.

Quero também agradecer a todos os ex-membros do "Membrane Traffic and Disease Group" com quem tive oportunidade de conviver e que muito contribuíram para a realização deste trabalho. Obrigada Xana, Cecília, Mafalda, Inês, Wanja, Rita, Joana, Filipe e Catarina por tudo aquilo que me ensinaram e pelos bons momentos que partilhámos. Agradeço em especial ao Hugo por toda a ajuda que me deu, pelas longas conversas e por acreditar sempre em mim.

Um especial "super" agradecimento a todas as pessoas que fazem ou fizeram parte do laboratório 2.7. Obrigada pela ajuda e pela constante boa disposição. Graças a vocês, as longas horas de laboratório foram sempre mais alegres e o ambiente de trabalho foi o melhor que poderia pedir.

Gostaria também de agradecer aos meus colegas do "PhD Committee". Duarte, Matilde, João e Rita, obrigada por todos os bons momentos que partilhamos. Foi, sem dúvida, uma experiência muito enriquecedora que me deu a oportunidade de participar na organização de eventos para tornar a comunidade do nosso instituto, numa comunidade mais unida.

Gostaria também de agradecer à NOVA Medical School e à NMS research pela oportunidade de realizar o meu projeto de doutoramento e pelo apoio prestado. Obrigada também a toda a comunidade deste instituto, incluindo todos os serviçoes, que de um modo prestável e com sentido crítico a nível científico, tornou esta experiência muito mais enriquecedora. Gostaria também de agradecer ao projeto LYSOCIL pela oportunidade de visitar o TIGEM e a Universidade de Münster para participar em dois workshops que me permitiram alargar o meu conhecimento científico. Agradeço também à Fundação para a Ciência e Tecnologia pelo financiamento da minha bolsa.

Agradeço à Doutora Florence Janody e ao Doutor Paulo Matos pelas sugestões e críticas construtivas que foram muito úteis na fase mais inicial deste trabalho.

Também quero agradecer a todos aqueles, que não fazendo parte da "família do trabalho", foram essenciais para que conseguisse superar este desafio.

Aos meus amigos de longa data, os melhores marienses e aqueles que me viram crescer e me acompanharam ao longo desta etapa. Aos que iniciaram esta aventura de doutoramento

comigo, os meus “amigos dos subúrbios” que são para mim um porto de abrigo e um lugar feliz na minha vida. Gosto muito de vocês.

À minha brasileira preferida, a minha Greice. Contigo partilhei uma casa, longas conversas e momentos que ficarão comigo para sempre. Obrigada por estares lá para me ouvir, para me apoiar e pelos teus conselhos e frontalidade. Considero-te uma das pessoas mais importantes da minha vida e espero que assim continue.

Um agradecimento especial ao “pessoalinho” da Refood Oeiras. O voluntariado é uma parte muito importante da minha vida e fazê-lo juntamente com um grupo de pessoas espetaculares, faz com que seja uma experiência ainda melhor.

Aos amigos que ficaram de aventuras passadas, em especial à minha Cristianinha e ao meu Paulinho. Com vocês partilhei momentos de pura alegria e “galhofa”, mas também pude sempre contar com o vosso ombro amigo, para desabafar e procurar consolo. São muito especiais para mim e espero que juntemos a “grupeta” em breve!

Quero agradecer também à minha família, de sangue e àquela que a vida felizmente me emprestou. Obrigada por me apoiarem nas minhas escolhas e por me incentivarem sempre a não desistir. São a melhor família que poderia pedir e sou muito feliz por vos ter na minha vida.

Ao meu irmão Rui pela amizade e verdadeira irmandade. Crescemos e vivemos juntos e essas vivências contribuíram para que me tornasse aquilo que sou hoje. Obrigada por puxares sempre por mim, por me desafiares a ser melhor e por seres meu amigo. Gosto muito de ti!

O meu maior agradecimento vai sem dúvida para as pessoas que diariamente me inspiram e que são o meu modelo de vida a seguir: os meus pais. Obrigada pelo amor incondicional, por poder contar sempre convosco e por fazerem de mim uma pessoa melhor. Espero um dia poder dar aos meus filhos aquilo que vocês me dão. Sou uma sortuda por vos ter como pais e todos os dias agradeço por isso! Obrigada do fundo do coração, adoro-vos muito.

Agradeço também ao Didi, à Maria José, ao Luís e à Ana por serem a minha família em Oeiras. Obrigada por todo o apoio que me dão e pelos momentos felizes que já vivemos.

Por fim, quero agradecer à pessoa que foi o meu pilar durante todo este percurso. Pedro, obrigada por seres o meu companheiro de vida e por me fazeres mesmo muito feliz, mesmo quando não o transmito tão bem. És um exemplo de dedicação, persistência e profissionalismo e, por isso, também te agradeço. Obrigada por sempre acreditares em mim e por dizeres a coisa certa na altura certa. Obrigada pelas palavras de conforto, pelos abraços apertados e por seres o meu porto seguro, a minha “casa”. Adoro-te muito!

Summary

Breast cancer (BC) is the most frequent type of cancer and the leading cause of cancer-related deaths in women. In recent years, the improvement in diagnosis techniques and consequent earlier detection of the disease led to a decline in the mortality from BC in developed countries. Furthermore, the development of more efficient therapies contributed for the reduction of the number of fatalities from this type of cancer. However, BC is still a major health issue, in which the formation of metastasis accounts for most BC-related deaths. Therefore, the development of therapies to impair metastasis is essential to reduce mortality and morbidity. To achieve this goal, it is paramount to understand the mechanisms underlying the progression from normal breast cells to breast carcinoma in situ and to invasive BC.

Emerging evidence indicates that membrane traffic is subverted by cancer cells to acquire proliferative, migratory, and invasive capacities. Indeed, members of the ADP-ribosylation factor (Arf) family, whcih regulate several steps of membrane traffic, have been shown to be upregulated in several malignancies and promote cancer progression. Furthermore, our group revealed that a member of the Arf-like (Arl) subfamily - ARL13B - regulates BC cell migration and invasion. This protein regulates primary cilia functions, although it also has been shown to regulate processes outside the cilia, including focal adhesion (FA) dynamics and the formation of circular dorsal ruffles (CDRs). However, the role of other ARLs in BC progression is still poorly understood. Therefore, the main aim of this PhD work was to identify new players in BC progression. We focused on the ARL subfamily of proteins, to unravel the underlying mechanisms that promote BC tumorigenic features, which can be targeted to impair tumor progression and the formation of metastases.

The results obtained in this work show that several ARL genes are upregulated in BC cell lines, namely ARL1, ARL2, ARL3, ARL4A, ARL5A, ARL5B, ARL6, ARL8A, ARL8B, ARL11, ARL13B, ARL14 and ARFRP1. Furthermore, a bioinformatic analysis using BC samples and normal adjacent tissues from the TCGA dataset revealed that ARL1, ARL8B, ARL11 and ARFRP1 are upregulated in BC. Moreover, we found that ARFRP1 regulates BC cell migration and invasion. This protein controls the transport of molecules at the trans-Golgi network (TGN) and was found to be important for the transport of proteins that are involved in cell-cell adhesion and planar cell polarity, which are involved in cell migration and invasion. We also found that ARL13B impairs the invasion of highly invasive BC cells using a 3D system, namely spheroids. Finally, our study revealed that the lysosomal

transport regulators ARL8A and ARL8B impair BC cell migration and ARL8B silencing decreases cell invasion in 3D and lysosome exocytosis in BC cells.

In the future, it would be important to investigate the signaling pathways involved in the regulation of BC migration and invasion promoted by ARFRP1. Furthermore, we previously proposed that ARL13B regulates BC cell migration and invasion through a cilia-independent mechanism likely mediated the non-canonical Sonic hedgehog (Shh) pathway. Future experiments to validate this hypothesis are necessary. ARL8A and ARL8B have been shown to regulate the movement of lysosomes to the cell periphery, although recent studies have shown that these proteins can also regulate the anterograde movement of endolysosomes. So, in future experiments it would be important to address what pathways are at play in the regulation of BC cell migration and invasion by ARL8A and ARL8B.

In conclusion, this work strongly suggests that ARFRP1, ARL13B, and ARL8 proteins could potentially serve as therapeutic targets to impair BC progression and reduce the high mortality and morbidity associated with this disease. Furthermore, the results obtained with this study reinforce the notion that membrane traffic regulators can be subverted by cancer cells, including BC cells, to promote migration and invasion. Thus, it highlights the importance of considering these proteins and the mechanisms regulated by them as targets for the design of new therapies for BC.

Sumário

O cancro de mama (CM) é o tipo de cancro mais frequente e a principal causa de morte associada ao cancro, em mulheres. Nos últimos anos, a melhoria das técnicas de diagnóstico e a consequente deteção mais precoce da doença levaram ao declínio da mortalidade por CM nos países desenvolvidos. Além disso, o desenvolvimento de terapias mais eficientes contribuiu para a redução do número de óbitos. No entanto, o CM ainda constitui um problema de saúde grave, no qual a formação de metástases é responsável pela maioria das mortes. Portanto, o desenvolvimento de terapias para impedir a formação de metástases é essencial para reduzir a mortalidade e a morbilidade. Para atingir este objetivo, é necessária a compreensão dos mecanismos moleculares subjacentes à progressão de células mamárias normais para células de carcinoma de mama in situ e de carcinoma de mama invasivo.

Vários estudos sugerem que o tráfego de membranas é subvertido por células cancerígenas para que estas adquiriram capacidades proliferativas, migratórias e invasivas. De facto, foi demonstrado que membros da família de fatores de ribosilação do ADP (Arf), que regulam várias etapas do tráfego de membranas, estão sobrexpressos em diferentes tipos de cancro e promovem a progressão desta doença. Além disso, o nosso grupo demonstrou que um membro da subfamília de proteínas Arf-like (Arls) - ARL13B - regula a migração e invasão de células de CM. Esta proteína regula mecanismos nos cílios primários, embora também regule processos fora dos cílios, incluindo a dinâmica de adesões focais e a formação de *circular dorsal ruffles*. No entanto, o papel de outras Arls na progressão do CM ainda é mal compreendido. Portanto, o principal objetivo deste trabalho de doutoramento foi identificar novos reguladores da progressão de CM, com foco na subfamília de proteínas Arl. Com isto, pretendemos desvendar os mecanismos subjacentes ao desenvolvimento desta doença e descobrir potenciais alvos terapêuticos para impedir a progressão do tumor e a formação de metástases.

Os resultados obtidos neste trabalho mostram que vários genes ARL estão sobrexpressos em linhas celulares de CM, nomeadamente ARL1, ARL2, ARL3, ARL4A, ARL5A, ARL5B, ARL6, ARL8A, ARL8B, ARL11, ARL13B, ARL14 e ARFRP1. Além disso, uma análise bioinformática usando a base de dados TCGA, que inclui amostras de CM e tecidos adjacentes normais mamários, revelou que os genes ARL1, ARL8B, ARL11 e ARFRP1 estão sobrexpressos em CM. Adicionalmente, descobrimos que a proteína ARFRP1 regula a migração e invasão de células de CM. Esta proteína regula o transporte

de moléculas na rede trans-Golgi e regula o transporte de proteínas que estão envolvidas em adesões célula-célula e na polaridade celular planar, processos que estão associados à migração e invasão celular. Também descobrimos que a ARL13B regula a invasão de células de CM altamente invasivas em 3D. Por fim, este estudo revelou que os reguladores de transporte de lisossomas, ARL8A e ARL8B, regulam a migração de células de CM e que o silenciamento da ARL8B diminui a invasão de células em 3D e a exocitose de lisossomas em células de CM.

No futuro, seria importante investigar quais as vias de sinalização envolvidas na regulação da migração e invasão de CM promovidas pela ARFRP1. Além disso, propusemos anteriormente que a AR13B regula a migração e invasão de células de CM, através de um mecanismo independente de cílios, potencialmente mediado pela via não canónica do *Sonic hedgehog.* Portanto, será importante realizar futuras experiências para validar esta hipótese. As proteínas ARL8A e ARL8B foram demonstradas regular o movimento dos lisossomas para a periferia da célula, embora estudos recentes tenham demonstrado que também podem regular o movimento anterógrado de endolisossomas. Assim, no futuro, seria importante abordar que vias, mediadas pelas proteínas ARL8A e ARL8B, regulam a migração e invasão de células de CM.

Em conclusão, este trabalho sugere que as proteínas ARFRP1, ARL13B e ARL8 podem ser potenciais alvos terapêuticos para impedir a progressão do CM e reduzir a alta mortalidade e morbilidade associadas a esta doença. Além disso, os resultados obtidos com este estudo reforçam a noção de que os reguladores de tráfego de membrana podem ser subvertidos por células cancerígenas, incluindo células de CM, para migrar e invadir. Estas evidências demonstram a importância de considerar estas proteínas e os mecanismos moleculares associados como alvos para o desenho de novas terapias para o tratamento do CM.

List of publications

Casalou C, **Ferreira A**, Barral DC. The Role of ARF Family Proteins and Their Regulators and Effectors in Cancer Progression: A Therapeutic Perspective. Front Cell Dev Biol 2020;8(April):1–13. 10.3389/fcell.2020.00217

Casalou C*, Faustino A*, Silva F, Ferreira IC, Vaqueirinho D, **Ferreira A**, Castanheira P, Barona T, Ramalho JS, Serpa J, Félix A, Barral DC. Arl13b regulates breast cancer cell migration and invasion by controlling integrin-mediated signaling. Cancers (Basel) 2019;11(10):1461. https:/www.mdpi.com/ 2072-6694/11/10/1461

Index

List of abbreviations and acronyms

2D - Two-dimensional

3D - Three- dimensional

A

ADF - Actin-depolymerizing factor

AJs - Adherent junctions

AP - Adaptor protein

Arf - ADP-ribosylation factor

ARF7EP - Arf7 effector protein

Arfrp1 - Arf-related protein 1

Arl - ADP-ribosylation factor-like

ARLTS1 - ADP-ribosylation factor-like tumor suppressor gene-1

ARNO - ARF nucleotide-binding site opener

ARP2/3 - Actin related protein 2/3

ATF3 - Activated transcription factor 3

B

BART - Binder of ARL2

BBS - Bardet-Biedl syndrome

BC - Breast cancer

BORC - BLOC-one-related complex

BM - Basement membrane

BMP - Bone morphogenic protein

BRCA - Breast cancer gene

C

$CaCl_2$ - Calcium chloride

CAFs - Cancer associated fibroblasts

CAIX - Carbonic anhydrase IX

Cdc42 - Cell division cycle 42

cDNA - complementary DNA

CDRs - Circular dorsal ruffles

CIDEC - Cell cycle arrest by upregulating the cell death inducing DFFA-like effector C

COP - Coat protein complex

CTCs - Circulating tumor cells

D

DCIS - Ductal carcinoma *in situ*

dH2O - Distilled water

DMEM - Dulbecco's modified Eagle medium

DMEM/F12 - DMEM/Nutrient Mixture F-12 Ham

DMSO - Dimethyl Sulfoxide

dNTPs - Deoxyribonucleotides triphosphate

DTT - Dithiothreitol

E

E-cadherin - Epithelial cadherin

E/M - Epithelial/mesenchymal

ECM - Extracellular matrix

EDTA - Ethylenediaminetetraacetic acid

EEs - Early endosomes

EGF - Epidermal growth factor

EGFR - Epidermal growth factor receptor

EGTA - Ethylene glycol-bis(β-aminoethyl ether)-N,N,N',N'-tetraacetic acid

EMT-Epithelial-to-mesenchymal transition

ER- Estrogen receptor

ERGIC - ER-Golgi intermediate compartment

ERK - Extracellular signal-regulated kinase

F

FBS - Fetal bovine serum

FDA - Fluorescein diacetate

FYCO1 - FYVE and coiled-coil domain-containing 1 protein

G

GAPDH – Glyceraldehyde-3-phosphate dehydrogenase

GAPs - GTPase-activating proteins

GARP - Golgi-associated retrograde protein

GDIs - Guanidine nucleotide dissociation inhibitor

GDP - Guanosine 5'-diphosphate

GEFs - Guanine nucleotide exchange factors

GFR - Growth factor reduced

GMF - Glia maturation factor

GST - Glutathione-S-transferase

GTP - Guanosine-5'-triphosphate

H

HBSS - Hank's balanced salt solution

Hh - Hedgehog

HER2 - Human epidermal factor receptor 2

HOPS - Homotypic protein sorting

HRP - Horseradish peroxidase

I

IDC - Invasive ductal carcinoma

IFT140 - Intraflagellar transport 140

IM - Interstitial matrix

INPP5E - Inositol polyphosphate-5-phosphatase E

J

JS - Joubert syndrome

L

LEs - Late endosomes

LXR - Liver X receptor

M

MET - Mesenchymal-to-epithelial transition

MHC - Major histocompatibility complex

MMPs - Matrix metalloproteinases

MRI - Magnetic resonance imaging

MT - Microtubule

MTT - 3-(4,5-Dimethylthiazol-2-yl)--2,5-Diphenyltetrazolium Bromide

N

N-cadherin - Neural cadherin

Nck1 - NCK Adaptor Protein 1

NMIIA - Non-muscle myosin IIA

NPFs - Nucleation promoting factors

NST - No special type

N-WASP - Neural Wiskott-Aldrich syndrome protein

O

OE - overexpression

ON - Overnight

P

PAK - p21-activated kinases

PBS - Phosphate Buffer Saline

Pen/Strep - Penicillin/Streptomycin

PI - Propidium iodide

PI3P - Phosphatidylinositol-3-phosphate

PI(3,4)P2 - Phosphatidylinositol (3,4)-bisphosphate

PIP5K1A - Phosphatidylinositol-4-phosphate--5-kinase type 1 alpha

PI(3,5)P2 - Phosphatidylinositol (3,5)-bisphosphate

PM - Plasma membrane

PR - Progesterone receptor

PSD4 - Pleckstrin and sec7 domain containing 4

PTEN - Phosphatase and tensin homolog

R

Rab - Ras-like in brain

Rac1 - RAS-related C3 botulinum toxin substrate 1

Ran - Ras-like nuclear

Ras - Rat sarcoma

RFS - Relapse free survival

Rho - Ras homologous

ROCK - Rho-associated kinase

RPMI - Roswell Park Memorial Institute

RT - Room temperature

RTKs - Receptor tyrosine kinases

S

Sar - Secretion-Associated RAS-related

SD -

SDS - Sodium dodecyl sulfate

Shh - Sonic hedgehog

SKIP - Sif-A and kinesin-interacting protein

SNAREs - N-ethylmaleimide-sensitive--factor attachment protein receptors

T

TBCD - Tubulin-specific chaperone D

TBS - Tris-buffered saline

TBST - Tris-buffered saline tween

TFs - Transcription factors

TGF-β - Transforming growth factor β

TGN - Trans-Golgi network

TJs - Tight junctions

Tks5 - tyrosine kinase substrate with 5 SH3 domains

TN -

TNBC - Triple- negative breast cancer

TP53 - Tumor protein p53

TRIM23 - TRIpartite Motif-containing protein 23

U

UCA1 - Urothelial Cancer Associated 1

ULA - Ultra-low attachment

V

Vangl2 - Van-Gogh-like 2

W

WASP - Wiskott–Aldrich syndrome protein

WAVE - WASP family verprolin-homologous

WHO - World Health Organization

WRC - WAVE regulatory complex

List of Figures

List of Tables

Chapter 1. Introduction

This chapter is partially based on the following manuscript:

Casalou C*, **Ferreira A***, Barral DC. The Role of ARF Family Proteins and Their Regulators and Effectors in Cancer Progression: A Therapeutic Perspective. Front Cell Dev Biol 2020;8(April):1–13. 10.3389/fcell.2020.00217

1.1. Breast cancer and cancer-associated mechanisms

1.1.1. Breast cancer epidemiology

In 2020, female breast cancer (BC) surpassed lung cancer and was reported by GLOBOCAN as the most common type of cancer worldwide, with an incidence of 2.3 million (11.7 %) new cases in one year (Figure 1A). Additionally, BC was responsible for the highest number of cancer-related deaths in women, accounting for 24.5% of the fatalities (Figure 1B) [1].

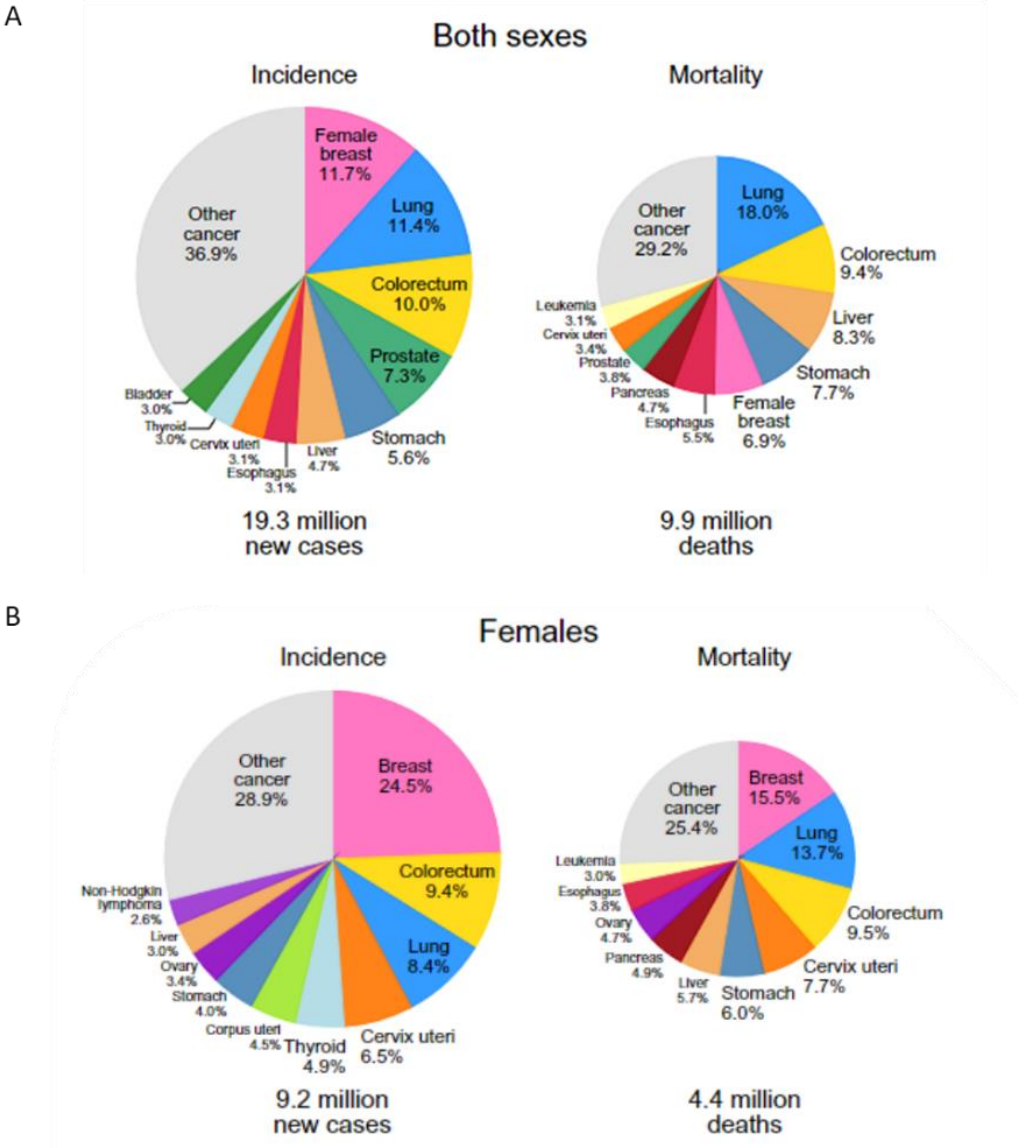

Figure 1 - Breast cancer incidence and mortality worldwide. A. Percentage of new cases and deaths in both sexes for the ten most common types of cancer. Female BC accounts for 11.7 % of new cases and 6.9 % of deaths. **B.** Percentage of new cases and deaths in women for the ten most common types of cancer. BC accounts for 24.5% of new cases and 15.5 % of deaths. Adapted from [1] .

In developing countries, the reported BC incidence rates are lower than those of high-income countries, due to early detection of the disease and easier access to better and more frequent diagnosis. However, mortality is higher in low-incoming nations, which is probably related with less access to state-of-the-art diagnoses and therapeutic options [2]. In Portugal, BC was responsible for the highest incidence and highest cancer-associated mortality in women, with around 7,000 new cases and 1,900 deaths in 2020 [3].

1.1.2. Breast cancer classification: physiology and subtypes

BC is a heterogeneous disease, and its classification follows established guidelines based on several clinical and pathological features [4]. Anatomically, the breast parenchyma comprises adipose tissue, glandular tissue, and fibrous (connective) tissue. Adipose tissue is supplied by a net of blood vessels, lymphatic vessels and nodes, and nerves, supported by fibrous tissue and ligaments. The glandular epithelium is divided in 15-20 lobes, which are composed of several lobules where the milk is produced. Lobes and lobules are connected by ducts that are responsible for transporting the milk toward the nipples [5,6] (Figure 2). Breast ducts are formed by two distinct layers of cells - epithelial (inner layer) and myoepithelial (outer layer) – which are surrounded by a basement membrane (BM) [5,6]. BM is a thin highly cross-linked layer mainly composed of collagen type IV, laminin, entactin/nidogen, and proteoglycans [7,8].

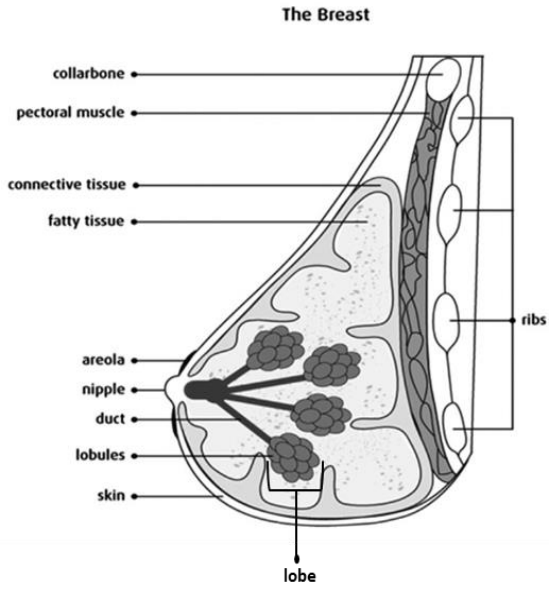

Figure 2 - Breast anatomy. The breast is composed by adipose, glandular epithelial, and connective tissues. The glandular epithelium is divided in lobes that are subdivided in lobules. Ducts connect the lobes to the lobules and carry the milk to the nipple. Adapted from [5].

The mechanisms underlying BC initiation and progression are still poorly understood. Nevertheless, it is thought that the clonal evolution model and the cancer stem cell model take place in this process [2]. The clone model, postulates that mutations and epigenetic alterations occur in cancer cells and the "fittest" cells will proliferate and give rise to a tumor [9]. Alternatively, according to the cancer stem cell model, only precursor cancer cells can initiate and sustain progression [10]. This scenario can get much more complex if we also consider that cancer stem cells can behave like clonal cells [11].

According to the established guidelines for histological classification, BC can be divided in carcinomas and sarcomas, depending whether the tumor originates from epithelial cells or other types of cells, respectively [12]. Carcinomas can be further subdivided in pre-invasive and invasive. Pre-invasive lesions include ductal carcinoma *in situ* (DCIS) or lobular carcinoma *in situ* depending on the cells of origin, namely duct cells or lobular cells, respectively. These tumors are mainly composed of BC cells that exhibit abnormal proliferation [13]. Invasive BC, on the other hand, is characterized by a malignant transformation of cells that can breach the BM and invade the surrounding tissues, and ultimately, lead to the formation of metastasis [14,15]. The most common forms of invasive breast cancer (IBC) are invasive ductal carcinoma (IDC) and invasive lobular carcinoma, depending on the cell's origin [16].

1.1.2.1. Ductal carcinoma *in situ*

Due to the implementation of mammography screening programs, the number of diagnosed cases of DCIS has increased in the last decades. Nowadays, around 25 % of diagnosed cases of BC are DCIS [17]. This lesion is considered an early stage of BC and is characterized by the neoplasia of the epithelial layer of cells that is surrounded by the myoepithelial cells and confined within the BM of the duct. DCIS is considered a non-obligatory precursor of IDC, which means that, in some cases, DCIS cells acquire an invasive phenotype, breach the BM and disseminate to the surrounding tissues (Figure 3) [18]. However, it is not known in which cases DCIS will progress to invasive IDC. Likewise, women that are diagnosed with DCIS have a high risk of having IDC, if not treated [4,18]. Classification parameters for DCIS are not standardized in the medical community. Nonetheless, DCIS can be classified according to the nuclear grade, which evaluates the nuclear features of tumor cells. Moreover, the presence or absence of comedonecrosis, or a buildup of necrotic cells inside the tumor, is also a commonly considered pathological feature. So, DCIS lesions can be divided in low

grade (grade 1), intermediate grade (grade 2), and high grade (grade 3) (Figure 3)[18]. Grade 1 is characterized by the presence of atypical ductal hyperplasia cells that can look like normal ductal cells. Grade 2 DCIS is very similar to the lower grade but in this stage, cells proliferate faster than normal breast cells [18]. However, this intermediate grade 2 is not always recognized [19]. Lastly, high-grade or grade 3 DCIS presents an even faster cell proliferation rate, with abnormal cell morphology and, frequently, comedonecrosis. Patients diagnosed with grade 3 DCIS are thought to be at higher risk to have IDC, as well as recurrences after treatment [17,20]. However, some studies suggest that the risk is independent of the grade [21,22]. In rare cases (around 1 % of diagnosed cases of BC), DCIS lesions can also present microinvasions [18]. These types of lesions contain a noninvasive DCIS component and an invasive component, which is described to be small (1 mm or less) [23]. Nonetheless, the prognosis for DCIS with microinvasions is closer to IDC than to pure DCIS [24]. DCIS can also be classified into different types, which include comedo, solid, cribriform, and papillary/micropapillary[25]. However, DCIS lesions are very heterogeneous and usually present morphological features of the different histological types [16,25,26].

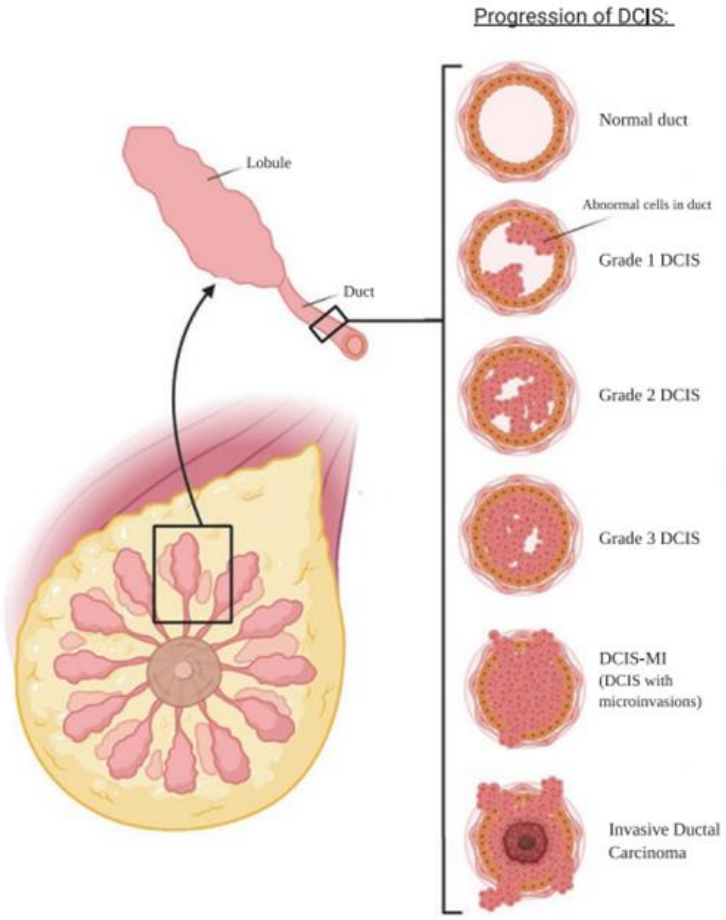

Figure 3 - legend on next page

Figure 3 - Ductal carcinoma *in situ* stages and progression. DCIS is considered an early stage of BC and is characterized by a neoplastic growth of the epithelial layer of cells surrounded by the myoepithelial cells and confined within the BM of the duct. DCIS lesions can be divided in low grade (grade 1), intermediate grade (grade 2), and high grade (grade 3). In rare cases, DCIS lesions can also present microinvasions (DCIS-MI). These types of lesions contain a noninvasive DCIS component and an invasive component. Lastly, DCIS can progress to IDC with BC cells breaching the BM and invading the surrounding tissues. Adapted from [18].

1.1.2.2. Invasive breast carcinoma

The World Health Organization (WHO) classification of the different histological types of IBC is based on several characteristics such as tumor cell type, architectural features, immunohistochemical profile, and extracellular secretion [27]. The most prevalent form of invasive or infiltrating BC, known as IDC "no special type" (NST), does not display any specific characteristics that can ground it as a specific type of BC and represents 70 % - 80 % of all IBC cases diagnosed [16]. Following IDC-NST, lobular carcinoma of the breast is the second most prevalent type of IBC, representing around 10% of the cases. A wide range of different histological subtypes is also included in the WHO classification, including microinvasive carcinomas, tubular carcinomas, mucinous carcinomas, micropapillary carcinomas, carcinomas with apocrine differentiation, metaplastic carcinomas, and other rare forms of IBC [14].

The histological grading system that is currently recommended by WHO is known as the Bloom–Richardson–Scarff classification in Elston–Ellis modification and is used to assess the degree of histopathological malignancy [28]. According to this grading system, the tumor grade is determined by scoring (from 1 to 3) tubule formation, nuclear pleomorphism, and mitotic count. The final score is obtained by the sum of all three scores: grade 1 (from 3-5), grade 2 (from 6-7), grade 3 (from 8-9) [28]. Tumors can also be classified according to the TNM classification system. It provides information about the size of the primary tumor (tumor or T), the extent of cancer at the regional lymph nodes (nodes or N), and the presence of distant metastasis (metastasis or M). The assessment of T, N, and M is then combined to generate five stages (stages 0–IV) [2,29].

IDC and DCIS can be classified according to their molecular characteristics. Over the years, the expression profiles of the estrogen receptor (ER), progesterone receptor (PR), and human epidermal growth factor receptor 2 (HER2) were used to unravel the heterogeneity of BC and helped in both prognosis and treatment strategies [30]. Moreover, gene expression profiling studies of BC samples performed by Perou and colleagues allowed the creation of different intrinsic subtypes:

luminal A, luminal B, HER2-overexpressing, basal-like and normal-like, although this last subtype is believed by some researchers to be an artifact due to contamination with normal cells. [31,32]

Luminal A is the most prevalent molecular subtype, with 60 % to 70 % of prevalence [2]. These tumors are characterized by a strong expression of ER and PR, absent HER2 expression and low Ki67 index, which is an indicator of cell proliferation. Luminal A tumors are associated with low grade lesions and a good prognosis [13]. Luminal B tumors express both ER and PR hormone receptors, but with a lower expression than luminal A tumors and are HER2-positive or HER2-negative. Also, Luminal B cancers have a high Ki67 index and present higher grades than luminal A tumors with an intermediate prognosis [2]. HER2-overexpressing or HER2- enriched tumors represent around 15 % of all IBCs and exhibit high HER2 gene expression levels. These tumors do not express ER and PR receptors and the Ki-67 index is high. Moreover, HER2-overexpressing tumors are likely to be high grade and are associated with poor prognosis [2]. Lastly, basal-like tumors represent around 10-15 % of IBCs. They are characterized by an expression pattern like normal mammary basal/myoepithelial cells, including the expression of cytokeratins 5, 6, and 17 and epidermal growth factor receptor (EGFR). They are considered triple-negative (TN) since the expression of ER, PR and HER is absent in these tumors. Histologically, these tumors are usually high grade with a high Ki67 index and poor prognosis [2].

Nowadays, it is widely accepted that “basal-like breast cancer” and TN breast cancer (TNBC) are not synonymous. Several studies showed that most TNBCs present basal-like intrinsic subtype characteristics. However, the TNBC immunohistochemistry subtype and the basal-like molecular subtype classified by genomic profiling do not perfectly match. Likewise, according to the most recent publications, TNBC tumors can be further divided into distinct groups: basal-like, mesenchymal, and luminal androgen receptor [33,34].The characteristics of the four molecular subtypes are summarized in Table 1.

Table 1 - Molecular subtypes of breast cancer – Estrogen receptor (ER), progesterone receptor (PR), and human epidermal growth factor receptor 2 (HER2) expression profile, Ki67 index, histological grade, prognosis, and prevalence of four molecular subtypes, excluding the normal-like BC. Based on [2].

	Luminal A	Luminal B	HER2+	Triple-negative
Receptor expression	ER+/PR+ (strong expression) HER2 -	ER+/PR+ (low expression) HER2 -/+	ER-/PR- HER2+	ER-/PR- HER2-
Ki67 Index	Low	High	High	High
Histological grade	Low	Higher that Luminal A	Higher than Luminal A	High
Prognosis	Good	Intermediate	Intermediate	Poor
Prevalence (% of BC)	60-70%	10-20%	10-15%	10-15%

1.1.3. Breast cancer causes, diagnosis, and treatment

Considered a multifactorial disease, BC has been linked to several factors that can increase the predisposition for the development of these tumors. Risk factors include both genetic or non-modifiable factors and non-genetic aspects, and it is not always possible to attribute one specific cause to a given diagnosed case of BC [35]. Gender is without a doubt one of the most important risk factors, given that 99% of BC cases occur in women and only 1% in men [36]. Age is also a crucial factor when it comes to BC progression, both in female and male BC. Although the incidence of BC is increasing in young women, most BC cases are still diagnosed in women with ages above 50 years old [35]. As for known BC-related genetic mutations, two genes are characterized by their high penetrance - breast cancer gene 1 (*BRCA1)* and 2 (*BRCA2)* [37]. Mutations in these genes have been mainly associated with hereditary syndromes but sporadic cases have been described [35]. Moreover, people that carry *BRCA1*/*BRCA2* mutations are estimated to have a 10-fold higher risk of developing BC [16]. Besides *BRCA1* and *BRCA2*, other high penetrance genes like tumor protein p53 (*TP53)* or phosphatase and tensin homolog (*PTEN)*, have also been associated with BC [38–41]. Non-modifiable risk factors for BC progression can also include other aspects like ethnicity and race, degree of economic development of the place of living, pregnancy/ breastfeeding, the density of breast tissue,

and radiation exposure [1,42–45]. As for the non-genetic/modifiable risk factors, several have been reported to increase the risk to develop BC. Examples are obesity and unhealthy diets, hormonal contraceptives and replacement therapy, physical inactivity, alcohol consumption, and smoking [46–52].

BC diagnosis is based on a combination of three tests that include clinical examination, imaging (mammography and/or ultrasonography), and biopsy [53]. Imaging evaluation can also be performed using MRI in cases where the conventional imaging techniques are inconclusive [2]. It is also important to refer that, due to the massive mammography screening campaigns, there is a debate about whether there is an overdiagnosis/overtreatment of DCIS lesions [17,54]. It is a current problem that has economic impacts and, more importantly, can affect the physical and phycological well-being of many women. As such, researchers and clinicians are putting enormous efforts into trying to understand which cases of DCIS will progress to IDC, to establish more appropriate guidelines for therapy.

In terms of treatment, the first option for early BC without metastases is surgery. This procedure is normally accompanied by neoadjuvant therapy (before surgery) in cases where the tumor is large or adjuvant therapy (after surgery) if there is an increased risk of recurrence [2]. Chemotherapy is a systemic treatment that can be used as neoadjuvant or adjuvant therapy. It includes different combinations of carboplatin, cyclophosphamide, 5-fluorouracil/capecitabine, taxanes (paclitaxel, docetaxel), and anthracyclines (doxorubicin, epirubicin) [35]. Endocrine therapy may also be used as neoadjuvant or adjuvant therapy and it is used in BC cases with an expression of hormone receptors (luminal BC). These treatments include drugs that block ERs (tamoxifen, toremifene, fulvestrant) and treatments that aim to decrease the levels of estrogen (letrozole, anastrozole, exemestane)[35]. Chemotherapy and endocrine therapy are often combined since this strategy has been linked with a reduction in mortality [55]. Regarding more localized therapies, radiotherapy is commonly used after surgery and/or chemotherapy. It is also widely used in cases where the tumors are unresectable or in metastatic BC [56]. Finally, targeted therapy can be provided at any stage of treatment. This type of therapy is often used in HER2-positive BC patients and includes anti-HER2 monoclonal antibodies like trastuzumab, and pertuzumab or HER2 inhibitors like lapatinib and neratinib [35]. Advanced cases of BC include both inoperable locally advanced breast cancer and metastatic BC and it is considered an incurable disease. Treatment options for these patients normally include therapies to alleviate their symptoms and prolong life expectancy while trying to keep the patient's life quality [2].

Over the years, progress has been made in increasing the efficacy and safety of the treatments for BC. However, side effects that can be acute (eg. nausea and fatigue) or more severe and chronic (such as cardiotoxicity or cognitive dysfunction) are still a reality for BC patients. Moreover, more aesthetical factors that come from partial and complete mastectomies or hair loss due to chemotherapy, often represent a high toll on the mental health of BC patients [2,35]. So, it is highly important to continue the research in this field to find more effective, and personalized therapies that can help to save more lives and conserve the quality of life of BC patients.

1.2. Hallmarks of cancer

The hallmarks of cancer are described as a combination of features that cells acquire during their transformation into a malignant state. These capabilities are essential for these cells to be able to form malignant tumors. Hanahan and Weinberg's first publication in 2000, suggested that the hallmarks of cancer could be divided into six categories: self-sufficiency in growth signals, insensitivity to anti-growth signals, limitless replicative potential, evading apoptosis, sustained angiogenesis, and tissue invasion and metastasis [57]. A decade later, this list was updated, and two new emerging hallmarks were added: reprogramming energy metabolism and evading the immune response. Also, two enabling traits were added: genome instability and mutation, and tumor-promoting inflammation. Enabling traits were described as cellular mechanisms that enable the acquisition of the hallmarks. The tumor microenvironment, which comprises a heterogeneous population of cancer and stromal cells, was later recognized as an important player in carcinogenesis and tumor progression[58]. More recently, another four parameters were added: two emerging hallmarks (unlocking phenotypic plasticity and epigenetic reprogramming) and two enabling traits (polymorphic microbiomes and senescent cells) (Figure 4) [59]. Also, this year, Ravi and colleagues proposed the introduction of pro-survival autophagy as a new hallmark of cancer, given the large evidence that highlights its role in cancer progression [60].

However, some researchers have challenged these proposals by posing the question: what is the definition of a hallmark? Indeed, in 2010, Lazebnik stated in his essay that a "hallmark" is defined as a distinguishable feature. So, in his view, the hallmarks of cancer should only include features that are different between normal cells and malignant cells and ruled out five of the six cancer hallmarks proposing that only invasion and metastases would fit in that definition [61]. Nonetheless, the constant updating and increasing complexity of the hallmarks of cancer, have been

useful to foster debate and discussion among the scientific community and, more importantly, to stimulate cancer research aiming at a better definition of cancer biology mechanisms.

1.3. The metastatic cascade

Metastasis formation accounts for most cancer-related deaths and is defined as an organ-selective and sequential multi-step process [62]. It is initiated by tumor cells that escape the primary tumor and ends with the colonization and propagation of tumor cells on distant organs. In general, this cascade of events can be divided in five steps: invasion, intravasation, dissemination, extravasation, and colonization (Figure 5) [63]. In the first step (invasion), cancer cells lose their cell-cell adhesion, allowing the dissociation of malignant tumor cells from the primary tumor. Also, cancer cells acquire the capacity to degrade the BM and stromal extracellular matrix (ECM) and invade neighboring tissues. Moreover, at this stage cells regulate the expression of proteins that control cell motility/migration [64]. During intravasation, cancer cells enter the vascular/lymphatic circulation whereby they can disseminate to distant locations. At this point, the circulating tumor cells (CTCs) are exposed to several types of stresses that include oxidative stress, shear forces, and immune system surveillance. Likewise, many CTCs die in circulation, and only a small percentage reaches the site of colonization [62]. When the CTCs arrive at the target site, they extravasate from the circulation to colonize the distant organ, which is achieved through the secretion of factors that induce vessel hyperpermeability [64]. After extravasation, cancer cells arrive at a new location in a new microenvironment, and they must adapt. So, these cells can reside in a dormancy state (for short or long periods) as single disseminated tumor cells or small micrometastatic clusters. When the ideal conditions are in place, cells start to actively proliferate at the colonization site and form macroscopic metastasis [65].

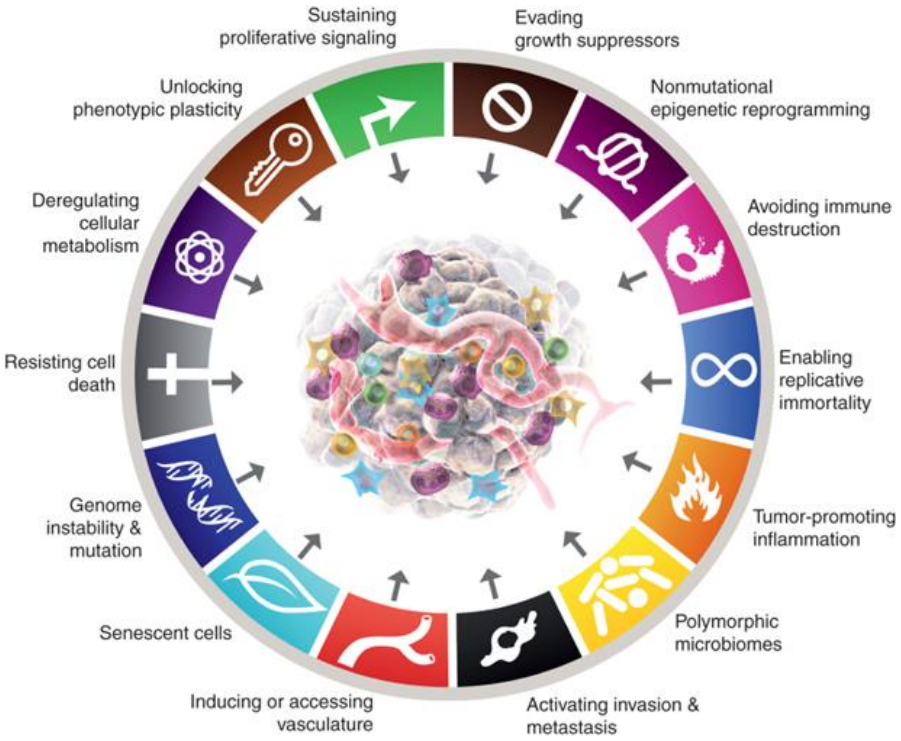

Figure 4 - Hallmarks of cancer. This illustration includes 10 hallmarks and 4 emerging traits proposed by Hanahan *et al*. The hallmarks include new emerging hallmarks - unlocking phenotypic plasticity and epigenetic reprogramming; and eight canonical hallmarks – sustaining proliferative signaling, evading growth suppressors, enabling replicative immortality, resisting cell death, inducing or assessing vasculature, activating invasion and metastasis, deregulating cellular metabolism and avoiding immune destruction. The enabling traits include new proposed traits - polymorphic microbiomes and senescent cells; and the canonical traits - non-mutational epigenetic reprogramming and tumor-promoting inflammation. Adapted from [59].

As mentioned before, it is widely accepted that metastasis is an organ-selective process. In other words, as initially suggested by the "seed and soil" hypothesis, certain types of cancer cells are more likely to form metastasis in specific tissues [66,67]. In the case of BC, the preferred metastatic sites are the bones, lungs, liver, brain, and lymph nodes [68]. Metastasis formation is a very complex and heterogeneous process, and, as mentioned before, it is the deadliest mechanism of cancer progression. All these reasons impose a continuing investment on research to uncover the molecular mechanisms underlying the multiple steps of the metastatic cascade, to find better therapeutic options.

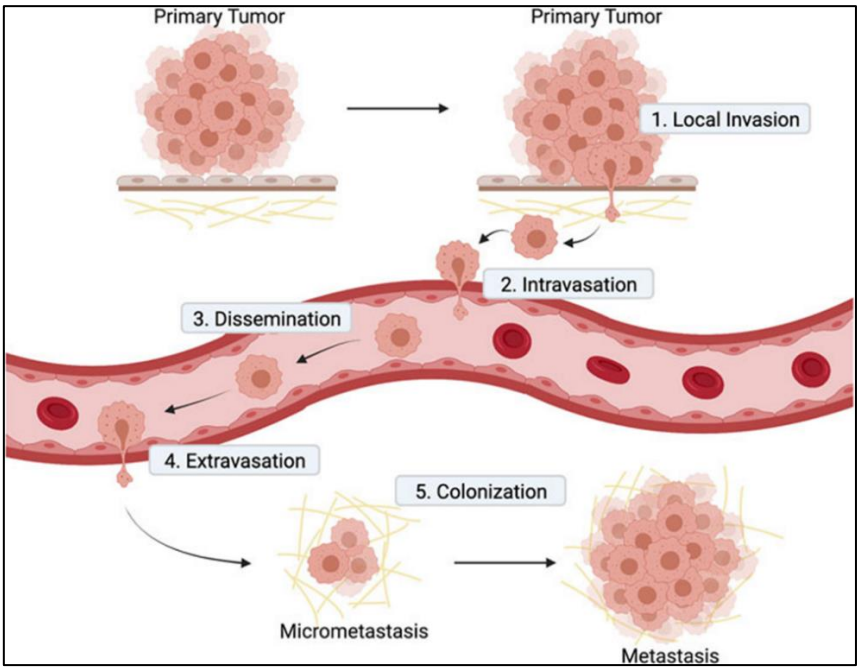

Figure 5 - Steps of the metastatic cascade. The formation of metastasis can be divided in five steps. 1. Local invasion; cancer cells at the primary tumor site acquire several features that enable the degradation of basement membrane/extracellular matrix and invasion of the surrounding tissues; 2. Intravasation: Cancer cells enter the vascular/lymphatic circulation; 3. Dissemination: Circulating tumor cells (CTCs) must survive in circulation until they reach the target site; 4. Extravasation – at the target organ, cancer cells extravasate from the vessels; 5. Colonization: at the secondary tumor site, cancer cells form micrometastases and once the ideal conditions are established, these cells proliferate and originate macroscopic metastasis. Adapted from [63]

1.3.1. Epithelial-to-mesenchymal transition

One of the mechanisms acquired by cancer cells during the metastatic process is the ability to activate the epithelial-to-mesenchymal transition (EMT) program. EMT is a cellular process broadly defined by the downregulation of epithelial features and acquisition of mesenchymal characteristics [69]. It was first described in early embryogenesis and is currently associated with different stages of development, wound healing, tissue fibrosis, and cancer [70,71]. In cancer, this process has been linked to several tumor-associated processes such as tumor initiation, malignant progression, stemness, cell migration, intravasation, colonization, and resistance to therapy [72–74]. Epithelial cells present apical-basal polarity and are connected by lateral tight junctions (TJs), adherent junctions (AJs), desmosomes, and gap junctions. Adherent junctions are formed by many different proteins, including the cell surface epithelial cadherin (E-cadherin) [69]. Moreover, epithelial cells interact with the BM through hemidesmosomes and α6β4 integrins [75]. Once EMT is activated, E-cadherin expression is decreased, leading to the loss of the polygonal, cobblestone morphology characteristic of the epithelia. In turn, the cells acquire a spindle-shaped mesenchymal morphology,

which is accompanied by the expression of proteins that are associated with a mesenchymal state, including neural cadherin (N- cadherin), vimentin, and fibronectin. This transformation also includes the increased expression of specific integrins, namely β1 and β3, and matrix metalloproteinases (MMPs) [75]. The alterations that occur during the EMT transformation promote both cell migration and invasion of cancer cells and are regulated by different transcription factors (TFs). TFs promote the downregulation of genes that are associated with an epithelial state and the overexpression of mesenchymal-associated genes. Various conserved TFs, including Snail (SNAI1), Slug (SNAI2), TWIST1, TWIST2, Zeb1 (previously known as TCF8) and Zeb2 (SIP1) have been identified as major regulators of EMT [76–82]. Additionally, there are several known inducers of EMT. For example, the Wnt signaling pathway increase leads to the upregulation of Slug, TWIST and N-cadherin, and represses the expression of E-cadherin in trastuzumab resistant HER2-overexpressing BC [83]. Also, the transforming growth factor β (TGF-β) signaling pathway can promote the expression of Slug and Snail, while Notch pathway has been linked to the regulation of EMT in different types of carcinomas, including BC [75,84,85]. The tumor microenvironment can also induce changes in EMT. Namely, cancer-associated fibroblasts (CAFs) and immune cells were shown to induce EMT in cancer cells by secreting cytokines and growth factors, like TGF-β, IL-6, epidermal growth factor (EGF), among others [75,86,87].

EMT is a reversible process, meaning that cells can activate several pathways to decrease the expression of mesenchymal markers and increase the expression of features associated with the epithelial state. This reverse process is called mesenchymal-to-epithelial transition (MET) and it is accepted that cancer cells need to undergo this transition during metastatic colonization and growth [75]. In fact, it is reported that metastases can present an epithelial morphology [71]. Over the years, several studies have been highlighting that carcinoma cells that activate EMT programs often express both epithelial and mesenchymal markers. Moreover, it is thought that cancer cells rarely reach a fully mesenchymal state during EMT [88]. In BC, several states of epithelial/mesenchymal (E/M) have been reported in cells from primary tumors and hybrid E/M states are enriched by CTCs released by primary breast tumors [89,90]. This plasticity of cancer cells may increase their capacity to adapt and respond to several physiological stresses and stimuli (Figure 6).

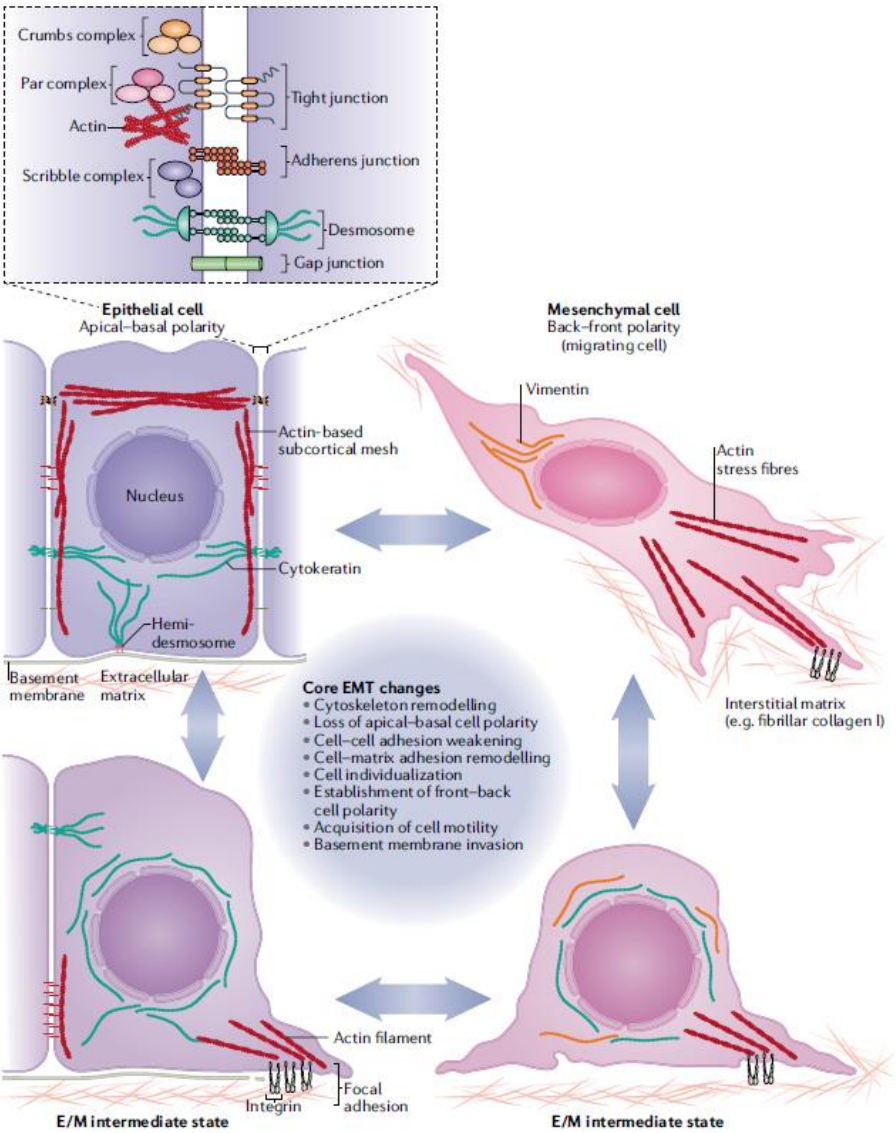

Figure 6 - Epithelial-to-mesenchymal transition process and states. Epithelial cells present apical-basal polarity and are connected to each other via lateral adherent junctions, tight junctions, desmosomes, and gap junctions. Adherent junctions are linked to cortical actin bundles and desmosomes bind to cytokeratin. Epithelial cells connect with the BM through hemidesmosomes and integrins. The apical versus basolateral domains of epithelial cells are defined by polarity complexes (Par, Crumbs and Scribble). Mesenchymal cells do not contain functional epithelial junctions and present back-front polarity. Also, they express vimentin-based intermediate filaments and attach to the extracellular matrix through focal adhesions The variable expression of epithelial/mesenchymal markers (E/M) leads to the creation of various intermediate states (bottom left and right) that interchange depending on external cues and imposed stresses. Adapted from [69].

1.3.2. Cancer cell migration

As previously mentioned, cancer cells need to acquire migratory features to invade through surrounding tissues and colonize distant organs. Cell migration in two-dimensional (2D) settings has been extensively studied over the years and can be described as a multistep process, involving spatiotemporal regulation and dynamics of the cytoskeleton components [actin microfilaments,

microtubules (MTs), and intermediate filaments (IFs)] [91,92]. However, in living organisms, cells experience a three-dimensional (3D) environment with different types of ECM and must adapt their migratory characteristics and morphology to each situation. Likewise, 3D cell migration exhibits a plethora of movements that can be executed in a single-cell or a collective mode [91,92].

1.3.2.1. Single-cell migration

Single cells in 3D can migrate using different types of locomotion that can be divided into mesenchymal, amoeboid, and lobopodial. It is described that cancer cells can interchange between mesenchymal and amoeboid migration types depending on the external cues of the microenvironment that surrounds them [93]. Mesenchymal and amoeboid migration modes are well documented. The mesenchymal migration is characteristic of cells with a spindle-like shape that undergo almost complete EMT. The speed of mesenchymal cell migration in 3D is rather slow, which is due to the slow turnover of focal adhesions (FAs) during this process. This mode of migration relies on protruded lamellipodia and/or filopodia at their leading-edge using actin polymerization stimulated by Rho family GTPases (*e.g.,* Ras-related C3 botulinum toxin substrate 1 (Rac1) and Cell division cycle 42 (Cdc42)]. Then, the leading-edge forms a new cell adhesion to the migratory surface/substrate, which in turn matures into focal adhesions, and the adhesion at the back/rear end of the cell is disassembled, usually via protease-dependent ECM degradation. This leads to a retraction of the back of the cell, via actomyosin contractility, promoted by Ras homolog family member A (RhoA), and the cycle repeats [91]. On the other hand, due to low attachment to the ECM, the velocity of amoeboid migration is relatively high, and these cells move within the 3D substrates through a protease-independent mechanism. In this type of cell movement, cells display enhanced contractility, which allows them to squeeze through the spaces between the ECM fibers or exert forces that deform the surrounding matrix. This process of actin cytoskeleton remodeling is regulated by RhoA and its effector Rho-associated kinase (ROCK). In this case, the tension is kept by cortical actomyosin, which results in membrane blebbing [94]. Finally, the lobopodial migration has only been observed in non-malignant cells and it is considered an intermediate state between amoeboid and mesenchymal migrations [95]. These cells are tightly adherent to the ECM and use actomyosin contractility, hydrostatic pressure, and nuclear repositioning to form bleb-like blunt protrusions called lobopodian (Figure 7) [92].

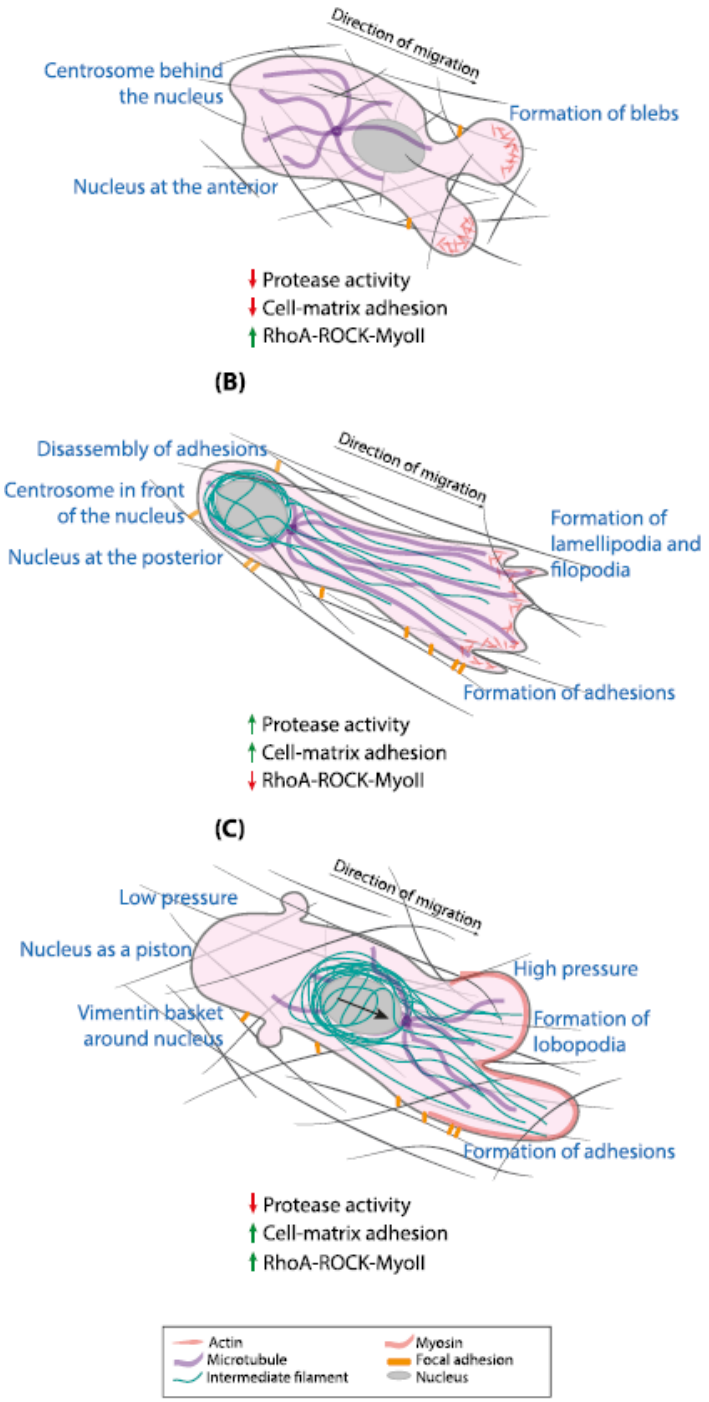

Figure 7 - Mechanisms of 3D single-cell migration. **A.** Amoeboid migration. This mechanism involves few adhesions and low protease activity. Movement is achieved through the formation of contraction-based blebs that allow cells to squeeze cells into the holes of ECM or deform it. **B**. Mesenchymal migration. Cells adhere strongly to the ECM at the leading edge through the formation of focal adhesions. Adherence at the back diminishes through the disassembly of focal adhesions and the actomyosin cytoskeleton contracts, leading to the retraction of the back of the cell and promoting directed cell migration. These cells also display proteolytic activity that remodels the ECM to facilitate cell dissemination. **C.** Lobopodial migration. In this process, cells form bleb-like blunt protrusions (lobopodia) by promoting strong adherence to the ECM, nuclear pistoning, actomyosin-dependent contraction, and hydrostatic pressure. Moreover, these cells display low protease activity and high RhoA-ROCK-MyoII contractility. Adapted from [92].

1.3.2.2. Collective cell migration

Cancer cells not only migrate individually, but they also undergo collective cell migration. This type of migration has been associated with the progression of different epithelial tumors, including BC [96,97]. Building evidence suggests that cells that move collectively display a higher capacity to successfully form metastases [97,98]. Cells that migrate collectively must be able to coordinate their movement to overcome the obstacles imposed by the tumor microenvironment. Namely, cells must use actin dynamics, integrin-mediated cell–ECM, protease-dependent ECM-remodeling and cell-cell interactions to move in a coordinated fashion [99]. Moreover, gradients of growth factors/chemokines can help guide the direction of collective cell migration [100]. The mechanism of collective cell migration is based on the "leader-follower" model. At the front, leader cells present a distinct, finger-like morphology and can detect extracellular cues from the surrounding environment through Rac-driven protrusions and integrin-mediated ECM adhesions. These cells also overexpress proteases to remodel the ECM and open the track for the trailing follower cells [99,101]. Curiously, evidence shows that stromal cells, like CAFs, can step in as "leader" cells during collective migration of cancer cells [102]. At the rear, follower cells, maintain tight symmetric cell-cell adhesions through the maintenance of AJs, TJs, and desmosomes. These cells also display apical-basal polarity. Leader cells maintain contact with the follower cells through cadherin-based AJs at their trailing edge, which means that although these cells present a more mesenchymal-like morphology, they still express markers of epithelial cells (Figure 8) [99–101]. In fact, recent studies have revealed that cancer cells that were found in clusters, display hybrid states of EMT, highlighting the heterogeneity and complexity of these processes [71].

1.3.2.3. Actin cytoskeleton dynamics during cancer cell migration and invasion

As described in the previous sections, cancer cell migration and invasion rely on contacts with the ECM, through the formation of actin-rich protrusions. These protrusions are formed through the coordinated polymerization of actin filaments that exert protrusive forces and drive the elongation/extension of the plasma membrane (PM) [103]. Actin filaments have two ends – the barbed or plus end, and the pointed or minus end. In migrating cells, actin subunits are added to the barbed of the filaments, to promote the elongation of actin protrusions at the PM [104]. The first step for the

assembly of actin filaments is nucleation, which depends on actin nucleators. The best described actin nucleator is the actin-related protein 2/3 (Arp2/3) complex, which comprises two actin-related proteins, Arp2 and Arp3, and five smaller subunits [105]. Due to its intrinsic inactivity, the Arp2/3 complex needs to be activated by class I nucleation promoting factors (NPFs), including the WAVE regulatory complex (WRC), the Wiskott–Aldrich syndrome protein (WASP), and neural WASP (N-WASP) [105,106]. Besides the Arp2/3 complex, other nucleators may regulate actin filament elongation, such as proteins from the formin and Ena/vasodilator-stimulated phosphoprotein (VASP) families, which promote elongation of unbranched actin filaments [104]. Also, capping proteins bind to actin filaments at the barbed ends, preventing the binding of actin monomers and their disassembly [107]. To guarantee that cells can form and maintain protrusions, actin monomers are disassembled for further recycling by severing factors [*e.g.,* actin-depolymerizing factor (ADF)/cofilin and gelsolin] and debranching factors like coronin or glia maturation factor (GMF), closer to the pointed ends of the actin filament [108–110].

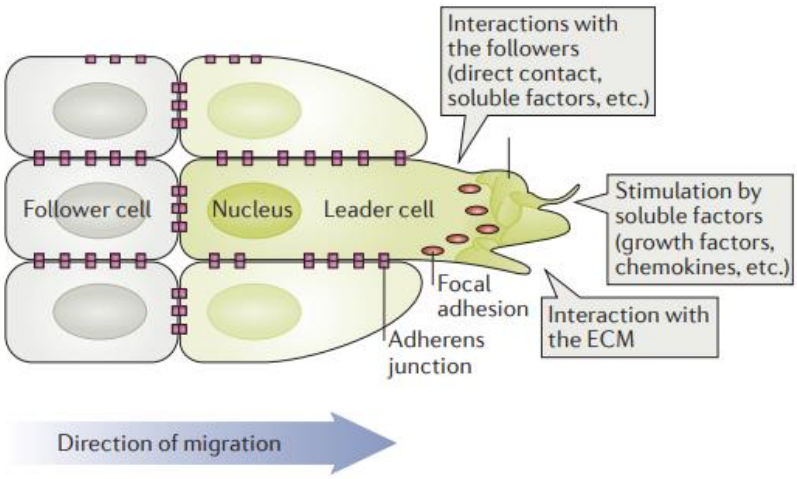

Figure 8 - Collective cell migration. In collective cell migration, leader cells are subjected to environmental cues and stimulated by several soluble factors. These cells also interact with the ECM and with follower cells. Adherent junctions restrict the formation and maintenance of focal adhesions to the front. The follower cells establish polarized cell-cell contacts. Adapted from [100].

During cancer cell migration and invasion, cells can form different types of protrusions, including lamellipodia and filopodia. Lamellipodia are planar protrusions, able to create pushing forces that are responsible for the movement of the leading edge of the cell. These protrusions are composed of branched filaments of actin, regulated by the Arp2/3 complex activity. Filopodia, on the other hand, are finger-like protrusions that act as antennae for cells to explore their surrounding environment [104]. These structures are formed by the elongation of parallel filaments of actin, likely mediated by formin and Ena/VASP proteins (Figure 9) [104].

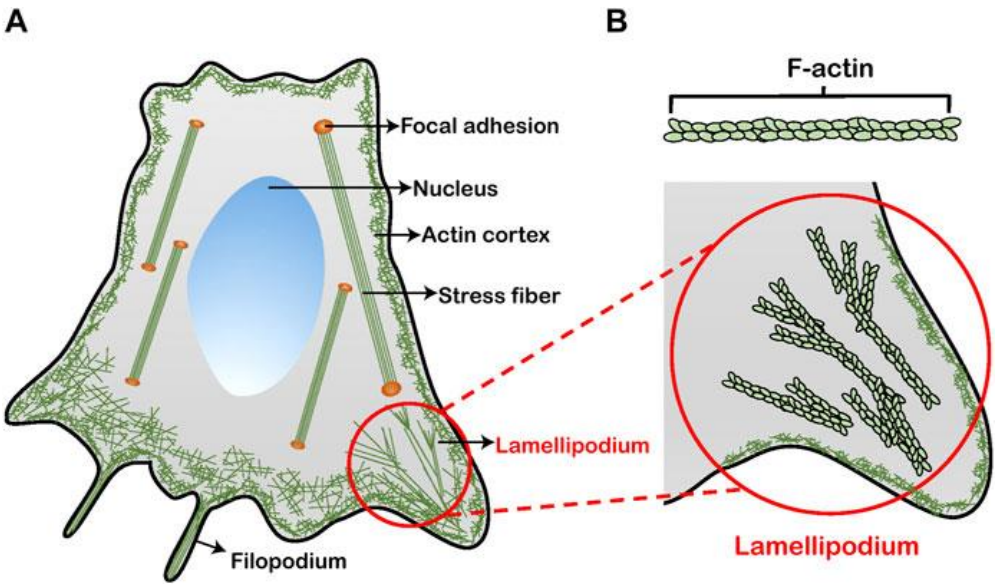

Figure 9 - Actin cytoskeleton dynamics. A. Cells can form several structures that are dependent on actin polymerization and dynamics, including actin cortex, stress fiber, filopodium, and lamellipodium. **B.** Lamellipodia are flat protrusions, formed by the branching of F-actin and are present in migrating cells. Adapted from [111].

1.3.2.3.1. Invadopodia

Cells also produce another type of specialized actin-rich protrusions, namely invadosomes. These structures are characterized by their ability to degrade the ECM via the secretion of MMPs. Invadosomes can be divided in podosomes, which are normally associated with non-malignant cells, such as immune cells, osteoclasts, and endothelial cells; and invadopodia, which are formed by cancer cells [112]. Podosomes and invadopodia share many structural and molecular similarities but the former are smaller, more abundant, short-lived, and less protrusive than invadopodia. On the other hand, invadopodia are less abundant, longer, and seem to have a lifespan of hours [112,113].

The presence of invadopodia has been associated with several steps of metastasis formation in different cancers [114]. Invadopodia formation is achieved through a sequence of temporal stages that can be divided into invadopodia precursor core initiation, invadopodia precursor stabilization, and invadopodia maturation (Figure 10) [113,115]. Invadopodia initiation can be prompted by different stimuli, including growth factors, cytokines, integrin-linked extracellular signals, acidic pH, increased matrix rigidity, hypoxia, and reactive oxygen species (ROS)[114,116]. These external cues lead to the activation of internal transducers, namely Src, p21-activated kinase (PAK), and Arg [117]. Invadopodia

initiation starts with the recruitment of core proteins, namely the Arp2/3 complex, cortactin, N-WASP, and cofilin. However, this core precursor is unstable and its stabilization involves tyrosine kinase substrate with 5 SH3 domains (Tks5)-mediated anchoring of the core to phosphatidylinositol-3,4-biphosphate ($PI(3,4)P_2$) at the PM [114,118]. At this stage, Mena and Arg are recruited to the invadopodium precursor, by lamellipoidin [119]. In turn, Mena interacts with SHIP2 that produces additional $PI(3,4)P_2$ for TKS5 binding and consequent core stabilization [114]. Actin polymerization is also included in the stabilization of the precursor core. This happens through a mechanism dependent on both cofilin and Arp2/3 complex [114]. Cofilin generates daughter filaments that further activate N-WASP-ARP2/3 complex-mediated nucleation of actin polymerization[120]. Furthermore, cofilin, Nck1, and N-WASP have been shown to activate the Arp 2/3 complex at the precursor core [114,115,121]. Lastly, β1- Integrin is also recruited to and activated in invadopodium precursors, promoting the maturation process, through interaction with Arg [122].

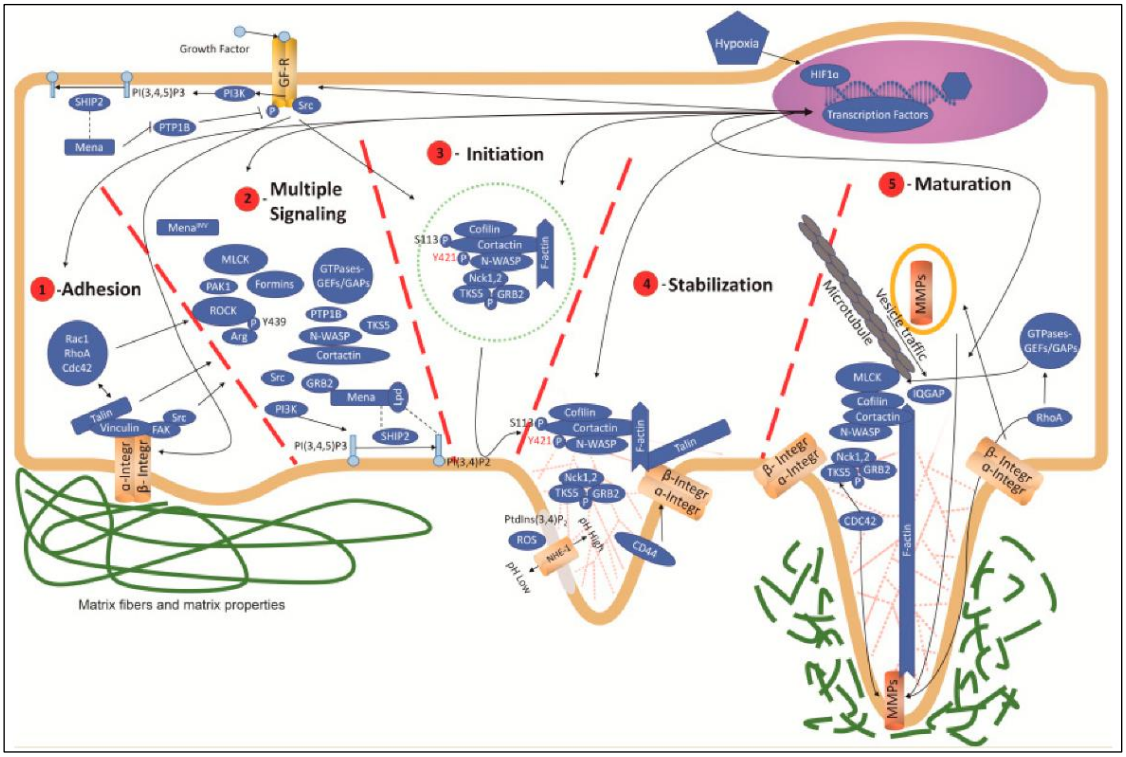

Figure 10 - Invadopodia formation. Representation of invadopodia stepwise formation triggered by cellular stimuli. Integrin and/or other membrane receptors 1. Adhesion mediated by integrins, and other membrane receptors activation generates signaling cues to the cell. 2. Generation of multiple signaling cues that trigger invadopodia formation. 3. Initiation of invadopodia formation via recruitment of actin polymerization-branching machinery to plasma membrane domains. 4. Stabilization of growing invadopodia in the plasma membrane 5. Maturation of invadopodia followed by MMP- dependent matrix degradation. Adapted from [113].

In the maturation stage, invadopodia growth and stabilization through actin polymerization take place. Maturation is also linked to the secretory machinery activation responsible for the

release of ECM-degrading proteases [113]. Cortactin is phosphorylated in tyrosine residues (Y421, Y466 and Y482) by Src and Arg, promoting the activation of cofilin. This leads to an increase in the free actin barbed ends available for polymerization via the Arp2/3 complex [123]. Furthermore, cortactin phosphorylation also leads to the activation of the NCK adaptor protein 1 (Nck1)-N-WASP-Arp 2/3 complex, promoting acting polymerization at invadopodia [124]. Mena^{INV} (Mena isoform) also promotes invadopodia maturation, probably by displacing phosphatases from the invadopodia core and, consequently, preventing cortactin dephosphorylation. Also, being an actin barbed end capping-protein antagonist, Mena promotes branched actin polymerization by displaying capping proteins from actin filaments [123]. Talins are also important regulators of invadopodia maturation and have been involved in actin polymerization, traction force production, and recruitment of MMP-loaded vesicles [125]. Once invadopodia formation is complete, cortactin is dephosphorylated, which leads to cofilin inhibition, allowing stabilization of invadopodia [126].

Invadopodia-dependent ECM degradation depends on MMPs and other proteases like proteins from the "a disintegrin and metalloprotease" (ADAM) family, serine proteases, cathepsins and the proteolytic system urokinase-type plasminogen activator receptor (uPAR) [113,127]. There are 23 MMPs described in humans. These enzymes are zinc-endopeptidases from the metzincin protease superfamily and can be classified into collagenases, gelatinases, matrilysins, stromelysins, membrane-type (MT)-MMPs and other MMPs, according to their structure and substrates [128]. Also, MMPs can be anchored to the PM or be secreted. All MMPs are initially inactive pro-enzymes, and are further activated via post-translational proteolytic cleavage [128,129]. From a large group of MMPs, 2 secreted forms (MMP-2 and -9) and 1 membrane-anchored MMP (MT1-MMP) have been often associated with mature functional invadopodia and cancer progression [129–132]. MMP-2 and MMP-9 are gelatinases that degrade gelatin, collagen (type IV, V, VIII, X, XI, and XIV), elastin, proteoglycan core proteins, fibronectin, laminin, and fibrillin-1 [133]. They are secreted as pro-enzymes and can be further activated extracellularly via an autocatalytic process or cleavage by other proteases (MMPs and others) [134]. Indeed, increased expression/activity of MMP-2 and MMP9 was associated with several types of cancers, including BC [129,135,136]. Moreover, there is evidence that these soluble proteases are relevant prognostic factors in BC [137]. MT1—MMP, or MMP-14, is a type 1 transmembrane protein generally found in invadopodia. It is synthesized as a proenzyme and it is activated at the Golgi through cleavage by the proprotein convertase furin [138] . Once activated, MT1-MMP can degrade a wide range of substrates, including gelatin, collagen (types I, II, and III), fibronectin, laminin-1, aggrecan, vitronectin, α2-macroglobulin, αl proteinase inhibitor, and

proteoglycans [133,134]. MT1-MMP is also known to cleave proMMP-2 and promote proMMP-9 activation through MT1-MMP/MMP2 axis, where MT1-MMP activates MMP-2, which in turn cleaves proMMP-9 [139]. Furthermore, MT1-MMP was described as an important prognostic marker, correlating with the metastatic potential of various cancers, including BC [132,133]. CAFs also express MT1-MMP and it was shown in a mouse model of BC that this expression contributes to cancer cell invasion and metastasis formation [140]. As previously described, invadopodia are an essential feature of cancer cells that enables ECM remodeling to allow cell invasion and metastasis formation. Therefore, numerous efforts have been made by the scientific community to use invadopodia markers to inhibit carcinogenesis, hoping that the inhibition of invadopodia formation can impair tumor progression.

1.4. Membrane Traffic

1.4.1. General Features

Membrane traffic is an essential cellular process that allows the communication and cargo exchange between membrane-bound organelles. Likewise, cellular fate is regulated by the formation, fusion, and movement of vesicles that control crucial processes within the cell, including cellular uptake, transport of nutrients for metabolic activity and pathogens/unwanted molecules for degradation, traffic of proteins, lipids, and solutes to specific locations, communication inside or outside cells, among others. These processes must be tightly regulated to ensure the correct functioning of the cell [141]. Moreover, membrane traffic can be divided in two main pathways: the endocytic and secretory pathway. The endocytic pathway includes the PM, endosomes, and lysosomes, while the secretory pathway includes the endoplasmic reticulum (ER), the Golgi apparatus and the PM. Importantly, both pathways communicate to regulate several biological processes. (Figure 11) [142].

Protein biosynthesis occurs at the ER, where correctly folded proteins are targeted for exocytosis by adaptor proteins, through coat protein complex (COP) II-coated vesicles. Then, these vesicles tether and fuse with the ER-Golgi intermediate compartment (ERGIC) and are subsequently delivered to the cis-Golgi, via tethering factors and complexes of ERGIC and Golgi-associated soluble N-ethylmaleimide-sensitive-factor attachment protein receptors (SNAREs) [143]. Afterward, cargo is

transported through the Golgi, where processing and post-translational modifications, specially glycosylation, take place. COPI vesicles are used to retrieve Golgi-resident enzymes that contribute to cargo movement through the cisternae [144]. These vesicles also participate in retrograde recycling from the ERGIC and Golgi and then to the ER [143,145]. Then, proteins leave the Golgi apparatus at the trans-Golgi network (TGN) and are transported to the PM or the endocytic pathway. Cargo that is targeted for secretion can be exocytosed via a constitutive or a regulated pathway. In the case of constitutive secretion, the carriers appear to be tubular [143]. On the other hand, regulated secretion cargoes are concentrated in granules that fuse with the PM through a SNARE-mediated and Ca^{2+}-dependent mechanism, a process that is facilitated by accessory proteins including synaptotagmins [146].

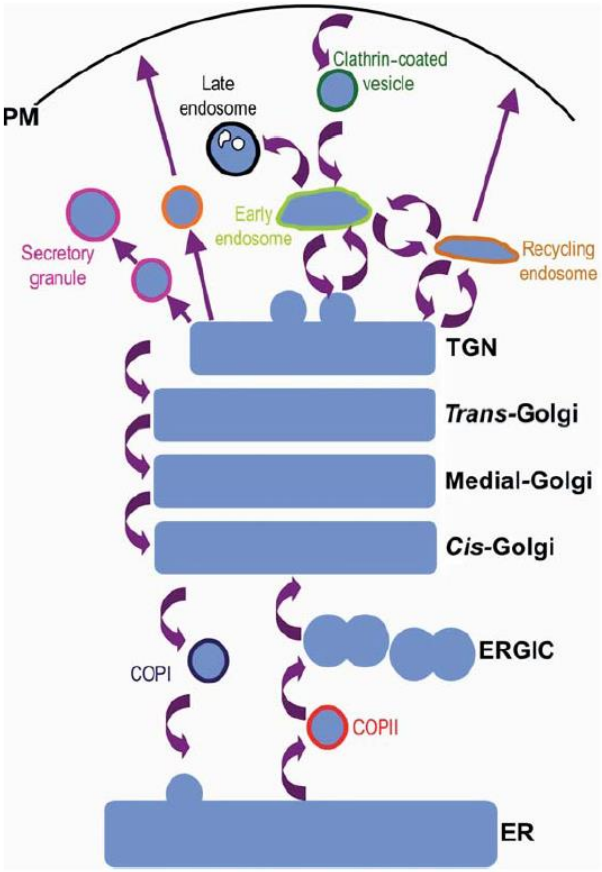

Figure 11 - Endocytic and secretory pathways. Proteins are synthesized in the endoplasmic reticulum (ER) and loaded into COPII-coated vesicles. These vesicles fuse to form the ER-Golgi intermediate compartment (ERGIC). COPI-coated vesicles recycle Golgi resident proteins and proteins from the ERGIC and the Golgi apparatus. Cargo moves through the Golgi and exits the apparatus through the trans-Golgi network (TGN). Then, cargo is transported to specific localizations by different coated vesicles and tubulovesicular carriers. Endocytosis takes place at the plasma membrane and cargo is transported to early endosomes. Then, cargo can be transported to lysosomes via late endosomes to be degraded. Alternatively, cargo can be transported to the TGN or to recycling endosomes to reach to the plasma membrane. Adapted from [142].

Clathrin-mediated endocytosis is the best characterized endocytosis route, whereby the membrane-deforming mold is defined by clathrin and mediated by cargo-binding adaptor complexes, like adaptor protein (AP) complex 2. Then AP-2 binds to clathrin and various accessory proteins and promotes the formation of a vesicle. Then, the scission GTPase dynamin is recruited and vesicles separate from the PM [143,147]. Afterward, the endocytic vesicles fuse and form early endosomes (EEs), followed by recruitment of Rab5 and phosphatidylinositol 3-phosphate (PI3P) effector proteins to the membrane of the endosome. EEs mature into late endosomes (LEs), with Rab5 being replaced by Rab7 and PI3P converts into phosphatidylinositol 3,5-bisphosphate [PI(3,5)P2]. Then, LEs fuse with lysosomes for cargo degradation [148,149]. Endocytic cargo can also escape from lysosomal-mediated degradation through recycling routes or by retrograde traffic to the Golgi apparatus [150].

1.4.2. Ras superfamily

The Rat sarcoma (Ras) superfamily of small GTPases includes over 150 members and is divided into five families that are conserved in eukaryotes and regulate several cellular processes: Ras, Ras homology (Rho), Ras-like in brain (Rab), ADP-ribosylation factor (Arf), and Ras-like nuclear (Ran). The Ras family is composed of 36 members and regulates signal transduction in cell proliferation, morphology, differentiation, and survival. Cytoskeleton dynamics, cell cycle, and gene expression are regulated by proteins of the Rho family (20 members). The Ran family only has 1 member and is the most abundant small GTPase in a cell. This protein regulates nuclear transport and structure. With more than 60 members, the Rab family is the largest, and together with the Arf family, it regulates vesicle traffic. [151,152]. Moreover, as small GTPases, proteins from the Ras superfamily cycle between an inactive guanidine-diphosphate (GDP)-bound state and an active guanidine-triphosphate (GTP)-bound state. When bound to GTP, small GTPases can bind effectors to regulate several processes within the cell. This is due to the higher affinity of the small GTPases towards the effectors, that is promoted by a conformational change in the switch I and II regions of the GTPase when GDP is exchanged by GTP. In some cases, GDP-bound GTPases can also interact with binding partners to promote different cellular responses. The GDP/GTP cycle is regulated by guanidine nucleotide exchange factors (GEFs) and GTPase activating proteins (GAPs). Moreover, guanidine nucleotide dissociation inhibitors (GDIs) also regulate the cycle for Rho and Rab proteins [153,154]. Binding affinities of small GTPases to GDP and GTP are within the picomolar range and

present a very slow off-rate. So, the rate of GDP to GTP exchange is intrinsically very slow. Therefore, GEFs catalyze the switch from GDP to GTP, producing the active form of the small GTPase, while GAPs promote the inactivation of the small GTPase, by catalyzing the hydrolysis of GTP into GDP. Lastly, GDIs sequester the GDP-bound form of Rhos and Rabs, which prevents the dissociation of GDP and, consequently, keep the small GTPases inactive (Figure 12)[152–154].

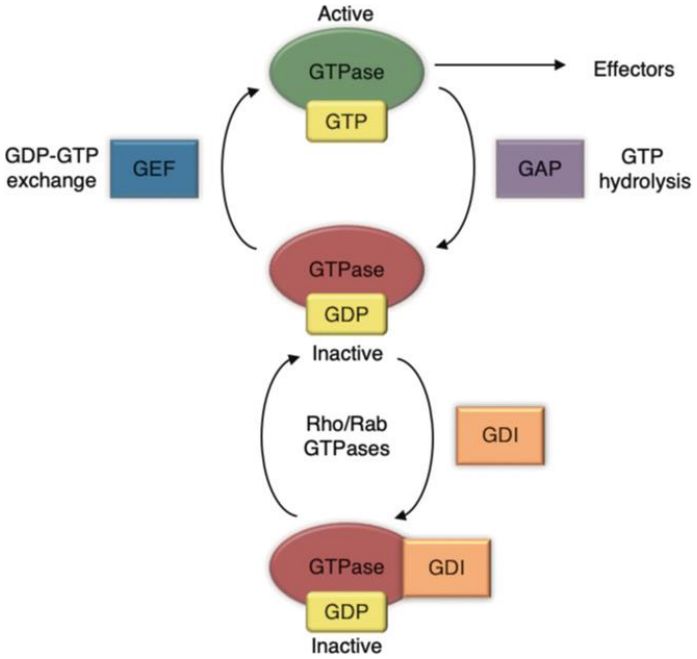

Figure 12 - Activation and inactivation of small GTPases. Small GTPases from the Ras superfamily cycle between an active GTP-bound state and an inactive GDP-bound state. Active GTP-bound GTPases bind to effectors to regulate various cellular processes. The GDP/GTP cycle is regulated by guanidine nucleotide exchange factors (GEFs), which catalyze the exchange of GDP by GTP and GTPase activating proteins (GAPs), which promote the hydrolysis of GTP by GDP. Rho and Rab small GTPases can also be kept in an inactive GDP-bound form by guanidine nucleotide dissociation inhibitors (GDIs), which sequester the protein bound to GDP and prevent its activation. Adapted from [152].

1.4.2.1. Arf family

All the members of the Arf family share a canonical G domain with nucleotide-sensitive loops (switch 1 and 2)[155,156]. Furthermore, Arf GTPases need to be recruited to membranes to be activated. Specifically, these proteins are recruited to the membrane via an N-terminal amphipathic helix in the GDP-bound state. After GDP to GTP GEF-mediated exchange, there is conformational rearrangement, which allows the insertion of a lipidic post-translational modification (*e.g.,* myristoylation, acetylation, or palmitoylation on the N-terminal) into the lipid bilayer, stabilizing the GTPase-membrane binding [156,157].

As mentioned before, Arfs are key regulators of membrane traffic [151]. In mammals, the Arf family includes around 30 proteins, comprising six Arfs (Arf1, Arf2, Arf3, Arf4, Arf5, and Arf6), 22 ARF-like (Arl) proteins, two Secretion-Associated RAS-related (Sar) and the TRIpartite Motif-containing protein 23 (TRIM23) (Figure 13) [156]. The six members of the Arf subfamily (five in humans since we lack Arf2) are highly conserved in structure and sequence. Based on sequence similarities, these proteins have been classified in three types: type I (Arf1-Arf3), which share more than 96 % sequence identity; type II (Arf4 and Arf5), which share 90% sequence identity; and type III (Arf6), which shares more than 65% sequence identity to type I and II Arfs [158]. Furthermore, these proteins can have overlapping localizations and similar functions within the cell. Arf1-5 have been more associated with the recruitment of coat proteins and vesicle formation in the Golgi apparatus [159,160]. On the other hand, Arf6 is the only Arf that does not localize to the Golgi, and can be found at the PM and in endosomes, where it regulates endosomal recycling and cortical actin dynamics [161]. The two Sars (Sar1a and Sar1b) are also highly identical, sharing around 90% of sequence identity. These two proteins localize to the ER and are essential players in ER-to-Golgi traffic, through the regulation of COPII-vesicle budding [156,162]. Finally, TRIM23 is implicated in antiviral defense by regulating autophagy and adipocyte differentiation [163,164]. Regarding sequence homology, ARLs are more divergent than Arfs or Sars, sharing between 40 % and 60 % of identity among them. These proteins also localize to several places within the cell and present more diverse cellular functions, which in some cases are parallel to Arfs [156]. In the next sections, a description of the main functions of each Arl protein is presented and is divided according to their main localization/function within the cell - Golgi, cilia, associated with cytoskeleton, and lysosomes). The described information is also summarized in Table 2. Arl5c, Arl10 and Arl13a were excluded from this description, since nothing is known about the function and localization of this small GTPase.

1.4.2.1.1. ARLs in the Golgi

Arl1 is the member of the Arl subfamily that presents higher sequence homology with Arfs. This protein localizes to the TGN, and it interacts with different proteins (*e.g.,* golgins and arfaptins) at this location regulating the secretion of different cargo, including insulin, chromogranin A and MMPs [156,165–168]. It can also be found in EEs, where it regulates the activation of Arf1 and Arf3 [169].

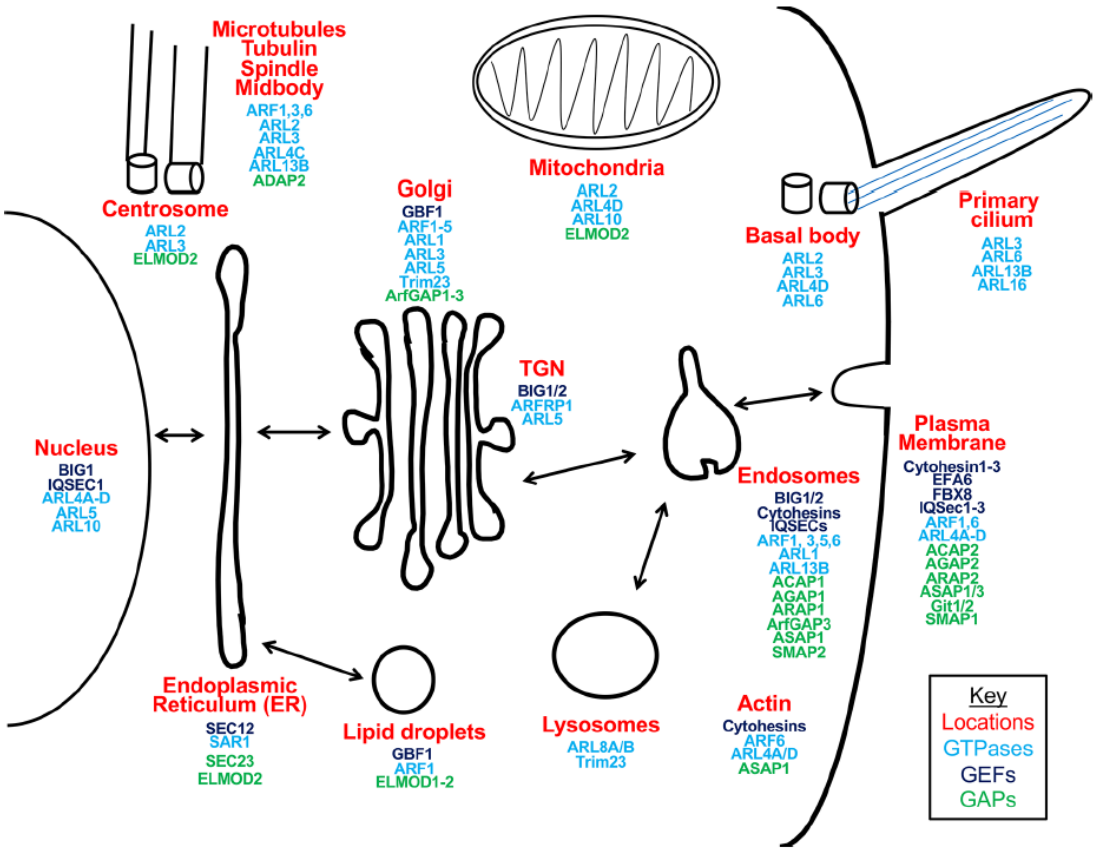

Figure 13 - Localization of ARF small GTPases, ARF GEFs, and ARF GAPs in the cell. Schematic representation of the cell with organelles (red), where the subcellular localization of ARF small GTPases (light blue), ARF GEFs (purple), and ARF GAPs (green) is depicted. Adapted from [156].

Arl5 presents three paralogs - Arl5a, Arl5b, and Arl5c (proposed to be a pseudogene). These proteins also localize to the TGN and Arl5 was found to regulate retrograde traffic from endosomes to Golgi, by recruiting the Golgi-associated retrograde protein (GARP) complex [170,171].

Arl15 (also known as ARFRP2) and has been extensively associated with metabolic disorders, including obesity in children, coronary heart disease, and type II diabetes [172]. Recently, Arl15 was shown to be localized to the Golgi and upregulated upon insulin stimulation[173]. This protein also regulates adipocyte differentiation in a process dependent on palmitoylation of this small GTPase, which is important for its Golgi localization [174].

Arf-related protein 1 (Arfrp1), previously known as Arl18, also localizes to the TGN. This small GTPase has been linked with the traffic of various cargo, such as glucose transporters and E-cadherin [175,176]. Furthermore, recent studies have shown that Arfrp1 regulates the recruitment of tethering factors to the TGN, through the recruitment of Arl1 and Arl5. In particular, this protein is involved in the recruitment of golgins (dependent on Arl1) and GARP (dependent on Arl5) (Figure 14) [177].

Table 2 - Localization and function of ArL small GTPases. TGN - trans-Golgi network, EEs - early endosomes, PM- plasma membrane, LEs - late endosomes, CDRs - circular dorsal ruffles, LPS - lipopossacharide, MHC - major histocompatibility complex II.

GTPase	Localization	Main function (s)
Arl1	Golgi, TGN, EEs	Endosome–Golgi secretory traffic
Arl2	Cytosol, mitochondria	Tubulin heterodimer assembly, mitochondrial motility/fusion
Arl4a	Cytosol, PM	Actin remodeling
Arl4c	Cytosol, PM	Cholesterol efflux
Arl4d	Cytosol, mitochondria, nucleus, PM, actin	Actin remodeling, regulation of mitochondrial function/morphology
Arl5a	Golgi	Endosome–Golgi traffic
Arl5b	Golgi	Endosome–Golgi traffic
Arl6	Cilia	Retrograde cilia transport
Arl8a	LEs/Lysosomes	LEs/Lysosomal traffic
Arl8b	LEs/Lysosomes	LEs/Lysosomal traffic
Arl9	n/a	Genetic links to visual system (*Xenopus*) and Vitiligo
Arl11	Nucleus, cytosol, cortical actin	LPS-induced macrophage activation
Arl13b	Cilia, CDRs	Cilia formation/maintenance Hh signaling, formation of CDRs
Arl14	Multi-vesicular bodies	MHC II transport along the actin cytoskeleton
Arl15	Cytosol, Golgi	Adipocyte differentiation
Arl16	Cilia	Golgi-cilia traffic
Arfrp1	TGN	TGN traffic

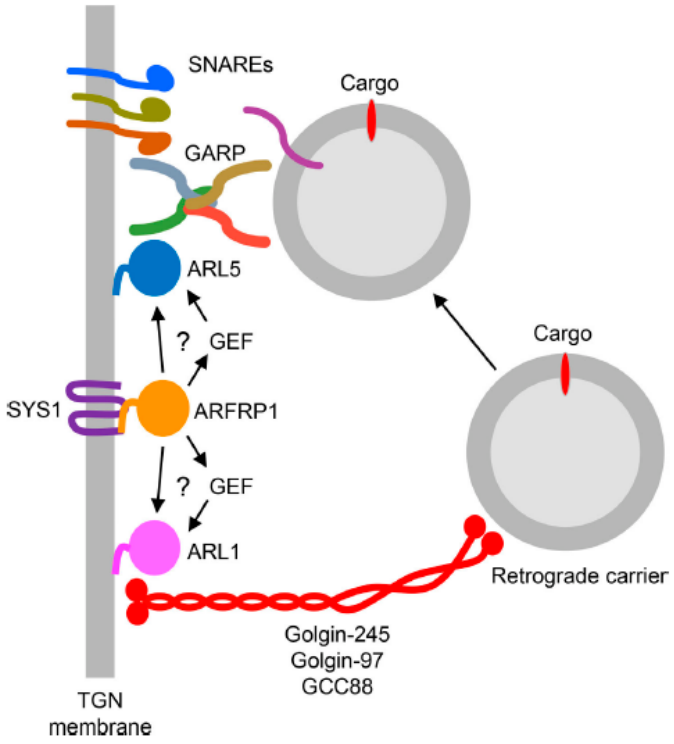

Figure 14 - ARFRP1-mediated recruitment of ARL1 and ARL5 to the trans-Golgi network. SYS1 recruits ARFRP1 to the TGN. Afterward, ARFRP1 promotes the recruitment and/or activation of ARL1 and ARL5 to the TGN. Activated ARL1 and ARL5 interact with the TGN membrane through the myristoylated N-terminal amphipathic helix. Then, ARL1 recruits Golgin-245, Golgin-97, and GRIP and coiled-coil domain containing 88 kDa (GCC88), which bind retrograde transport carriers loaded with cargo, while ARL5 recruits the GARP complex. Golgins go through a conformational collapse that transports the carriers closer to the TGN and enables their transfer to the GARP complex. GARP in turn stimulates the assembly of the *trans*-SNARE complex and fuses the carrier to the TGN membranes, leading to the delivery of the cargo to the TGN [177].

1.4.2.1.2. ARLs in cilia

Arl3, Arl6, Arl13b, and Arl16 localize to primary cilia, which are cellular structures that act as sensors of various extracellular stimuli [156]. Specifically, depletion of Arl3 in mammalian cells leads to an impairment of ciliary transport [178,179] and Arl16 was found to regulate the traffic of intraflagellar transport 140 (IFT140) and inositol polyphosphate-5-phosphatase E (INPP5E) from the Golgi to the cilia [180].

Arl6, was the first Arl to be linked to an autosomal recessive ciliopathy, namely Bardet-Biedl syndrome (BBS) [181]. Also, Arl6 regulates the retrograde transport of Sonic hedgehog (Shh) and Wnt in cilia and also promotes the recruitment of the BBSome complex, which controls ciliary traffic [182–184]. Recently, a phylogenetic profile analysis has determined that *ARL6* is almost completely absent from eukaryotic species that do not possess cilia cells or stages [180].

Arl13 presents two paralogs (Arl13a and Arl13b) that only share around 43 % sequence homology [172]. Arl13b differs from the other members of the subfamily because it has almost twice the size and presents an abnormally long C-terminal region [156]. Moreover, and probably due to its distinctive structure, it is the only Arl that was reported to act as a GEF (for Arl3) [185,186]. Studies in zebrafish and mice revealed that the depletion of Arl13b results in defects in cilia structure and signaling. Namely, the mutant mice revealed many of the typical phenotypes presented by Joubert Syndrome (JS) patients. Moreover, the cilia of the mutant mice are shorter and present defects in Shh and bone morphogenic protein (BMP) signaling pathways in combination with overexpression of Wnt ligands [187,188]. Activated Arl13b was also found to bind to subunits of the exocist complex (Sec5 and Sec8) and regulate cilia function [189]. Recently, tubulin was found to interact directly to Arl13b, to promote an even distribution of this small GTPase throughout the membrane of the cilia [190]. Furthermore, Arl13b regulates the formation of circular dorsal ruffles (CDRs) and, consequently cell migration, through the interaction with the actin cytoskeleton. This interaction is mediated by the non-muscle myosin IIA (NMIIA), which was identified as an effector of Arl13b [191]. The role of Arl13b in cell migration was also demonstrated in interneurons and fibroblasts of mutant mice, through cilia-dependent mechanisms [192,193]. The function of Arl13a remains unknown.

1.4.2.1.3. ARLs associated with the cytoskeleton

Arl2 is highly conserved, and it was shown to interact with tubulin-specific chaperone D (TBCD), which in turn mediates the interaction with β-tubulin. This interaction is necessary for the αβ-tubulin biogenesis and microtubule dynamics [194,195]. Arl2 was also found to localize to mitochondria, where it regulates mitochondrial motility, fusion, and ATP levels, through the interaction with its GAP ELMOD2 [196,197].

Arl4 has three paralogs (Arl4a, Arl4c, and Arl4d), which present a distinct extended C-terminal region with basic amino acids, allowing the binding to importin-α. Therefore, the C-terminal region works as a nuclear localization signal [172,198]. All three paralogs were found to localize to the PM, with some accumulation of Arl4d in the nucleus [172]. These proteins also promote the recruitment of the GEF Arf nucleotide-binding site opener (ARNO) to the PM, where it activates Arf6, which has a role in actin remodeling, endocytosis, and cell adhesion [199]. Besides ARNO (also known as cytohesin-2), Arl4 paralogs also recruit other ARF GEFs to the PM, including cytohesin-1,

cytohesin-3, and cytohesin-4 [172,199]. Arl4a also controls actin dynamics via the interaction with ELMO, which controls actin cytoskeleton remodeling through DOCK-180 and Rac signaling pathways [200]. Arl4c (previously known as ARL7) shares a 71 % amino acid sequence identity with Arl4a [172]. Further studies revealed that Arl4c is involved in the liver X receptor (LXR)-dependent cholesterol efflux [201]. This small GTPase was also found to interact with α-tubulin and to play a role in transferrin receptors transport from EEs to recycling endosomes [202]. The third paralog, Arl4d shares 59% identity with Arl4c, and it localizes to the PM in its active GTP-bound state. However, when bound to GDP, Arl4d localizes to mitochondria, where it regulates the function and morphology of this organelle [172,203].

Originally, *ARL11*, which is also named ADP-ribosylation factor-like tumor suppressor gene-1 (*ARLTS1*), was described as a tumor suppressor gene [204]. However, the information about its cellular function is scarce. A recent publication points out that Arl11 localizes to the nucleus, cytosol, and cortical actin [205]. In the same study, the authors found that Arl11 is essential for lipopolysaccharide (LPS)-induced macrophage activation, through interaction with phosphorylated extracellular signal-regulated kinase (ERK) 1/2 on actin structures [205].

1.4.2.1.4. ARLs on lysosomes

Arl8 contains two paralogs, and it is localized to lysosomes. Arl8a and Arl8b share 91 % sequence identity and lack a glycine residue, essential for myristoylation. In the case of Arl8a, the glycine is replaced by isoleucine, while in the case of Arl8b it is replaced by leucine [206]. These modifications allow the acetylation of the N-terminal methionine, which together with the presence of hydrophobic residues in the amphipathic helix is crucial for the lysosomal localization of Arl8a and Arl8b [206,207]. Although both paralogs localize to the same organelle, the biological functions of Arl8a are still poorly understood. Also, it is not known if both paralogs have redundant functions and if the loss-of-function of one is compensated by the other. Arl8b is recruited to the lysosome membrane by the BLOC-one-related complex (BORC) and mediates the kinesin-dependent movement of lysosomes towards the cell periphery (anterograde movement). It has also been shown that the Sif-A and kinesin-interacting protein (SKIP) acts as a downstream effector of Arl8b and this interaction results in the recruitment of kinesin-1 to lysosomes [208,209]. Moreover, Arl8a/b were shown to regulate the anterograde movement of lysosomes by direct interaction with kinesin-3 [210]. Lysosomal movement along microtubules is also regulated by the homotypic protein sorting

(HOPS) complex, which was found to be an effector of Arl8b. In mammalian cells, Arl8b binds to the HOPS subunit Vps41 and promotes the interaction between HOPS and the lysosomal membrane. Furthermore, Arl8bB effector SKIP was shown to recruit another subunit of HOPS – Vps39, to lysosomes [211]. On the other hand, Rab7 which localizes to LEs was shown to regulate the retrograde movement of lysosomes (towards the perinuclear region). In this case, Rab7 effector Rab-interacting lysosomal protein (RILP) binds to both the HOPS complex and dynactin (dynein adaptor), promoting the movement of LEs/lysosomes to the perinuclear region [206,212]. Curiously, two very recent reports showed evidence that Arl8 also regulates long-range endolysosomal retrograde movement. In these studies, two new Arl8a and Arl8b effectors are described – RUN and FYVE domain-containing protein (RUFY) 3 and RUFY4. RUFY3 recruits the JIP4-dynein-dynactin complex and mediates the movement of lysosomes towards the perinuclear region, while RUFY4 was also shown to interact with dynein-dynectin [213,214]. So, these new findings add a new layer of complexity to the regulation of endolysosomal movement and positioning by Arl8a and Arl8b (Figure 15).

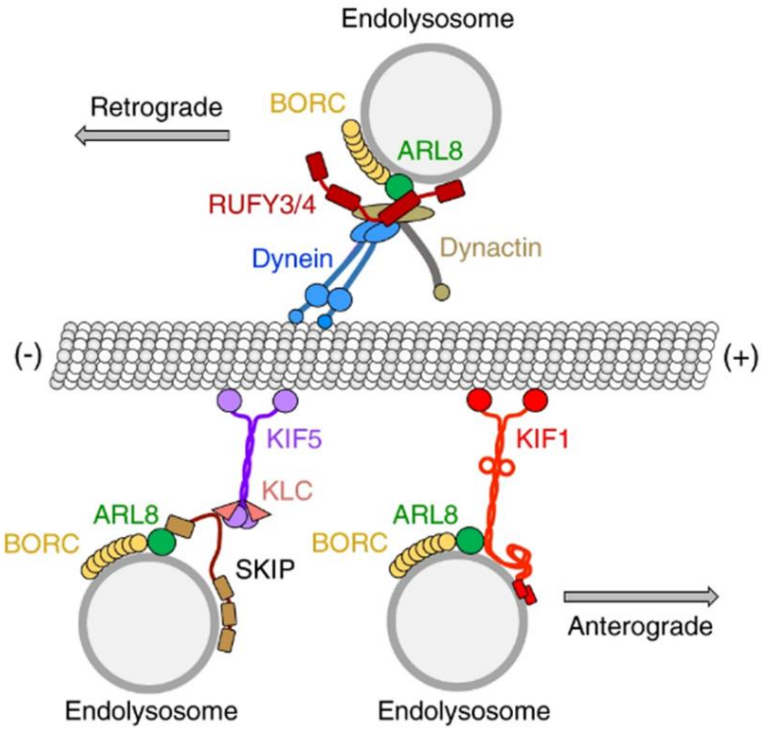

Figure 15 - ARL8 regulates the anterograde and retrograde movement of endolysosomes. ARL8 is recruited to endolysosomes by BORC. ARL8 then recruits RUFY3 and RUFY4, which bind to dynein-dynectin, promoting the transport of endolysosomes from the plus end to the minus end of microtubules (retrograde movement). On the other hand, ARL8 binds to its effector SKIP and recruits kinesin-1 ($KIF5_2$-KLC_2). Also, ARL8 can bind directly to kinesin-3 (KIF1). Binding to both kinesins promotes the movement of endolysosomes towards the cell periphery (anterograde movemen)t. Adapted from [213].

1.4.2.1.4.1. Lysosome exocytosis

Lysosomes are characterized by an acidic luminal pH and are responsible for the degradation of intracellular and extracellular cargo. Moreover, lysosomes contain around 60 hydrolases within their lumen, which digest all cellular macromolecules, including proteins, lipids, and nucleic acids. The digested products are then transported to the cytoplasm where they are used to fulfill different cellular needs. Besides their intracellular role, lysosomes can also release their content extracellularly, through lysosomal exocytosis [215].

Lysosome exocytosis is defined by the release of lysosomal enzymes to the extracellular space. For this, lysosomes are transported from the perinuclear region to the cell periphery, where they fuse with the PM and secrete their contents [216]. Exocytosis of lysosomes, which is generally regulated by Ca^{2+}, is often associated with two main processes – membrane remodeling and secretion. PM repair requires a localized release of Ca^{2+}, which promotes lysosomal fusion with this structure. This allows the replacement of the damaged membrane with the lysosomal membrane [217]. Moreover, lysosome exocytosis leads to the secretion of enzymes that promote the endocytosis of the damaged membranes and consequently, complete the process of repair [218]. Secretion of lysosomal enzymes has been associated with several biological functions in different cell types. For example, bone resorption by osteoclasts is affected by impaired lysosomal exocytosis [219]. Also, lysosomal enzymes released by immune cells promote the digestion of pathogens, linking lysosomal exocytosis to immune defense [220].

The link between lysosome exocytosis and disease is also very important. Several studies have highlighted that the secretion of lysosomes is especially relevant in cancer progression. As previously explained, invasive cancer cells require the formation of invadopodia. Lysosome exocytosis has been proposed to be as required for cell invasion since it promotes the release of hydrolases to degrade/remodel the ECM and participate in membrane remodeling involved in protrusion formation [221]. Lysosome exocytosis is also relevant in anticancer drug resistance since the drugs are sequestered by lysosomes, and then released to the extracellular medium without reaching their initial intracellular target [222].

1.4.2.1.5. Arl9 and Arl14

For some members of the Arl subfamily, very little information is known about their localization and function within the cell. In Xenopus, *arl9* was described as a neurogenic gene important for the development of the visual system [223]. Moreover, a genetic study showed that *ARL9* is associated with a chronic skin disease (Vitiligo) [224]. However, no studies regarding the physiological role of this small GTPases have been conducted.

Arl14 was described to colocalize with phosphatidylinositol-4-phosphate 5-kinase Type 1 alpha (PIP5K1A) and localize to the multi-vesicular bodies. In this study, the authors found that pleckstrin and sec7 domain containing 4 (PSD4) acts as a GEF to activate Arl14, which in turn recruits Arf7 effector protein (ARF7EP). ARF7EP binds to myosin-1E and regulates the transport of major histocompatibility complex (MHC) class II along the actin cytoskeleton [225].

1.4.2.1.6. ARLs in cancer

Members of the ARL sub-family have been associated with different types of pathologies, including cancer. Several reports describe that many ARLs present an altered expression in different types of cancers. Moreover, the mechanistic insights on how some ARLs promote and/or inhibit carcinogenic progression, have been documented in different studies [226,227].

Although there are no studies about the functional role of ARL1 in cancer, a bioinformatics study revealed that this gene is upregulated in cutaneous melanoma [228].

On the other hand, ARL2 has been involved in different types of cancer, both in promoting tumorigenesis or inhibiting it. In pancreatic cancer cells, active ARL2 binds to binder of ARL2 (BART), which in turn inhibits the ARL2-mediated inhibition of RhoA, leading to a decrease in cancer cell invasiveness [229]. Recently, it was found that ARL2 is required for homologous recombination in the nucleus, which is involved in colon cancer stem cell population maintenance [230]. *ARL2* was also found to be upregulated in both tumor samples and cell lines in hepatocellular and cervical cancers, as well as in osteosarcoma cell lines [231–233]. Also, several microRNAs (miRs) have been proposed to impair cancer progression by targeting ARL2. One example is the miR-195, which is regulated by Urothelial Cancer Associated 1 (UCA1). *In vivo* studies using mouse models revealed that bladder tumor size is reduced upon UCA1 silencing and the expression of miR-195 is increased, which leads

to ARL2 downregulation. The phenotype mediated by UCA1/miR-195/ARL2 in bladder cancer cells was found to be caused by defects in mitochondrial metabolism, which is regulated by ARL2 [234]. The role of ARL2 in colorectal cancer is not very clear. While the protein levels are increased in tumor samples when compared to normal samples, the depletion of this small GTPase leads to increased proliferation, migration, and invasion, suggesting an inhibitory role for ARL2 in this type of cancer [235]. Moreover, in glioma samples, ARL2 expression was found to be decreased when compared with normal samples. Also, ARL2 downregulation was associated with poor prognosis of glioma patients, while the overexpression of this protein decreases proliferation, migration, and tumorigenicity of glioma cells, by regulating the receptor tyrosine kinase AXL [236].

Protein and mRNA levels of ARL3 were shown to be decreased in gliomas. In the same study, bioinformatics analysis suggested that ARL3 is involved in angiogenesis and immune cell infiltration in tumors [237].

ARL4C was shown to be upregulated and regulate tumorigenic progression in several types of cancers including colorectal, lung, lung and tongue squamous, gastric, hepatocellular, pancreatic, renal cell carcinomas, as well as leiomyosarcoma type II [238–244]. In colorectal and lung cancers, ARL4C downregulation leads to a decrease in cell proliferation, migration, and invasion *in vitro*, as well as tumor growth *in vivo*, through a mechanism dependent on Wnt/β-catenin and EGF/RAS signaling pathways [238]. Also, ARL4C overexpression was associated with a poor prognosis in patients with endometriosis-associated ovarian cancer and PTEN-deficient glioblastomas [245,246]. Furthermore, in gastric cancer cells, ARL4C silencing results in a decrease of the EMT marker SLUG, as well as a reduction in lamellipodia and filopodia formation [240]. ARL4C was also found to regulate EMT functioning as a downstream effector of the Wnt/ β-catenin signaling pathway in clear cell renal cell carcinoma [247]. Upregulation of ARL4C in pancreatic cancer cells promoted an invasive behavior of these cells and it was also associated with self-renewal, stemness, and drug resistance in this type of cancer [248]. On the other hand, ARL4C was associated with a reduction in metastasis formation in ovarian cancer cells, by inhibiting cell motility. Curiously, in this study, the authors found that ARL4C low expression is associated with poor treatment response by ovarian cancer patients [249].

ARL4D was initially identified as a glioma-associated antigen [250]. A few years later, ARL4D expression in gliomas was found to be dependent on PTEN tumor suppressor loss, which leads to the activation of the Akt/mammalian Target of Rapamycin (mTOR) pathway [251]. Recently, *ARL4D* mRNA levels were found to be upregulated on an oral cavity squamous cell carcinoma cell line [252].

ARL5A was found to be highly expressed in colorectal cancer and a target of miR-202-3P, which regulates colorectal cancer cell proliferation [253]. In the case of ARL5B, it was recently found to be overexpressed in ovarian cancer cells and targeted by miR-145, which in turn regulates mitochondrial metabolic reprogramming in these cells [254].

A study from 2016 described the role of ARL6 in rhabdomyosarcoma. It was found that ARL6 is upregulated in cilia-dependent cancer cells and that the downregulation of this protein leads to a decrease in cell proliferation and increased apoptosis of rhabdomyosarcoma cancer cells, caused by impairment of ciliogenesis and Hh signaling [255].

In prostate cancer cells, ARL8B silencing leads to a decrease in invasion and protease secretion, as well as tumor growth in mice. Moreover, the mechanisms by which ARL8B regulates prostate cancer progression were found to be dependent on the regulation of lysosomal movement and protease secretion, leading to ECM degradation and cell invasion, as well as lipid metabolism regulation to sustain cell proliferation [256].

ARLTS1 (*ARL11*) was initially described as a potential low-penetrance tumor suppressor gene in different types of cancers, including melanoma and chronic lymphocytic leukemia [204]. Moreover, different variants of *ARLTS1* have been linked to familial and sporadic cancers and the mutations Trp149Stop and Cys148Arg are the best characterized [257]. One of them, Trp149Stop, is a nonsense mutation that results in the production of a truncated protein that cannot bind to GTP, leading to decreased apoptosis in these cells [258]. Both Trp149Stop and Cys148Arg variants were found to be associated with hematological tumors [259]. Also, melanoma and both familial and sporadic forms of colorectal cancers were associated with the variant Cys148Arg [260,261]. *ARLTS1* expression was also found to be downregulated in ovarian, lung and prostate cancers, as well as chronic lymphocytic leukemia [257,262]. Finally, a study on ovarian cancer revealed that ARLST1 increases cancer cell sensitivity to chemotherapeutic agents, through the regulation of apoptosis [263].

In 2018, two studies described the cilia-dependent role of ARL13B in the progression of medulloblastoma and gastric cancer [264,265]. Bay and his team showed that ARL13B depletion in medulloblastoma cells leads to a decrease in oncogenic hedgehog (Hh) signaling [264]. Moreover, *in vitro,* and *in vivo* experiments suggested that ARL13B promotes cell proliferation, migration, and invasion of gastric cancer cells, via activation of Smoothened, which in turn activates Hh signaling [265]. More recently, it was shown that ARL13B interaction with purine biosynthetic enzyme inosine-50-monophosphate dehydrogenase 2 (IMPDH2) leads to epigenetic modifications of the small GTPase, and consequently, to temozolomide resistance in glioblastoma cells [266].

ARL14 was shown to be involved in lung adenocarcinoma cell proliferation. Specifically, the downregulation of *ARL14* blocks ERK1/2 and p28 signaling and leads to cell cycle arrest by upregulating the cell death inducing DFFA-like effector C (CIDEC) [267]. Furthermore, ARL14 protein levels were found to be increased in non-small cell lung cancer and this higher expression was correlated with poor survival of the patients [268]. A poor prognosis of bladder cancer patients was found to be associated with the hypermethylation of *ARL14* [269].

In the case of ARFRP1, it was found to be upregulated in gastric cancer [270].

1.4.2.1.6.1 ARLs in breast cancer

There are only a few studies linking the expression and function of ARLs to the development and progression of BC. A recent study describes that *ARL1* is downregulated in TNBC samples that are positive for carbonic anhydrase IX (*CAIX*), a hypoxia-related gene [271].

In the case of ARL2, it was shown to regulate α/β-tubulin polymerization in the BC cell line MCF-7. It was also shown that a lower expression of ARL2 in MCF-7 cells leads to enhanced resistance to cytotoxic agents [272,273]. This ARL2-mediated mechanism of resistance is also regulated by Protein Phosphatase 2A (PP2A), which fails to dephosphorylate p53 when ARL2 expression is low [273]. A follow-up study by the same group showed that ARL2-depleted BC cells have less contact inhibition, enhanced clonogenic potential, and proliferation, as well as impaired tumor growth in experiments using orthotopic mouse models [274]. Therefore, these studies strongly suggest that ARL2 expression impairs BC progression.

ARL4C was shown to be downregulated in BC samples. Furthermore, the low levels of ARL4C in BC correlates to those of the activated transcription factor 3 (ATF3). The authors also found that ATF3 promotes the transcription of *ARL4C,* which in turn acts as a negative regulator of tumor progression in BC. Indeed, the overexpression of ARL4C was shown to decrease BC cell proliferation, migration, and invasion, leading to cell cycle arrest [275].

ARL8A and ARL8B were found to be upregulated in both luminal A and TNBC cell lines, upon silencing of TBC1 domain family member 9 (TBC1D9), which is associated with negative regulation of TNBC progression [276]. Moreover, a previous study from the same group had identified ARL8A as a binding partner of TBC1D9 [277]. A recent publication by Wu *et al.*, showed evidence that the lysosomal movement mediated by ARL8B and its interacting partner BORC promotes the invasion

of radiation-surviving BC cells [278]. In this study, the authors found that there is a higher activation of ARL8B in invasive BC cells that survived ionizing radiation treatment. Moreover, this process seems to be regulated by BORC, which recruits ARL8B to lysosomes. The recruitment and activation of ARL8B leads to binding to the effector SKIP and increased BC cell invasion *in vitro*, as well as tumor metastasis *in vivo*, through lysosome exocytosis and consequent release of ECM-degrading proteases [278].

As previously mentioned, *ARL11* is known as a tumor suppressor gene in different cancers. This is also the case in BC, where the Trp149Stop and Cys148Arg were associated with familial cases of this malignancy [257,279].

A recent publication from our group has shown evidence suggesting a role for ARL13B in BC progression, through a mechanism likely independent of cilia [280]. In this study, the silencing of *ARL13B* in BC cells resulted in impairment of both cell migration and invasion *in vitro*, as well as decreased tumor growth and metastasis *in vivo*. Furthermore, a new mechanism of tumor progression regulation by ARL13B was revealed. Specifically, we found evidence that ARL13B promotes BC cell migration and invasion through the regulation of cell-ECM adhesion, mediated by integrin-dependent signaling [280].

In summary, emerging evidence show that members of the ARL subfamily of small GTPases are important for cancer development, including BC. However, further studies need to be conducted to unravel the molecular mechanisms that are regulated by ARLs and subverted by cancer cells to promote tumor progression.

Objectives

Despite all the efforts to find better therapeutic options and the significant improvement in diagnostic techniques that are currently available, BC is still the leading cause of cancer mortality in women. So, there is an unmet need to find better therapeutic options to impair the progression of BC and the formation of metastases, which represents the main cause of death. To achieve this, it is essential to have a deeper understanding of the mechanisms that are involved in BC progression and that cancer cells subvert to be able to proliferate, migrate and invade surrounding tissues, overcoming the barriers imposed by the microenvironment.

Several studies have highlighted the role of membrane traffic in cancer progression. In fact, many known regulators of membrane traffic are involved in the tumorigenesis of different malignancies, including BC. Among these regulators, proteins from the ARF family have been linked to different types of cancers, where they can regulate several steps of the tumorigenic process. Moreover, there is already much evidence linking members of the ARF subfamily to BC progression, but little is known about the role of ARLs in this disease.

Main objectives and hypothesis

The main objective of this PhD thesis is to identify new players in BC progression and unravel the underlying mechanisms that promote the required tumorigenic features, which can be targeted to impair tumor progression and the formation of metastases. To do this, we focused on the ARL subfamily of proteins and studied their role in BC progression. We hypothesized that different ARLs may be upregulated in BC and positively regulate the progression of this disease, by promoting cell proliferation, migration, and invasion. In the end, we hope that this work contributes to the growing knowledge of the role of ARLs in BC tumorigenesis, aiming to identify candidates that can represent potential therapeutic targets to impair cancer cell invasion and the formation of metastases, a pressing clinical need.

To achieve our main objective, we planned three specific aims:

Specific aim 1 - Assess the expression of ARLs in different breast cancer cell lines and samples.

In this task, we aimed to assess which ARLs are differently expressed in BC. We started by performing a screen to evaluate the mRNA expression levels of all the *ARL* genes by real-time qPCR, using non-tumorigenic cell lines and BC cell lines with different invasive capacities. From this first screen, we selected the most promising candidates to conduct a bioinformatic analysis to assess the expression of *ARL* genes in BC samples using available datasets. Finally, we also conducted a real-time qPCR analysis to evaluate the mRNA levels of *ARL* genes in BC samples.

Specific aim 2 - Determine the role of candidate ARLs in breast cancer cell proliferation, migration, and invasion.

To assess the functional role of ARLs in BC progression, we selected candidates from the results obtained in specific aim 1 and modulated their expression in BC cell lines. Specifically, we aimed to unravel the role of these candidates on BC cell proliferation, migration, and invasion, using 2D and 3D *in vitro* assays.

Specific aim 3 - Determine the role of ARL8 and lysosome exocytosis in breast cancer progression

It is well established that ARL8 is a lysosomal marker that regulates lysosome positioning, and more specifically the movement of these organelles to the cell periphery. Also, it is known that lysosome positioning and exocytosis are involved in cancer progression. Therefore, we aimed to assess the role of ARL8A and ARL8B in BC cell proliferation, migration, and invasion. Furthermore, we also analyzed whether the modulation of ARL8B expression affects lysosome exocytosis in BC cells. Finally, we aimed to determine whether ARL8B impairs EMT on invasive BC cell lines.

Chapter 2. Materials and Methods

2.1. Cell culture

2.1.1. Cell culture in 2D

All human cell lines were cultured at 37 ºC and 5 % CO_2, in a humidified incubator. MCF10A cells were a kind gift from Dr. Florence Janody (i3S, Oporto, Portugal) while MCF10DCIS.com were obtained from Barbara Ann Karmanos Cancer Institute (Wayne State University, Detroit, USA). MCF10DCIS.com cells were maintained in high calcium medium – Dulbecco's Modified Eagle Medium/ Nutrient Mixture F-12 (DMEM/F12) GlutaMAX (Gibco), 5 % (v/v) horse serum (Sigma-Aldrich), 10 mM HEPES (Gibco), 1.05 mM calcium chloride ($CaCl_2$, Sigma) 100 U/mL penicillin, 100 µg/mL streptomycin (Pen/Strep, GIBCO). MCF10A were cultured in high calcium medium supplemented with 20 ng/mL EGF (Sigma), 10 µg/mL insulin (Gibco), 0.5 µg/mL hydrocortisone (Sigma-Aldrich), 100 ng/mL cholera toxin (Sigma-Aldrich). MCF-7 and MDA-MB-231, kindly provided by Dr. Gabriela Silva (iBET, Lisbon, Portugal), and HEK-Star-Rdpro cells, a gift from Dr. José Ramalho (NOVA Medical School, Lisbon, Portugal), were maintained in DMEM complete medium – DMEM, 10 % (v/v) fetal bovine serum (FBS, Gibco), 5 mM GlutaMAX (Gibco), 15 mM HEPES and Pen/strep. Finally, HCC1806 cells, provided by Dr. Catarina Brito (ITQB/iBET, Lisbon, Portugal) and BT-474 (ATCC) were cultured in RPMI complete medium - Roswell Park Memorial Institute (RPMI) GlutaMAX medium (Gibco), 10 % (v/v) FBS, 0,6 % (v/v) HEPES and Pen/Strep.

2.1.2. Spheroid formation

Spheroids were formed using two approaches: agarose-coated plates and ultra-low attachment (ULA) plates. In the first approach, MDA-MB-231 cells were seeded in 96-well round-bottom tissue culture plates (TPP) coated with 1.5 % agarose (SeaKem), at 1000 cells/well in 200 µL DMEM complete medium. The next day, 6 µg/mL collagen I, Rat tail (Corning), were added, so that the final concentration of collagen I on each well was 3 µg/mL. Spheroids were allowed to grow for 5 days before use.

In the second approach, cells were seeded on ULA plates, either Nunclon™ Sphera™ 96-well plate (Thermofisher) or BIOFLOAT™ 96-well plate (FaCellitate) at 2000 cells/well (HCC1806 and MDA-MB-231) or 1000 cells/well (MCF10DCIS.com), in 200 µL of the appropriate complete medium.

In the case of *ARFRP1* silenced MDA-MB-231 cells, spheroids were mixed with 0.6 % (w/v) methylcellulose (Sigma), kindly provided by Dr. Ana Cavaco (IMM, Universidade de Lisboa) at 25 % (v/v) in DMEM complete medium. Spheroids were allowed to grow for three days before use.

For *ARL13B* silenced MDA-MB-231 cells, cells were seeded in 100 µL of DMEM complete medium. Then, the plate was centrifuged for 3 minutes at 290 x g, RT, and incubated at 37 ºC, 5 % CO_2, and 95 % humidity. On the following day, 100 µL of DMEM complete medium supplemented with 3 µg/mL collagen I, Rat tail (Corning), so that the final concentration of collagen I on each well was 1.5 µg/mL and the plate was centrifuged for 3 minutes at 100 x g before incubation at 37 ºC, 5 % CO_2, 95 % humidity. After one day, 100 µL of DMEM complete medium were added to each well, and the spheroids were allowed to form for 3 days before use. In all experiments, half the volume of the medium was carefully changed every other day until spheroids were used for other experiments.

2.2. Bioinformatic analysis of human BC samples

The TIMER 2.0 online tool (http://timer.cistrome.org/) [281] was used to assess the expression of *ARL* genes in BC samples and normal adjacent breast tissues, using the GENE_DE module. This analysis included 1093 BC samples and 112 normal adjacent breast tissues available from the TCGA dataset.

2.3. Human BC patient samples

BC samples and the paired adjacent parenchyma tissues were obtained from patients that were not subjected to any treatment. The samples were freshly collected in TRIzol by surgeons at Hospital Beatriz Ângelo, Lisbon, and stored at -80 ºC. This study was approved by the hospital ethics committee and NMS ethics committee and a written informed consent was obtained from each patient. Patient and samples detailed information about molecular subtype, histological evaluation, and stage of BC, are detailed in Table 3.

Table 3 - List of *ARL* genes analyzed and clinicopathological characteristics of breast cancer patient samples.

Number	Genes	Age	BC subtype	Histological grade	ER	PR	HER2	Molecular subtype
1	*ARL1, ARL2, ARL8B, ARFRP1*	n/a	DCIS	n/a	n/a	n/a	n/a	n/a
2	*ARL1, ARL2, ARL8B, ARFRP1*	n/a	IDC	I	+	+	-	LA
3	*ARL1, ARL2, ARL8B, ARFRP1*	n/a	IDC	I	+	+	-	LA
4	*ARL1, ARL2, ARL8B*	n/a	IDC	I	+	+	-	LA
5	*ARL1, ARL2, ARL8B, ARFRP1*	48	IDC	II	+	+	-	LA
6	*ARL1, ARL2, ARL8B, ARFRP1*	n/a	IDC	II	+	+	-	LA
7	*ARL1, ARL2, ARL8B, ARFRP1*	n/a	IDC	II	+	+	-	LA
8	*ARL1, ARL2, ARFRP1*	62	IDC	II	+	+	-	LA
9	*ARL1, ARL2, ARL8B*	60	IDC	n/a	+	+	+	LB

DCIS - ductal carcinoma in situ, IDC - invasive ductal carcinoma, LA - Luminal A, LB - luminal B, n/a - not available

2.4. RNA extraction, complementary DNA synthesis, and quantitative real-time PCR

Total RNA, was extracted from cells, using the Rneasy kit (Qiagen) following the manufacturer's instructions. RNA from human BC patient samples was extracted with TRIzol (Invitrogen), following the manufacturer's instructions, after tissue disruption using a mortar and pestle with liquid nitrogen. RNA extracted from human tissues was treated with DNAseI (Thermo Fisher) to eliminate any contamination with DNA. cDNA synthesis was carried out using the established protocol for Superscript™ II Reverse Transcriptase (Invitrogen). Briefly, 500 ng of RNA were used as a template and mixed with 1 µL Random Primers 3 µg/mL (Roche), 1 µL of deoxyribonucleotide triphosphate (dNTPs) 10 mM mix (Thermo Fisher), and Rnase free water (Qiagen) up to 12 µL and incubated at 65ºC for 5 minutes. Then, 4 µL of 5x First-Strand Buffer, 2 µL of dithiothreitol (DTT), and 1 µL RnaseOUT™ 40 U/µL (Invitrogen) were added to each tube and the mix was incubated at 25ºC for 2 minutes. Finally, 1 µL SuperScript™ II Reverse Transcriptase 200 U/µL was added to each tube and the samples were incubated at 25°C for 15 minutes, at 42 °C for

50 minutes, and 70 ºC for 15 minutes. The synthesized cDNAs were diluted 5x in RNase-free water and stored at – 20 ºC until use.

Quantitative real-time PCR was carried out on a LightCycler 96 system (Roche), using the following protocol: pre-incubation at 95 ºC for 10 minutes; 45 amplification cycles at 95 °C for 10 seconds, 60 °C for 10 seconds, and 72 ºC for 20 seconds; melting at 95 °C for 10 seconds, 65 °C for 1 minute and 97 °C for 1 second. The samples were prepared with the FastStart Essential DNA Green Master kit (Roche), according to the manufacturer's instructions. The sequences of the specific primers used for each gene amplification are listed in Table 4. The quantification of relative mRNA expression was calculated using the LightCycler® 96 Version 1.1.0.1320. software and Glyceraldehyde 3-phosphate dehydrogenase (*GAPDH*) was used as the reference housekeeping gene.

Table 4 - List of primers used for real-time qPCR.

Gene	Primer Forward (5'-3')	Primer Forward (5'-3')
ARL1	AGTCTGTTTGGAACTCGGGAA	AGGTTTTTGTACGTCACCGTCT
ARL2	GCACTGTCCTCTAACGCCAT	TCATCCAGGAGCCAGTCGAT
ARL3	TGAAGAGACGGGTCAGGAAC	GATGAGCACTGGCACACAAC
ARL4A	GTCCAACCTGCCTTCATTTCAG	GTCTTTCCAGCACAGTCCAA
ARL4C	CACCACCTATCACGTCCAGC	CTTGAGGGACTTCCTGCGTT
ARL4D	ACCACTTGACTGAGATGGCG	CTCCTTGAACTTGAGGCGGT
ARL5A	GTTCAATCACCAGGAGCACAA	TCTTGGCCACCAATATCCCA
ARL5B	GGCTGATCTTCGCCAAACTG	CCCTGCATTATCCAGTCCCA
ARL5C	GCCGAAGACCCACTTCTTCA	ATAGCTCCTCCCGAGTGGTC
ARL6	AAAGTGTCTCAGTTGCTGTGTT	GCAAGCCTTCTCCTTTTATGGC
ARL8A	CCGGGAGCATTGGATGAGAA	CAGCAGATCTCTCGGTCCTG
ARL8B	TCAATGTCATCGCGTCAGGT	TGCTTCGAAATCGGGGTTGT
ARL9	TGGCTCAGAGATACCCTCCA	CAGCCAGCTGTGCAATCAAG
ARL10	GCTGGGTCTACAGGCTATCG	AGGCTCTTCAAAGGTGGGTC
ARL11	GTCCTGAACGACCCCAACAT	TAAGCAGCGGAAGTGCATCA
ARL13A	CATGCCGAGTAGAGCCATGT	CGAGGTAGGTGGTAGTTGGC
ARL13B	GTGACTCTTTTGATGGTGGGAC	AGGGTATTCTCCTTGGATTCCC
ARL14	GACATGCCTGGAGCTCTGAC	CACAGCAGGGTTGCACATAC
ARL15	TCTCCGAATAACTGAGGCGT	AGGCCTATGCAAACCAGGTC
ARL16	AAGCACGGAATGTGTCTCCT	GTAAGATTGGTGCCCACCGT
ARFRP1	CGGCTCATGTTCTGGGACTT	GTAGATGACGCCGTGACACT
GAPDH	CATTTCCTGGTATGACAACGA	GTCTACATGGCAACTGTGAG

2.5. Lentiviral production and cell transduction

All shRNAs as well as the empty vector (pLKO.1 puro) were obtained from Broad RNAi Consortium (Cambridge, MA, USA) and the sequences are listed in Table 5. psPAX2 and pCMV-VSGV-G plasmids were a kind gift from Dr. José Ramalho. The plasmids used to overexpress ARL8B-Flag and Glutathione S-transferase (GST)-Flag were obtained from GenScript. Briefly, ARL8B and GST cDNAs were cloned into pGenLenti vector using AsiSI and BsiWI restriction enzymes. Finally, mcherry and ARL13B-mcherry were cloned into pLenti6/V5-DEST in-house by a former lab member with the help of Dr. José Ramalho (NMS Research). To produce lentiviral particles carrying the above-listed plasmids, HEKStar Rd-pro cells were used. In brief, 9 x 10^5 cells were seeded in 6 cm^2 plates in DMEM complete medium without antibiotics. On the next day, cells were transfected with a 3-plasmid mix containing 0.9 µg of packaging plasmid (psPAX2), 0.1 µg of envelope plasmid (pCMV-VSV-G), and 1 µg of the target expression vector (pLKO.1, pGenLenti or pLenti6/V5-DEST) using Fugene 6 (Promega) transfection agent diluted in Opti-MEM (Gibco). After 22 hours, DMEM complete medium with 30% FBS was added to the cells to boost lentiviral particle production. Lentiviral particles were harvested from the cell supernatant 40 hours and 60 hours post-transfection, pooled together. After a centrifugation at 1250 rpm for 5 minutes, to remove cell debris, lentiviral particles were stored at - 80ºC in small aliquots.

For cell transduction, 1.5 x 10^5 MDA-MB-231, MCF-7 and HCC1806 cells/well or 3 x 10^5 MCF10DCIS.com cells/well were plated in 6-well plates. When cells achieved 50% - 60% confluency, they were transduced with lentiviral particles in the appropriate complete medium without antibiotics and supplemented with 8 µg/mL polybrene (hexadimethrine bromide, Sigma Aldrich). Twenty-four hours post-transduction, the medium was changed to selection medium – complete medium supplemented with puromycin (pLKO. 1 and pGenLenti) (Gibco) or blasticidin (pLenti/V5-DEST) (Gibco). The antibiotic concentrations used for each cell line are summarized in Table 6 Transduced cells were selected at least for 5 days before performing functional assays and gene silencing efficiency was evaluated by real-time qPCR.

Table 5 - List of shRNA target sequences used for gene silencing.

Gene	Accession number	Hairpin	Clone ID	Target sequence (5'-3')
ARL1	NM_001177.6	1 (G3)	TRCN0000048060	GCCTTGATGAGGCAATGGAAT
		2 (G5)	TRCN0000048062	GAACTCGGGAAATGAGAATTT
ARL8A	NM_138795.4	1 (C11)	TRCN0000072951	GTGGGTTTCAACATGCGCAAA
		2 (C12)	TRCN0000072952	CCCGGTCTTAGTCCTGGGTAA
ARL8B	NM_018184.3	1 (B7)	TRCN0000072854	GCTTCCCGAAATGAGCTACAT
		2 (B9)	TRCN0000072856	GTGGCTTATTCAGCATTCAAA
ARL13B	NM_182896.3	1 (E4)	TRCN0000064950	CCAGCCAATAGCATCTGTAAT
		2 (E6)	TRCN0000064952	CCTATATTGGTGTTGGCAAAT
ARFRP1	NM_003224.6	1 (C1)	TRCN0000047758	CGAAGACAAACTTTCCTCTAT
		2 (C3)	TRCN0000047760	GCAGTCTTTGTGGGACAAGTA

Table 6 - Concentrations of puromycin and blasticidin used to select breast cell lines.

Antibiotic / Cell line	Puromycin (µg/mL)	Blasticidin (µg/mL)
MCF10DCIS.com	1	2
HCC1806	0.5	-
MDA-MB-231	1.5	-

2.6. Cell proliferation

2.6.1. MTT assay and Trypan Blue exclusion method

To evaluate the metabolic activity of MDA-MB-231 and HCC1806 BC cell lines, 25,000 cells/well were seeded in a 96-well flat-bottom tissue culture plate (TPP Techno Plastic Products AG). On the following day, the medium was removed, and cells were washed twice with phosphate-buffered saline (PBS) 1x. Next, 50 µL of 3-(4,5-dimethylthiazol-2-yl)-2,5-diphenyltetrazolium bromide (MTT) (Sigma-Aldrich) at 0.5 mg/mL, diluted in serum-free medium, were added to each well, and cells were incubated for 3 hours, at 37 °C. The formed formazan crystals were dissolved with dimethyl sulfoxide (DMSO) (Sigma-Aldrich) and absorbance was measured at 570 nm and 690

nm using a SpectraMax i3x Multi-Mode Microplate Reader (Molecular Devices). The final absorbance values were calculated by subtracting the absorbance at 690 nm to the absorbance at 570nm.

To assess cell growth, 1 x 10^5 HCC1806 cells/well were seeded on a 24-well plate and incubated for 48 hours. Afterwards, cells were detached and counted with trypan blue (Sigma) on a Neubauer chamber. Cell viability was calculated by counting the number of live cells in each condition.

2.6.2. Cell viability in 3D

Cell proliferation was evaluated in 3D spheroids using CellTiter-Glo® 3D kit (Promega), following the manufacturer's instructions. Briefly, triplicates of 3-day old HCC1806 spheroids, were transferred to a 96-well black opaque-walled plate (Greiner) in 100 µL. Next, the same volume of CellTiter-Glo® 3D reagent was added to each well by pipetting vigorously for 5 minutes to lyse the cells. The luminescence signal was allowed to stabilize for 25 minutes at room temperature (RT) before being measured with an integration time of 0.140 seconds on a Spectramax i3x Multi-Mode Microplate Reader (Molecular Devices).

2.7. FDA/PI spheroid staining

Fluorescein diacetate (FDA, Sigma-Aldrich) and propidium iodide (PI, Invitrogen) were used to assess viability in HCC1806 spheroids, starved for 7 days in serum-free medium. Live and dead cells were labeled by incubating HCC1806 spheroids with FDA (5 µg/mL) and PI (8 µg/mL), respectively, in PBS 1x for 20 minutes at 37ºC. Immediately after, spheroids images were acquired using a Zeiss LSM 710 confocal microscope equipped with a Plan-Neofluor 10x/0.3 DIC lens.

2.8. Scratch "Wound-healing" assay

Collective cell migration was assessed using scratch assays. HCC1806 and MDA-MB-231 cells were seeded at 2 x 10^5 cells/well, on a 24-well plate, to allow the formation of a confluent cell monolayer. On the next day, serum-free medium supplemented with 0.5 % bovine serum albumin (BSA) (Sigma-Aldrich) was added to the cells, followed by incubation at 37 °C, 5 % CO_2, and 95 %

humidity overnight (ON). After, cells were treated with 2.5 µg/mL mitomycin C (Calbiochem) for 2 hours at 37 ºC, to inhibit cell proliferation. Then, a scratch was made on each well, using a 200 µL pipette tip. The detached cells were washed with PBS 1 x and complete medium was added to promote cell migration. Images from two fields of each well were acquired in Axiovert 40 (Zeiss) microscope equipped with a digital camera (AxioCam MRc) and ZEN 2 software (blue edition), immediately after the scratch and at several time points. The scratched areas were measured using Fiji software. To calculate the percentages of wound closure, the following formula was applied: [1-(wound area at t = x hours/gap area at t = 0 hours) ×100].

2.9. Transwell migration assays

To assess single-cell migration, 8.0 µm pore size polycarbonate membrane inserts (Corning) were used. The lower membrane of each transwell was pretreated with 10 µg/mL of fibronectin (Gibco), ON at 4ºC. On the next day, transwells were washed with PBS 1x and the upper chamber was allowed to hydrate in serum-free medium supplemented with 0.5 % BSA, for 1 hour at 37 ºC, 5 % CO_2, and 95 % humidity. Then, HCC1806 cells, that were starved in serum-free medium with 0.5 % BSA, ON, were seeded at 5 x 10^4 cells/transwell in the same media. Complete medium was added to the lower chamber to induce migration. After 6 hours of migration, the upper membrane surface was wiped with a cotton swab to remove cells that did not migrate. Then, cells were fixed with 4 % (v/v) paraformaldehyde (PFA; Alfa Aesar) for 15 minutes at RT and the nuclei were stained with 0.2 % (w/v) crystal violet (Sigma-Aldrich) in 20% methanol for 15 minutes. Transwells were then washed with MilliQ water to remove the excess of crystal violet and the inserts were left to dry at RT. Finally, images of 5 randomly selected fields of each transwell were acquired on Axiovert 40 (Zeiss) microscope using a digital camera (AxioCam MRc) and ZEN 2 software (blue edition) and analyzed with Fiji software.

2.10. 3D invasion assays

Cell invasion in a 3D setting was evaluated by embedding cell spheroids in either Matrigel growth factor reduced (GFR) or collagen I Rat tail (Corning).

For the experiments using Matrigel, two protocols were used. On the first approach, HCC1806 and MDA-MB-231 fully formed spheroids were transferred in 30 µL medium to a 96-well flat bottom plate (TPP) containing 30 µL Matrigel GFR, on ice, using cut cold tips pre-washed with PBS 1x. For experiments using MCF10DCIS.com spheroids, the medium from each spheroid-containing well was carefully removed and 45 µL Matrigel GFR at 5 mg/mL was directly added to the plate. Finally, the matrix was allowed to solidify for 1 hour at 37 °C, 5 % CO_2, 95 % humidity, and 100 µL/well of complete medium supplemented or not with 50 ng/mL epidermal growth factor (EGF) were added to MCF10DCIS.com and MDA-MB-231/HCC1806 spheroids, respectively. Cell invasion was monitored for several days. To assess Matrigel GFR degradation, DQ™ Red BSA (Gibco) was used. Briefly, the same protocol described for the first approach was performed, but Matrigel GFR was mixed with DQ-BSA ™ at 30 µg/mL. These experiments were then performed in serum-free medium instead of complete medium.

For the experiments using collagen I Rat tail, the medium was removed from the spheroid containing wells and 50 µL of collagen Mix – 1.75 mg/mL collagen I Rat tail, 15 mM NaOH, DMEM with GlutaMax, HEPES - were added to each well. The collagen was allowed to solidify for 1 hour at 37 °C, 5 % CO_2, 95 % humidity, 100 µL of complete medium was added to each well and cell invasion was monitored for several days.

Cell invasion was monitored by acquiring pictures on Axiovert 40 (Zeiss) microscope using a digital camera (AxioCam MRc) and ZEN 2 software (blue edition) and Zeiss LSM 710 confocal microscope equipped with a Plan-Neofluor 10x/0.3 DIC objective and Zen Blue 2010b SP1 software. All images were analyzed with Fiji software.

2.11. Gelatin Degradation Assay

Sterile glass coverslips in 24-well plates were coated with 50 µg/mL poly-D-Lysine (Sigma-Aldrich) in PBS 1x, for 1 hour at RT. After washing the coverslips 3 times with PBS 1x, 0.5 % glutaraldehyde in PBS 1x was added for 15 minutes at RT. After 3 washes with PBS 1x, coverslips were turned onto a parafilm containing a 40 µL droplet of gelatin from pig skin, Oregon Green ® conjugate (Invitrogen) at 0.2 mg/mL in PBS 1x with 0.2 % sucrose, for 10 minutes at RT. After incubation, coverslips were transferred to the 24-well plate, washed 3 times with PBS 1x, and incubated with a fresh solution of sodium borohydride (Sigma-Aldrich) at 5 mg/mL in PBS 1x, for 15 minutes at RT. Finally, coverslips were washed 3 times with PBS 1x and stored at 4°C in PBS 1x,

protected from the light, until further use. Before each experiment, Gelatin-coated coverslips were washed with PBS 1x and incubated with DMEM complete medium for at least 1 hour at 37 ºC, 5 % CO_2, and 95% humidity. Afterwards, 5 x 10^4 cells/well of MDA-MB-231 cells silenced for ARFRP1 were plated on the gelatin-coated coverslips and incubated for 6 hours at 37 ºC, 5 % CO_2, and 95 % humidity, to allow gelatin degradation. Then, cells were washed with PBS 1x and fixed with PFA 4 % for 15 minutes at RT. After fixation, cells were washed again with PBS 1x and permeabilized/blocked with PerBlock buffer (PBS 1x + 0.5% BSA + 0.1% saponin) (Sigma) for 30 minutes at RT. Then, cells were incubated with mouse cortactin clone 4F11 antibody (Milipore, #05-180), diluted at 1:300 in the PerBlock, for 1 hour at RT. After washing 3 times with PBS 1x, goat Alexa Fluor™ 568 goat anti-mouse antibody (Invitrogen, #A11004), diluted at 1:1000 in PerBlock, was added for 1 hour at RT. Finally, coverslips were washed 3 times with PBS 1x and mounted in Fluoromount-G™ with DAPI. Image acquisition was performed using a Zeiss LSM 710 confocal microscope equipped with a Plan-Apochromat 63/1.40 Oil Ph3 lens and Zen Blue 2010b SP1 software.

2.12. Immunoblotting

Protein was extracted using IGEPAL lysis buffer containing 50 mM Tris-HCl pH 7.5, 150 mM NaCl, 1 mM ethylenediaminetetraacetic acid (EDTA), 1mM ethylene glycol-bis(β-aminoethyl ether)-N,N,N',N'-tetraacetic acid (EGTA), 2 mM magnesium chloride, 1 mM DTT and 0.1% sodium dodecyl sulfate (SDS), protease inhibitor cocktail (Roche), 1 µM sodium orthovanadate and 1% IGEPAL (IGEPAL, 2D cultures), on agitation for 30 minutes at 4 ºC. Then, the lysed cells were centrifuged at 13 800 x g, for 30 minutes at 4 ºC and the supernatants were collected to a new tube for protein quantification using the DC protein assay kit (Bio-Rad), following the manufacturer's instructions. SDS-polyacrylamide gel electrophoresis (SDS-PAGE) was performed by loading 30-50 µg of total protein per lane in 10 % or 12 % polyacrylamide gels. Proteins were separated at 0.02 amperes in running buffer (25 mM Tris, 192 mM glycine, 0.1 % SDS). Proteins were transferred to a nitrocellulose membrane (0.2 µm pore, Cytiva), in chilled transfer buffer (25 mM Tris, 192 mM glycine, 0.025 % SDS, 20 % ethanol), for 53-60 minutes at 100 volts. Afterward, membranes were blocked with blocking buffer - 5 % low-fat milk in Tris-buffered saline (TBS 1x) with 0.1 % Tween-20 (TBST) - for 1 hour at RT, on agitation. Primary antibodies were diluted in 5 % BSA in TBST and incubated ON at 4 ºC, on agitation. On the following day, membranes were washed 3 times with TBST and incubated with horseradish peroxidase (HRP)- conjugated secondary antibodies diluted in

blocking buffer, for 1 hour at RT, on agitation. Then, membranes were washed 3 times with TBST, and chemiluminescence was acquired using ECL Select/Prime Western Blotting Detection Reagents (Cytiva) in ChemiDoc™ Touch Imaging System (Bio-Rad) equipment. All antibodies and respective working dilutions are listed in Table 7.

Table 6. List of antibodies used for immunoblotting.

Antibody/Dye	Species (antigen)	Raised in	Brand (reference)	Dilution
Anti-ARL8B	human	rabbit	Production described in [282]	1:300
Anti-Slug (C19G7)	human	rabbit	Cell Signaling (9585T)	1:2000
Anti-E-Cadherin (24E10)	human	rabbit	Cell Signaling (3195T)	1:2000
Anti-GAPDH	human	Goat	Sicgen (#AB0049-200)	1:2000
Anti-CANX (calnexin)	human	Goat	Sicgen (#AB0037-200)	1:1000
Donkey anti-goat HRP (secondary)	mouse	Goat	Invitrogen (#A16005)	1:5000
Goat anti-rabbit HRP (secondary)	rabbit	Goat	Bio-Rad (#1706515)	1:5000

2.13. Transfection and immunofluorescence of HCC1806

HCC1806 cells (5 x 10^4 cells/well) were seeded in glass coverslips (13 mm, 1.5 mm thickness, VWR) in 24-well plates, in RPMI complete medium and incubated at 37 °C, 5 % CO_2, 95 % humidity. On the following day, cells were transfected with human ARL8B-GFP (pEFGP-N1, a kind gift from Dr. Jaime Mota, FCT) and control GFP (pEGFP-C3), using FuGENE 6 (Promega) transfection reagent following the manufacturer's instructions. Briefly, a mix containing 1 µg DNA/2 µl of FuGENE was prepared in Opti-MEM and added to the cells. After 24 hours, cells were fixed in 4 % PFA for 15 minutes at RT and used for immunofluorescence assays.

For immunofluorescence, cells were permeabilized/blocked with PerBlock buffer (PBS 1x + 0.5% BSA + 0.1% saponin) (Sigma) for 30 minutes at RT. LEs/lysosomes were labeled with mouse LAMP1-647 clone H4A3 (Biolegend, #328611) in PerBlock buffer for 1 hour at RT. Then the coverslips

were washed 3 times with PBS 1x and mounted in slides (VWR – cut edged frosted) using Fluoromount-G™ with DAPI mounting medium (Invitrogen). Imaging was performed using the Zeiss LSM 710 confocal microscope equipped with a Plan-Apochromat 63/1.40 Air Ph3 lens and Zen Blue 2010b SP1 software.

2.14. Lysosome exocytosis

2.14.1. Flow cytometry

HCC1806 cells were seeded in 24-well plates at 1.3 x 10^5 cells/well in RPMI complete medium. After two days, calcium-triggered lysosome exocytosis was induced by incubating cells with 10 µM ionomycin and 4 mM of $CaCl_2$ in HBSS for 10 minutes at 37 ºC, 5 % CO_2, and 95 % humidity. Cells were placed on ice and detached with TrypLE. After two washes with flow cytometry buffer – PBS 1x, 1 % FBS and 2mM EDTA, cells were incubated with anti-human LAMP1 conjugated with Alexa Fluor 488 (clone H4A3, Biolegend, Table V) for 30 minutes at 4° C. Cells were washed 1x with flow cytometry buffer before being resuspended in 200 µL of the same buffer. Immediately before acquisition, cells were incubated with propidium iodide (PI) (Invitrogen), at a final concentration of 0.5 µg/mL**.** Samples were acquired in a FACS CANTO II flow cytometer and at least 30,000 cells were analyzed using FlowJo version 10.1r7 software.

2.14.2. Beta-hexosaminidase release assay

HCC1806 were seeded in 6-well plates at 6 x 10^5 cells/well in RPMI complete medium. Two days after seeding, calcium-triggered lysosome exocytosis was evaluated. For that, cells were incubated with 10 µM ionomycin and 4 mM of $CaCl_2$ in Hank's Balanced Salt Solution (HBSS) for 10 minutes at 37 ºC, 5 % CO_2, and 95 % humidity. Cells were then placed on ice and the supernatants were collected. Simultaneously, cells were lysed with 1% IGEPAL. Both supernatants and cell lysates were centrifuged at 11.000 xg for 5 minutes, 4 ºC. To determine β -hexosaminidase activity, 100 µl of cell supernatants/lysates were incubated on a 96-well opaque black plate (Corning) with 100 µl of 6 mM of β-hexosaminidase substrate 4-methylumbelliferyl- N-acetyl-β-d-glucosaminide (4-MU-β-D-GlcNAc; Glycosynth), resuspended in HBSS with 40 mM sodium citrate and 88 mM Na_2PO_4 pH

4.5, for 15 minutes at 37 °C. Fluorescence was then measured in Spectramax i3x Multi-Mode Microplate Reader (Molecular Devices) at 365 nm excitation and 450 nm emission**.** Additionally, total protein from cell supernatants/lysates was quantified using the BCA protein assay kit (Pierce Laboratories) following the manufacturer's instructions, and absorbance was measured at 560 nm using the previously mentioned plate reader. IGEPAL lysis buffer and HBSS were used as background controls. β-hexosaminidase (β-hex) activity was calculated for each sample normalizing to total protein amount, using the following formulas:

$$\boldsymbol{\beta - \text{hex activity in supernatant}} = \frac{\text{sample fluorescence}\left(\frac{365}{450}\right) - \text{HBSS alone}\ \left(\frac{365}{450}\right)}{\text{protein (µL)}}$$

$$\boldsymbol{\beta - \text{hex activity in cell lysate}} = \frac{\text{sample fluorescence}\ \left(\frac{365}{450}\right) - \text{IGEPAL alone}\ \left(\frac{365}{450}\right)}{\text{protein (µL)}}$$

$$\boldsymbol{\text{Total } \beta - \text{hex activity}} = \beta - \text{hex activity in supernatant} + \beta - \text{hex activity in cell lysate}$$

Finally, the percentage of β-hex release was calculated as follows:

$$\boldsymbol{\beta - \text{hex release}}\ (\%) = 100\ \text{x}\ \left(\frac{\beta - \text{hex activity in the supernatant}}{\text{Total } \beta - \text{hex acitivity}}\right)$$

2.15. Statistical analysis

All results are presented as mean ± standard deviation (SD). GraphPad Prism software (version 6) was used to perform the statistical analysis and the statistical tests used in each dataset are indicated in the respective figure legends.

Chapter 3. Results

3.1. Role of membrane traffic regulators from the ARL subfamily in breast cancer progression

All the work presented in this section was performed by Andreia Ferreira (all Figures), Diana Coito (Figure 16) and Madalena Lopes (Figure 16).

Currently, BC is the type of cancer with the higher number of cases and mortality in women, worldwide [1]. Although significant advances have been achieved in terms of diagnostic tools and therapeutic options, BC is still considered a major health issue, and strategies to increase the life expectancy and quality of life of BC patients are urgently needed. To find more and better solutions, it is fundamental to understand the molecular mechanisms that foster the progression of BC and allow the transformation of non-malignant breast cells into tumor cells.

Cancer cells, including BC cells, subvert different cellular mechanisms to acquire proliferative, migratory, and invasive capacities. Specifically, membrane traffic regulators were shown to be crucial for the transformation of "normal" cells into malignant cells with invasive capacities [283,284]. Several proteins belonging to the Rab and Arf families of small GTPases, which can regulate the traffic of organelles and vesicles [285], were shown to be involved in the progression of diverse types of cancers [227,286]. Moreover, our lab and others have been deeply interested in understanding the role of membrane traffic regulators in cancer processes. Namely, we found that ARL13B, which belongs to the ARF family of small GTPases, has a role in BC cell migration and invasion through an integrin-dependent mechanism[280]. Other groups described the role of different ARLs as tumor suppressors for BC. One example is ARL11, which has been associated with familial and sporadic forms of BC, where at least two variants of the *ARLST1* gene have been extensively studied[257,279]. Also, ARL2 has been described as an inhibitor of BC progression, via the regulation of α/β tubulin polymerization of a luminal A BC cell line, MCF-7 [272].Thus, given the previous studies that point to a key role of membrane traffic regulators in BC progression and the current scarce knowledge on the association of proteins from the ARL subfamily with this disease, we decided to study the role of these proteins in BC.

ARL genes are differentially expressed in breast cancer cell lines and samples

To assess the role or ARLs in BC progression, we started by performing a real-time qPCR screen to assess which *ARL* genes are differentially expressed in BC cell lines. For this approach, we chose a non-malignant breast cell line (MCF10A) [287], a non-invasive *in situ* BC cell line (MFC10DCIS.com) [288], a poorly invasive luminal A BC cell line (MCF-7) [289] and a highly invasive triple-negative BC cell line (MDA-MB-231) [289]. The results obtained with this preliminary screen showed that several ARLs, namely *ARL1*, *ARL2*, *ARL3, ARL4A*, *ARL5A, ARL5B*, *ARL6*, *ARL8A*, *ARL8B*, *ARL11, ARL13B, ARL14* and *ARFRP1,* have an increased mRNA expression from non-tumoral/non-invasive

cell lines (MCF10A and MCF10DCIS.com) to poorly/highly invasive BC cell lines (MCF-7 or MDA-MB-231) (Figure 16). Additionally, for some of the above-mentioned targets, we could observe a tendency for a higher mRNA expression with a positive correlation with invasiveness, meaning that we observed an increase in expression from non-invasive MCF10A/MCF10DCIS.com to poorly invasive MCF-7 and from MCF-7 to highly invasive MDA-MB-231 cell lines – *ARL1*, *ARL2,* and *ARFRP1* (Figure 16).

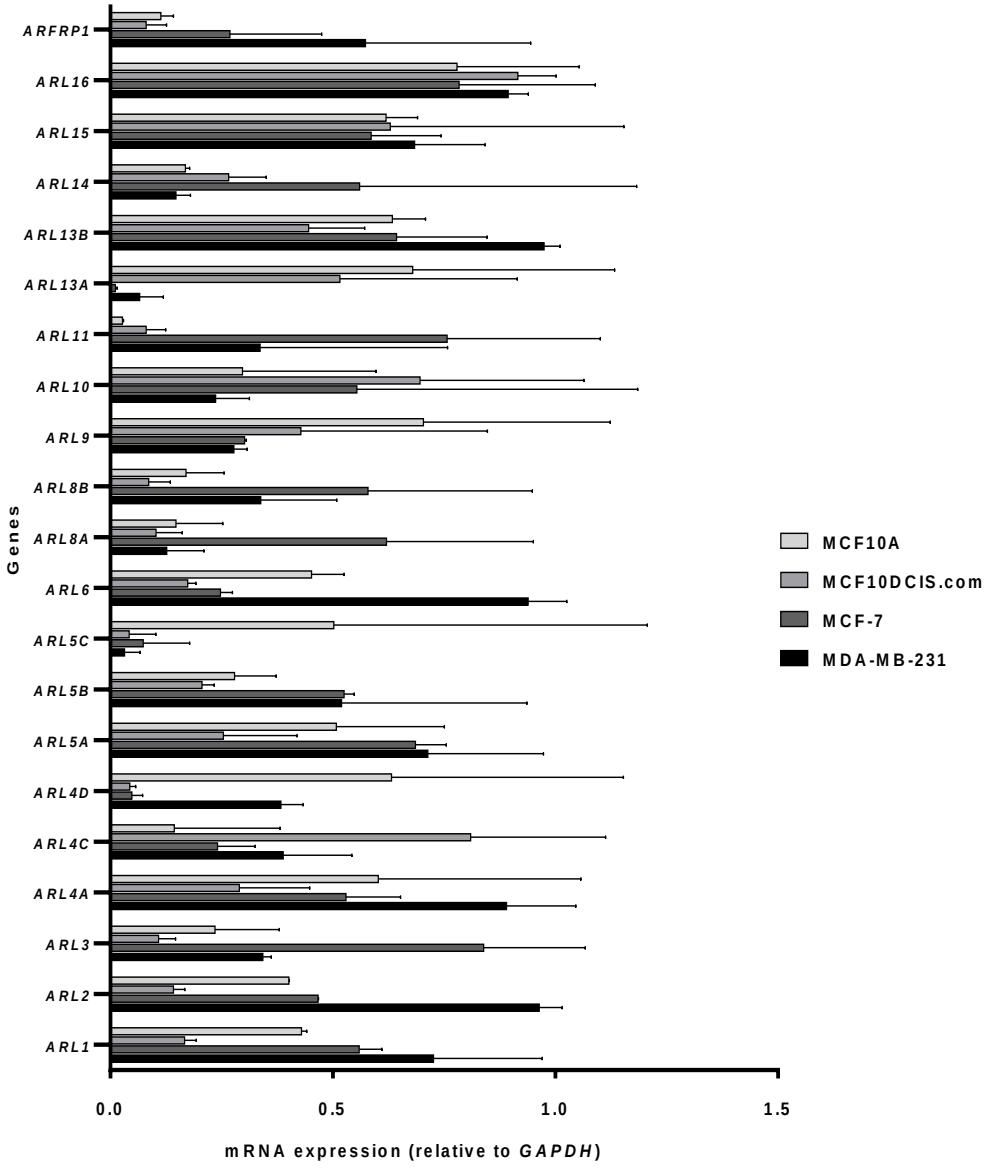

Figure 16 - ARLs mRNA expression screen in normal breast and BC cell lines. mRNA levels were measured by real time qPCR using cDNAs obtained from non-tumorigenic MCF10-A, non-invasive ductal carcinoma in situ MCF10DCIS.com, poorly invasive MCF-7 (Luminal A) and highly invasive MDA-MB-231 (Triple negative B) BC cells. The housekeeping *GAPDH* gene was used to normalize the expression of different *ARLs*. Results show the relative ratios normalized from 0 to 1 between mRNA expression levels of *ARLs* and *GAPDH* and error bars represent mean ± SD of at least two independent experiments.

Besides assessing the mRNA expression levels in different cell lines with increasing invasive capacities, we also conducted a bioinformatic analysis of the most promising candidates, chosen from the screen (Figure 16). Specifically, we chose *ARL1, ARL2*, *ARL5A*, *ARL5B*, *ARL6, ARL8B*, *ARL11*, and *ARFRP1*, which show a more striking upregulation in the highly invasive cell line MDA-MB-231, when compared with MCF10A and MCF10DCIS.com. For this, we used the TIMER 2.0 online tool (http://timer.cistrome.org/)[281] to assess the expression of the selected *ARLs* in BC samples and normal adjacent breast tissues. As depicted in Figure 17, the expression of *ARL1*, *ARL8B, ARL11* and *ARFRP1* is significantly increased in tumor BC samples (BRCA.Tumor), when compared with normal adjacent tissues (BRCA. Normal). On the other hand, the expression of *ARL2* and *ARL6* were decreased in BC samples when compared with normal adjacent tissues. Finally, we did not find any significant differences in expression of *ARL5A* and *ARL5B* between BC samples and normal tissues.

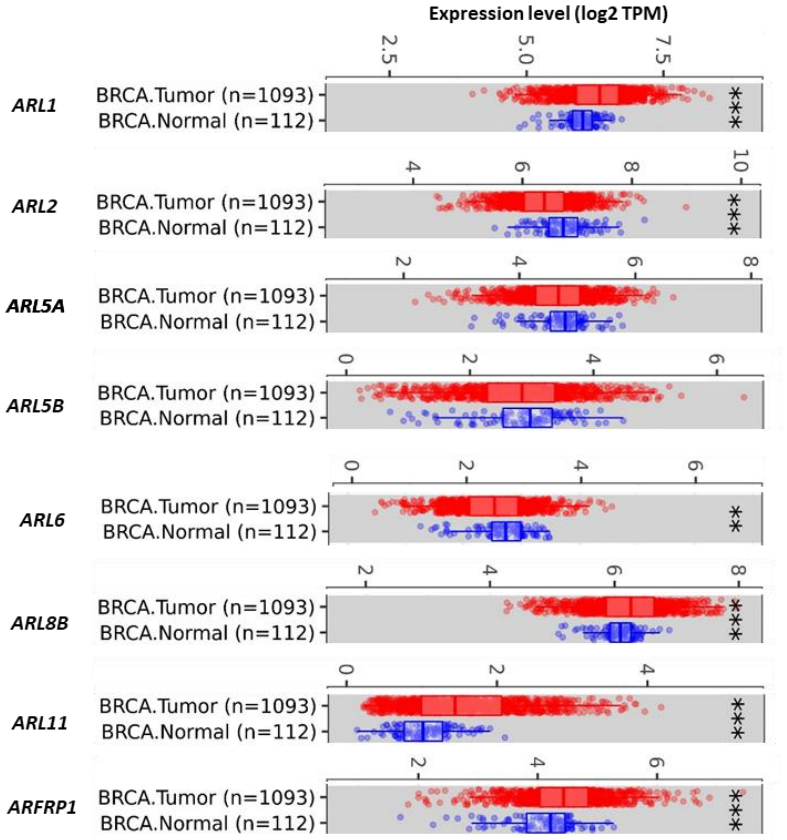

Figure 17 - Expression analysis of *ARL* genes in normal and tumor samples. Plots were generated using TIMER 2.0 online tool (Gene_DE module) to assess the differential expression of *ARLs* between BC tumor samples (BCRA Tumor – red dots) and adjacent normal tissues (BCRA Normal – blue dots). The distribution of mRNA expression levels is represented as box plots and statistical analyses were performed using the Wilcoxon test, *** p <0.001. Transcripts Per Million (TPM). This analysis was performed using the TCGA dataset.

We also analyzed the mRNA levels by real-time qPCR of selected *ARL* genes in BC samples and normal adjacent breast tissues. In this analysis we included *ARL* genes that were shown to be

significantly increased/decreased in BC samples in the bioinformatic analysis and compare with the normal adjacent tissue (*ARL1*, *ARL2*, *ARL6*, *ARL8B, ARL11 and ARFRP1*). Due to a low number of available samples, we decided to exclude *ARL6* and *ARL11* from this analysis. The results depicted in Figure 18 show that none of the *ARL* genes analyzed show a significant difference in mRNA expression between normal and tumor samples. As mentioned before, a low number of samples were available to perform this analysis, which could help to explain the lack of statistical significance of the results obtained. Nonetheless, it is possible to observe a tendency for a decrease in mRNA expression from normal samples to tumor BC samples in *ARL2* and *ARFRP1*. In fact, the results obtained for *ARL2* corroborate the ones obtained from patient samples with the bioinformatic analysis performed with the TIMER platform. For the other two targets, *ARL1* and *ARL8B*, no difference was observed between normal adjacent tissues and BC samples.

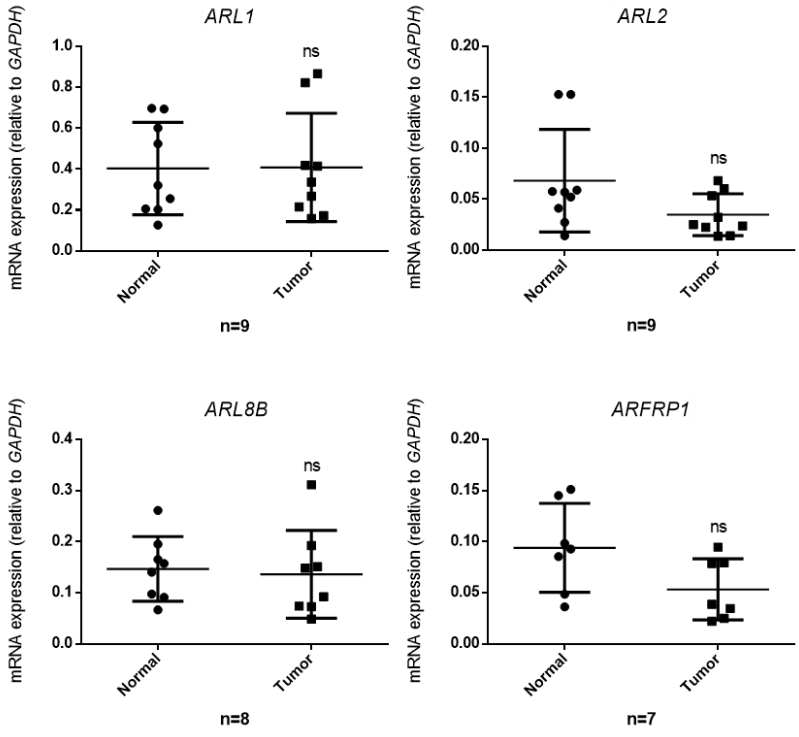

Figure 18 - Analysis of *ARLs* mRNA expression in normal tissues and breast cancer samples. Total RNA was extracted from tumor samples and normal adjacent breast tissue of BC patients. The extracted RNA was used to synthesize cDNA and the mRNA expression of *ARL1, ARL2, ARL8B, and ARFRP1* was assessed by real-time qPCR, using *GAPDH* as the housekeeping gene. Error bars represent mean ± SD. The statistical analysis was performed by applying a paired Student's t-test.

Altogether, the results obtained from the mRNA screen in cell lines and the bioinformatic analysis using BC patient samples, have shown that *ARL1*, *ARL8B* and *ARFRP1* are upregulated in BC, suggesting that these proteins may play a role in BC progression.

ARFRP1 regulates breast cancer collective cell migration

Cancer cells, including BC cells, must acquire several features to survive and disseminate to distant locations. These processes include proliferation, migration, invasion, and survival to cell death, among others [59]. Cell migration is essential for cancer cells to move locally within tissue and from one tissue to another. Also, collective cell migration is thought to be the main way by which cancer cells can disseminate and form metastases [97,98]. Different studies have shown that the modulation of ARLs has an impact on cancer cell migration. For example, *ARL13B* silencing was shown by our group to impair single-cell migration and collective cell migration capacity of BC cells [280]. Also, Fuji *et al.,* described that *ARL4C* depletion leads to a decrease in both single-cell and collective cell migration in colon and lung cancer cells [238].

From the previous qPCR screen using BC cell lines and bioinformatic analysis, we selected ARL1, ARL8B, and ARFRP1 which are upregulated in BC, to assess the effect of modulating their expression in BC cells in the migratory capacity of these cells. For this, highly invasive TNBC MDA-MB-231 cells were transduced with lentiviruses encoding specific shRNAs to silence the selected target genes. Gene silencing efficiency was evaluated by real-time qPCR. For that, the mRNA expression was analyzed in cells transduced with a non-targeting shRNA control (Mission) compared with cells expressing 2 specific shRNAs targeting *ARL1, ARL8B* or *ARFRP1*. The results depicted in Table 7 show that silencing efficiencies of at least 40 % were obtained for all the shRNAs tested, without compromising cell viability or inducing major morphological alterations in cells.

Table 7 - Silencing efficiencies of the shRNAs. Lentiviruses were used to transduce MDA-MB-231 with different shRNAs to silence *ARL1, ARL8B, or ARFRP1*. mRNA expression was measured by real-time qPCR, using GAPDH as a housekeeping gene and the silencing was calculated as follows: 100%- [relative expression shRNA ARL/relative expression shRNA control (Mission)].

	Silencing (%) – relative to shRNA control (Mission)	
	shRNA 1	shRNA 2
ARL1	68.4 - 88.0	94.6 - 96.4
ARL8B	71.3 - 80.8	56.0 - 59.2
ARFRP1	43.2 - 65.9	83.4 - 87.2

Once the silencing for all the shRNAs was confirmed, transduced MDA-MB-231 cells were used to perform a wound-healing (“scratch”) assay to assess the collective migratory capacity of these cells in 2D. In this analysis, proliferation was inhibited with serum-free medium and treatment with

mitomycin-C. The migratory capacity was evaluated by measuring the wound area at 0 hours and 8 hours. The wound closure percentage was calculated for each shRNA and compared with shRNA control (Mission). We observed no differences in the percentage of wound closure for the silencing of *ARL1* and *ARL8B*. Lastly, we can observe that *ARFRP1* silencing with shRNA 1 (C1) or shRNA 2 (C3) showed a significant decrease (around 38 %) in wound closure percentage when compared with shRNA control (Mission) (Figure 19 A and B). These results suggest that ARFRP1 may have a role in the collective cell migration of MDA-MB-231 cells.

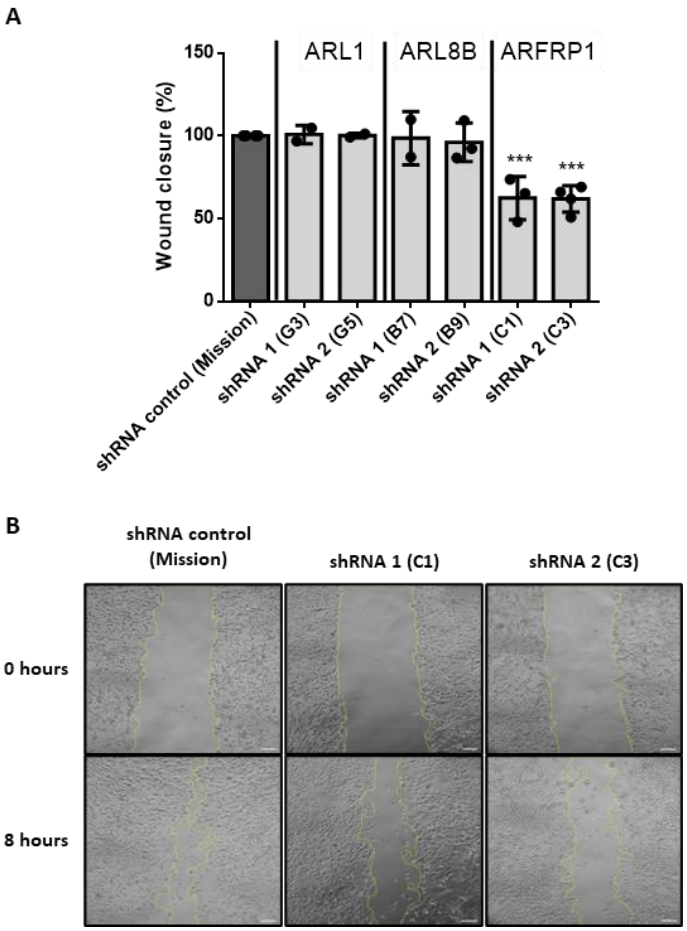

Figure 19 - *ARFRP1* silencing decreases collective cell migration in MDA-MB-231 cells. A. Wound closure percentage was calculated using the following formula: as [1 - (gap area at t = 10 hours/gap area at t = 0 hours) x 100] upon silencing of ARL1, ARL8B and ARFRP1. The results were normalized to shRNA control (Mission). For each condition, four areas were measured, using ImageJ software. Results are represented as mean ± SD of at least two independent experiments The statistical analysis was performed applying a One-ANOVA with Dunnett's test, ***p<0.001. **B.** Representative taken at 0 hours and 8 hours of MDA-MB-231 wound closure upon *ARFRP1* silencing. Yellow lines represent the wound area measured with Fiji software. Scale bar: 100 µm.

ARFRP1 silencing does not impair the metabolic activity of MDA-MB-231 cells

To date, the role of ARFRP1 in cancer progression has not been described. Only one study reported that ARFRP1 is upregulated in gastric cancer[270]. Given that we observed a decreased migratory capacity of

MDA-MB-231 cells upon *ARFRP1* silencing, we decided to further explore if this protein is involved in BC progression. One of the cancer hallmarks is the uncontrolled cell division that allows cancer cells to survive in a harsh microenvironment[60]. These increased proliferation rates have been extensively associated with BC progression, and they are caused by mutations/alterations in cell signaling pathways that control the cell cycle[290].

To evaluate if ARFRP1 regulates BC cell proliferation, we used the MTT assay to measure metabolic activity. In brief, MDA-MB-231 cells silenced for *ARFRP1* were incubated with MTT reagent, which is a substrate of NAD(P)H-dependent oxidoreductase enzymes present in viable cells[291]. MTT is reduced to purple formazan crystals that are dissolved in DMSO and absorbance can be measured on a spectrophotometer. In this experiment we included cells transduced with the empty vector as a control - shRNA control (Empty). As shown in Figure 20, *ARFRP1* silencing does not impair cell metabolic activity of MDA-MB-231 cells, suggesting that BC cell proliferation is not regulated by ARFRP1.

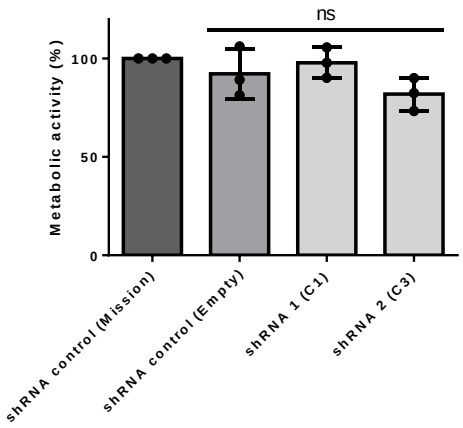

Figure 20 - *ARFRP1* silencing does not affect cell metabolic activity of MDA-MB-231 BC cells. MDA-MB-231 cells silenced for *ARFRP1* were seeded in 96-well plates. Afterward, cells were incubated with MTT, and the formazan crystals formed were dissolved with DMSO. Absorbance was measured at 570nm and 690 nm. Absorbances were calculated as A570 nm - A690 nm and were normalized to shRNA control (Mission). Results are represented as mean ± SD of three independent experiments. The statistical analysis was performed applying a One-ANOVA with Dunnett's test, ns - non-significant.

ARFRP1 silencing impairs MDA-MB-231 cell invasion in collagen I

Successful cancer metastasis formation requires not only cell migration but also cell invasion. This process is characterized by the acquisition of several features that allow the cancer cells to degrade and remodel the surrounding ECM [62]. Therefore, we decided to assess whether BC cell invasion is regulated by the modulation of *ARFRP1*. For that, we used a 3D setting, namely BC cell spheroids, which better mimic the architecture of tumors *in vivo* [292]. Spheroids were formed in 96-well plates coated with agarose to inhibit cell adherence to the bottom of the well and promote cell

aggregation [293]. Collagen I was added to each spheroid to promote spheroid compaction. Then, fully formed spheroids were embedded in Matrigel and cell invasion was monitored for two days. Cell invasion was quantified by dividing the total area of invasion by the core area. After one experiment, we were not able to see any difference in BC spheroid cell invasion into Matrigel upon silencing of *ARFRP1* (Figure 21). However, the protocol needed further optimizations to improve cell aggregation and spheroid uniformity. Moreover, as shown in Figure 21 A (lower panel), the cell spheroid core (yellow line) did not appear compact and was very hard to define after 48 hours of invasion, probably leading to inaccurate results.

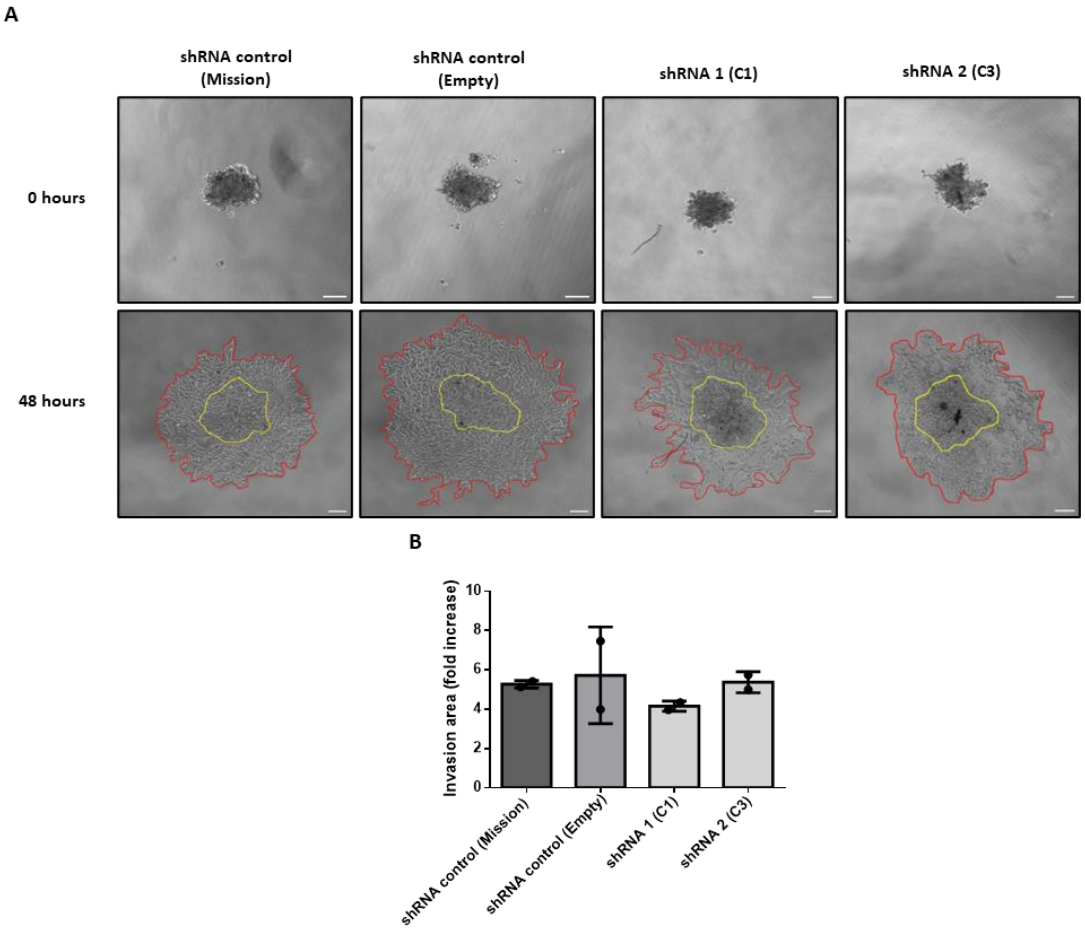

Figure 21 - *ARFRP1* silencing does not affect MDA-MB-231 cell invasion into Matrigel. MDA-MB-231 cells silenced for ARFRP1 were used to form spheroids. Then, fully formed spheroids were embedded in Matrigel, and invasion was monitored for 2 days. **A.** Representative images were taken at 0 hours and 48 hours. Yellow lines represent the spheroid core area and red lines represent the total spheroid area (core + invasion area). Scale bar: 100 µm. **B.** Invasion area quantification, calculated by dividing the total spheroid area by the core area Results are represented as mean ± SD of two spheroids per condition from one experiment.

To improve spheroid aggregation and uniformity, we decided to apply a different methodology. Spheroids were formed in ultra-low attachment (ULA) plates that are treated with a special coating to avoid cell adherence and promote uniform aggregation. We also doubled the

number of cells per well and mixed them with methylcellulose, which is an inert compound that derives from cellulose and promotes cell aggregation [294]. Furthermore, we decided to embed the spheroids into collagen I instead of Matrigel, since collagen I is the main component of the interstitial space and was found to be important for metastases formation [295]. Results show that the protocol optimizations improved cell aggregation, leading to more compact and uniform spheroids (Figure 22 A). More importantly, we found that *ARFRP1* silencing in MDA-MB-231 cells led to a significant decrease in cell invasion into collagen I. Specifically, we observed a reduction of almost 60 % in cell invasion for both shRNA 1 (C1) and shRNA 2 (C3), when compared with shRNA control (Mission) (Figure 22 A and B). However, it is important to highlight that, at 0 hours, the spheroid corresponding to shRNA 2 (C3) appeared to be less compact, which was probably caused by an effect of the silencing and can explain why we observed an increased spheroid core area (yellow line) after 48 hours (Figure 22 A). Nonetheless, these results suggest that ARFRP1 has a role in the regulation of BC 3D cell invasion in collagen I.

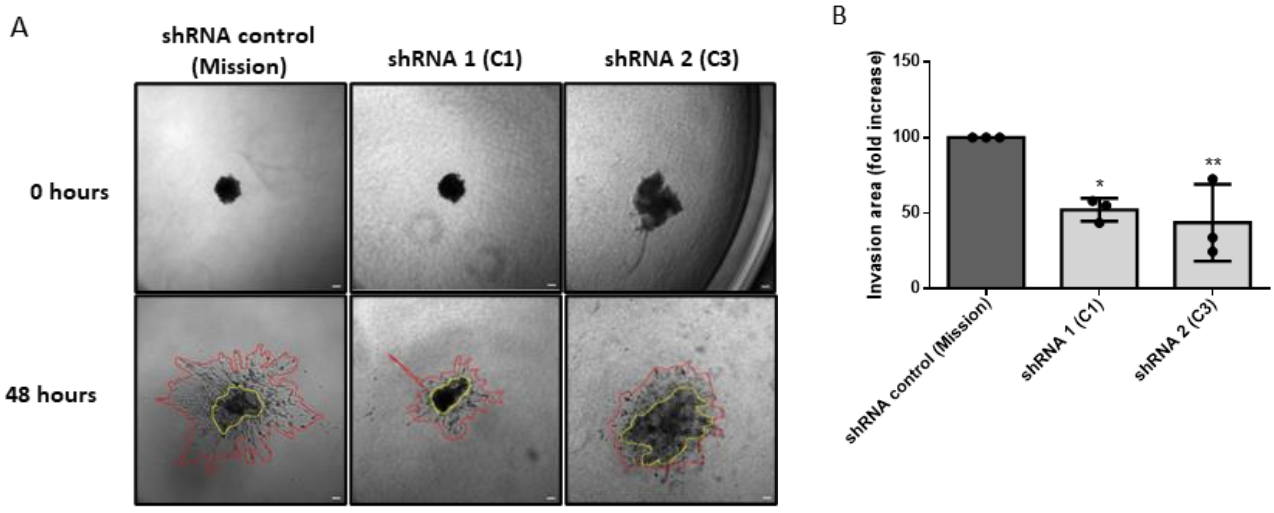

Figure 22 - *ARFRP1* silencing reduces MDA-MB-231 cell invasion into collagen I. MDA-MB-231 cells silenced for ARFRP1 were used to form spheroids in methylcellulose. Fully formed spheroids were embedded in collagen I. **A.** Representative images were taken at 0 hours and 48 hours. Yellow lines represent the spheroid core area and red lines represent the total spheroid area (core + invasion area). Scale bar: 100 µm. **B.** Invasion area quantification was calculated by dividing the total spheroid area by the core one. The results were normalized to shRNA control (Mission) and are represented as mean ± SD of at least three independent experiments. The statistical analysis was performed applying a One-ANOVA with Dunnett's test, * $p<0.05$, ** $p<0.01$.

ARFRP1 silencing does not impair invadopodia activity in MDA-MB-231 cells

An important feature of invading cells is their ability to degrade the ECM. They do so by forming invadopodia, which are specialized actin-rich structures where proteases are locally

secreted, including MMPs that can hydrolyze the ECM [114]. To evaluate if ARFRP1 is involved in invadopodia formation and activity, a gelatin degradation assay was performed. For this, MDA-MB-231 cells silenced for *ARFRP1* were seeded on top of fluorescent-gelatin-coated coverslips. After 6 hours, cells were stained with cortactin, which is a marker of actin-rich structures including invadopodia [114], followed by confocal microscopy analysis. Invadopodia activity was measured by calculating the percentage of cells that showed invadopodia co-localizing with black spots (*i.e.*, gelatin-degraded areas). Surprisingly, we observed that *ARFRP1* silencing does not affect invadopodia activity since we could only detect a decrease in the percentage of cells with active invadopodia for shRNA 1 (C1), which was not statistically significant (Figure 23), suggesting that ARFRP1 does not impair the formation of invadopodia nor the degradation of gelatin.

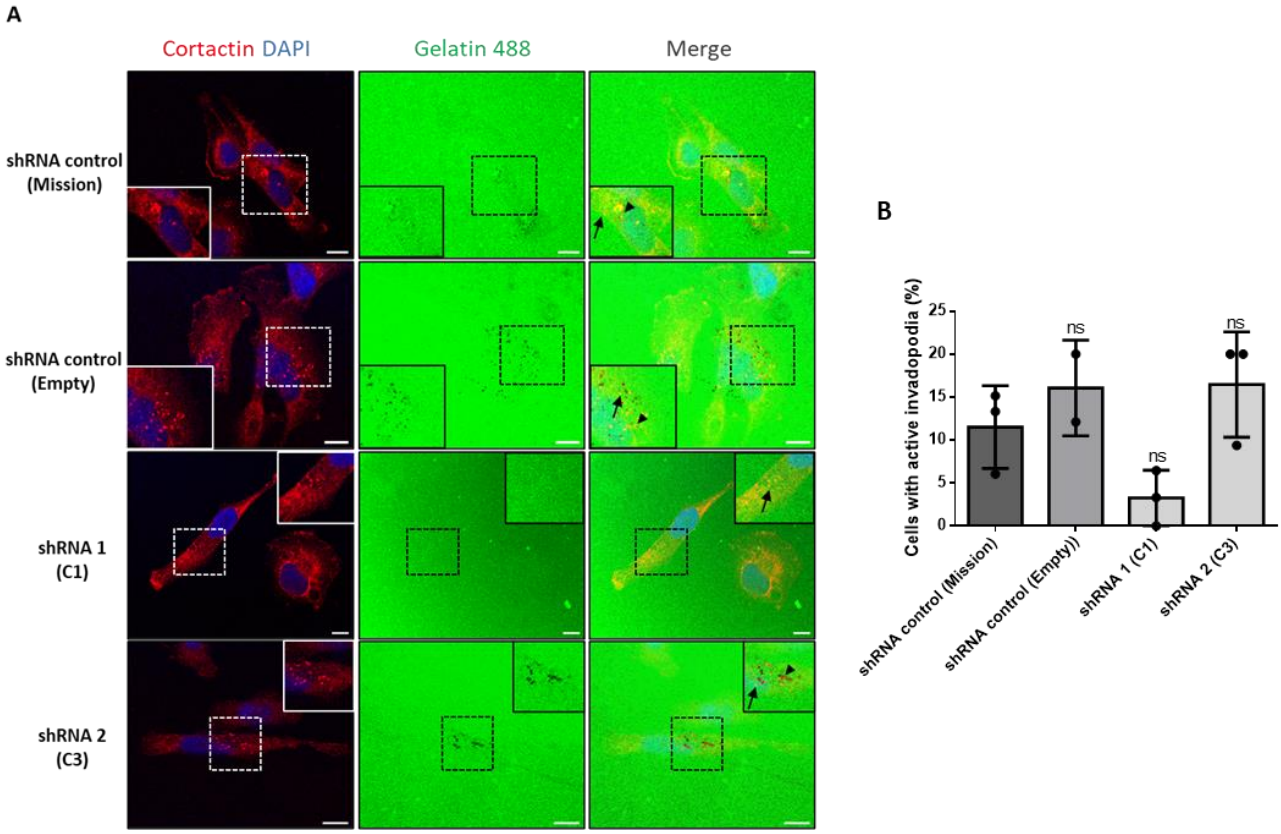

Figure 23 - *ARFRP1* silencing does not impair invadopodia activity in MDA-MB-231 cells. A. Representative images of MDA-MB-231 cells silenced for *ARFRP1* seeded on top coverslips coated with gelatin from pig skin (Oregon Green™ 488) labeled with cortactin (red) and nuclei (DAPI - blue). Black spots indicate the areas of gelatin degradation. The insets are magnified images of dashed regions. Gelatin degradation spots colocalizing with cortactin (active invadopodia) are indicated by arrowheads and degradation spots that do not co-localize with cortactin (inactive invadopodia) are indicated by arrows. Scale bar: 10 µm. **B**. Percentage of cells with active invadopodia. Results are represented as mean ± SD of three independent experiments. The statistical analysis was performed applying a One-ANOVA with Dunnett's test, ns, non-significant.

Overall, the obtained results suggest that ARFRP1 is required for ECM degradation of collagen I, indicating a role for this small GTPase in BC cell invasion. Furthermore, the mechanism by which ARFRP1 modulates cell invasion is probably independent on invadopodia formation.

ARL13B regulates 3D cell invasion of breast cancer cells

Recently, our group has shown evidence that ARL13B plays a role in BC progression, through a cilia-independent mechanism. Specifically, the depletion of ARL13B in BC cells leads to a reduction in migration and invasion *in vitro* and impairs tumor growth and metastasis formation *in vivo* [280].

In this study we also found that ARL13B is upregulated in BC cell lines (Figure 16). Likewise, given our previous results and extensive knowledge of this protein, we decided to validate our observations on a 3D setting, by evaluating whether *ARL13B* silencing in MDA-MB-231 cells leads to a decrease in cell invasion. For this, we introduced some changes to the protocol, given that we found that cells were not as compact as they should for *ARFRP1* shRNA 1 (C3) (Figure 22). So, spheroids were formed in ULA plates with 1.5 µg/mL of collagen I. After embedding spheroids in Matrigel, cell invasion was quantified using the same method shown for ARFRP1 3D invasion experiments. As shown in Figure 24, ARL13B silencing in MDA-MB-231 leads to a decrease in 3D invasion, Specifically, we observed a reduction in cell invasion area of around 55% in the case of shRNA 1 (E4) and around 20% with shRNA 2 (E6) compared with shRNA control (Mission). Figure 24 C displays *ARL13B* mRNA expression upon silencing with shRNA 1 (E4) and shRNA 2 (E6) in MDA-MB-231 BC cells, measured by real-time qPCR. Silencing efficiencies of 30% and 87%, were obtained for shRNA 1 (E4) and shRNA 2 (E6), respectively, compared with shRNA control (Mission). Therefore, these results suggest that ARL13B regulates 3D BC cell invasion, validating the results previously obtained by us in 2D and *in vivo* models [280].

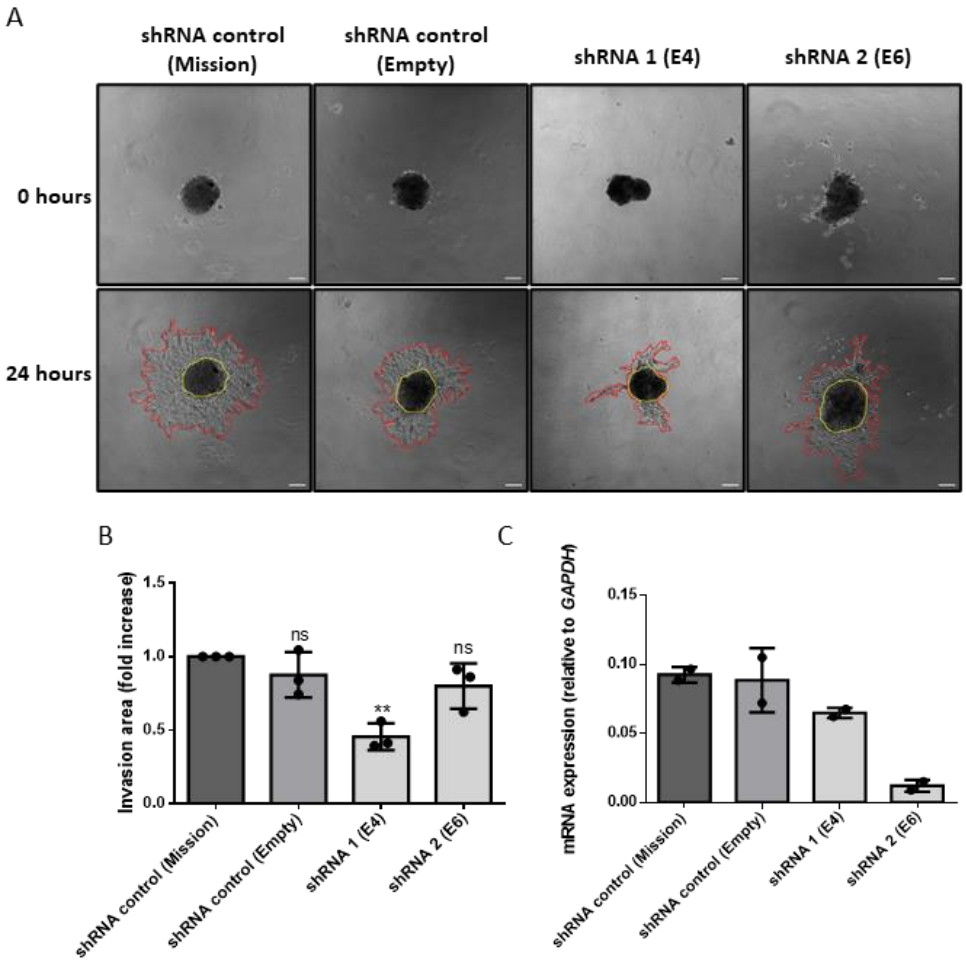

Figure 24 - *ARL13B* silencing reduces MDA-MB-231 cell invasion into Matrigel. MDA-MB-231 cells silenced for *ARL13B* were used to form spheroids. Then, fully formed spheroids were embedded in Matrigel, and invasion was monitored for 24 hours. **A.** Representative images were taken at 0 hours and 24 hours. Yellow lines represent the spheroid core area and red lines represent the total spheroid area (core + invasion area). Scale bar: 100 µm. **B.** Invasion area quantification was obtained by dividing the total spheroid area by the core area. The results were normalized to shRNA control (Mission) and are represented as mean ± SD of three independent experiments. The statistical analysis was performed applying a One-ANOVA with Dunnett's test, ns, non-significant, **p<0.01. **C.** ARL13B silencing measured by real-time qPCR. Results are represented as mean ± SD of two independent experiments.

Afterwards, we also wanted to evaluate if the overexpression of ARL13B in non-invasive MCF10DCIS.com promotes an invasive behavior and if this small GTPase is involved in the transition from *in situ* to invasive BC. For this, we transduced MCF10DCIS.com cells with lentiviruses encoding mCherry or ARL13B-mCherry. After selection, successful transduction was monitored by microscopy to evaluate mCherry expression. As depicted in Figure 25, MCF10DCIS.com expressed mCherry and ARL13B-mCherry, although the mCherry expression was found to be stronger. This may be explained by the differences in the expression pattern of mCherry and ARL13B-mCherry, where the first is expressed all over the cell cytoplasm and the second is expressed in small, confined structures of

the cell like FAs [280]. Therefore, the expression levels may be different between mCherry and ARL13B-mCherry.

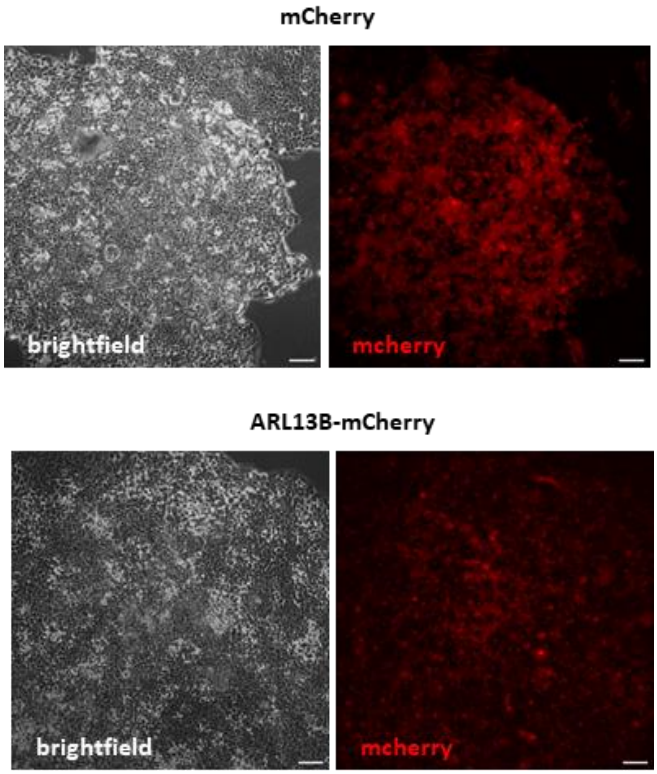

Figure 25 – ARL13B-mCherry and mCherry expression in MCF10DCIS.com cells. MCF10DCIS.com cells were transduced with lentivirus encoding mCherry and ARL13B-mCherry. After selection, representative images of brightfield and mCherry (red) were acquired. Scale bar: 100 µm.

Then, transduced MCF10DCIS.com cells were used to form spheroids that were embedded in Matrigel after formation. Spheroids were monitored for 8 days, and the invasion area was quantified as follows: total spheroid area at 8 days divided by total spheroid area at 0 days. Although we could observe an increasing trend in spheroid invasion area in cells expressing ARL13B-mCherry, it was not significant (Figure 26). Furthermore, it is also important to highlight that the setup of this experiment is not ideal, since we compared the total area of the spheroid at 8 hours and at 0 hours, which can be affected by cell proliferation.

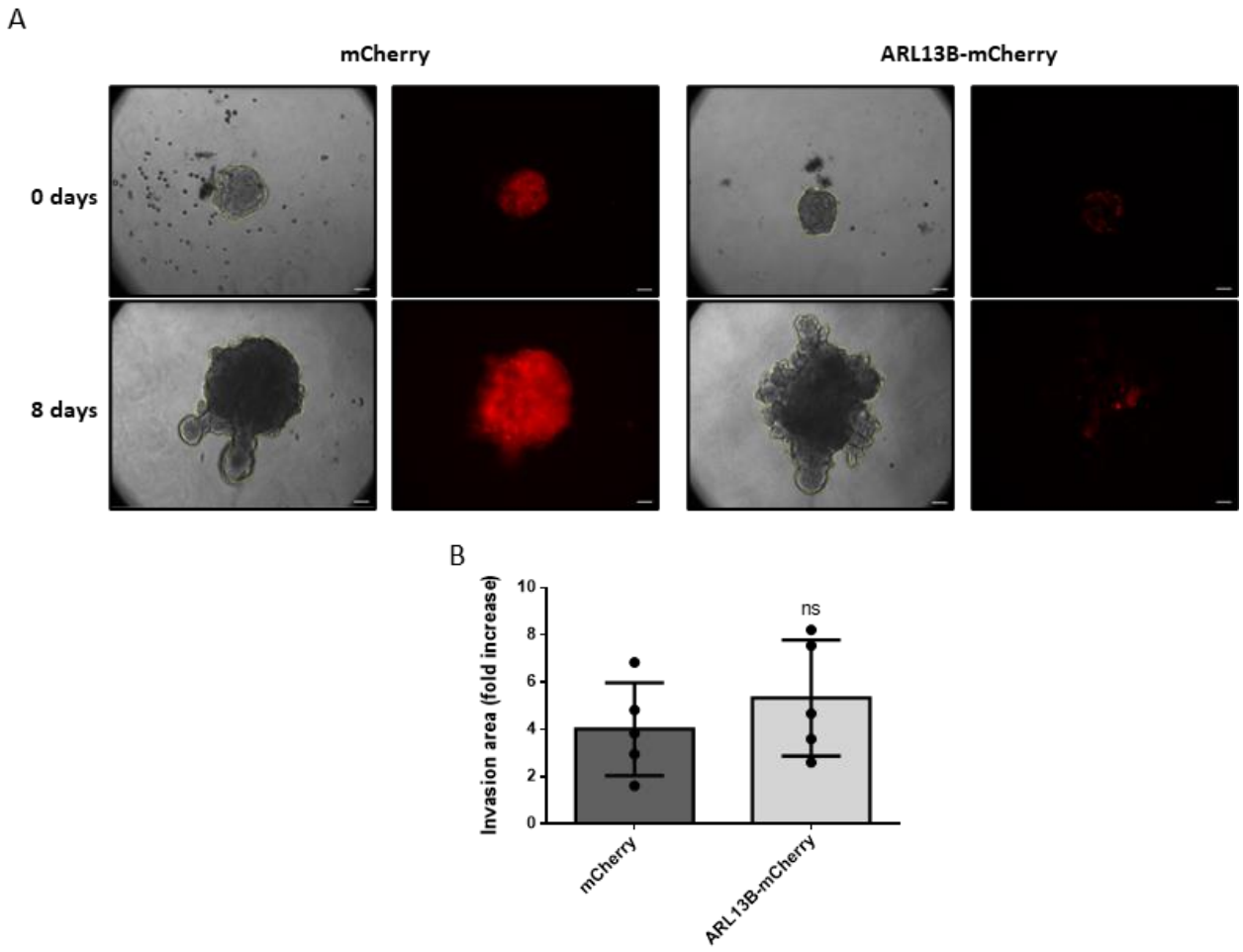

Figure 26 - ARL13B does not affect MCF10DCIS.com cell invasion capacity. MCF10DCIS.com cells were transduced with lentiviruses encoding mCherry and ARL13B-mCherry and used to form spheroids. Then, fully formed spheroids were embedded in Matrigel, and invasion was monitored for 8 days. A. Representative images were taken at 0 days and 8 days. Yellow lines represent the total spheroid area (core + invasion area) measured on day 0 and day 8. Scale bar: 100 µm. B. Invasion area quantification, calculated by dividing the total spheroid area at day 8 by the total spheroid area at day 0. The results are represented as mean ± SD of five independent experiments. The statistical analysis was performed applying an unpaired two-tailed Student's t-test (Mann-Whitney). ns, non-significant.

3.2. Role of ARL8 and lysosome exocytosis in breast cancer progression

All the work presented in this section was performed by Andreia Ferreira (all figures), Cristina Escrevente (Figures 43 and 44), Diana Coito (Figure 27) and Madalena Lopes (Figures 27, 31, 33, 34, 35, 36, 37, 40 and 45)

Part of the results were included in the following thesis:

Diana Coito - "Modulating membrane traffic regulators to impair breast cancer progression", NMS Research, NOVA Medical School and NOVA School of Science and Technology, Universidade NOVA de Lisboa, 2021, Master thesis.

ARL8 is a small GTPase from the Arl subfamily that regulates lysosomal movement from the perinuclear region to the cell periphery (anterograde movement). It has two paralogs, ARL8A and ARL8B, which are thought to have redundant functions, and both were shown to regulate lysosomal transport [208].

In cancer, ARL8B has been associated with the growth and progression of prostate cancer. In this study, the authors showed that ARL8B depletion impairs the invasiveness of prostate cancer cells, through the regulation of lysosomal positioning and protease secretion. They also gathered evidence to support that ARL8B controls prostate cancer cell proliferation by controlling lipid metabolism [256]. Moreover, a recent study shows that ARL8B is involved in BC cancer cell resistance to radiation [278]. In this study, it was shown that irradiated MDA-MB-231 cells are less invasive upon depletion of ARL8B. On the other hand, no studies so far have described the regulation of carcinogenic progression by ARL8A. Also, its effectors and specific binding partners are far less studied. Therefore, given the role of ARL8B in both prostate and BC and the growing interest of our laboratory to understand the role of lysosomal function in this disease, we decided to explore whether ARL8A and ARL8B would regulate BC progression.

ARL8A and ARL8B are upregulated in breast cancer cell lines

Our screen (Figure 16) showed that ARL8B mRNA levels increased from MCF10A cells to MDA-MB-231 cells, while the mRNA expression of ARL8A is increased in luminal A BC MCF-7 cells, when compared with non-tumoral MCF10A cells. However, we were not able to detect any changes in the migratory capacity of MDA-MB-231 cells upon ARL8B silencing (Figure 19). So, we decided to assess *ARL8A* and *ARL8B* mRNA expression by real-time qPCR in other cell lines, including one luminal B BC cell line - BT-474 - and one TNBC cell line - HCC1806. As shown in Figure 27, *ARL8A* mRNA levels are increased in both luminal cell lines MCF-7 and BT-474 and significantly higher in TNBC HCC1806 cells, when compared with non-tumoral MCF10A cells. Moreover, we observed the same trend for ARL8B, although a slight increase in MDA-MB-231 cells was also detected (Figure 27 B). Finally, the mRNA levels of both ARL8A and ARL8B in non-invasive MCF10DCIS.com are similar to non-tumoral MCF10A cells (Figure 27 A and B).

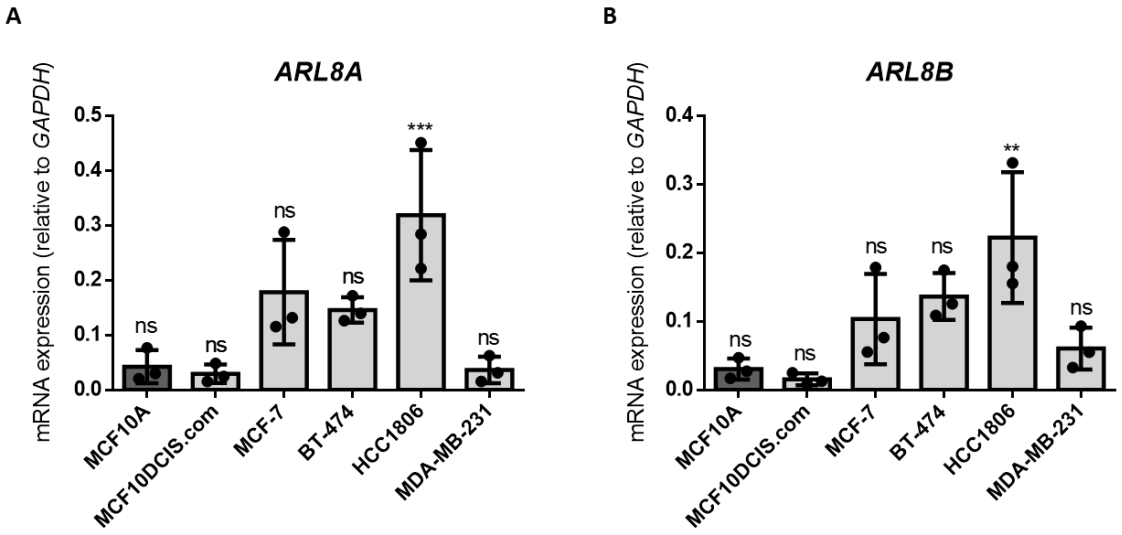

Figure 27 - *ARL8A* and *ARL8B* mRNA expression is increased in breast cancer cell lines. mRNA levels were measured by real-time qPCR using cDNA obtained from non-tumorigenic MCF10-A, non-invasive ductal carcinoma *in situ* MCF10DCIS.com, MCF-7 (luminal A), BT-474 (luminal B), HCC1806 (triple negative), MDA-MB-231 (triple negative) BC cells. Results show the relative ratios normalized to the *GAPDH* housekeeping gene. Error bars represent the mean ± SD of three independent experiments. The statistical analysis was performed applying a One-ANOVA with Dunnett's test. ns – non-significant, ** $P<0.01$, *** $P<0.001$.

Next, we wanted to evaluate if protein expression was also altered in BC cell lines when compared with non-tumoral MCF10A and non-invasive MCF10DCIS.com cells. For this, we obtained lysates of the cell lines used in the previous section and performed an immunoblot analysis. The antibody used for this analysis was raised against ARL8B [282], but it can detect both ARL8A and ARL8B proteins.

As depicted in Figure 28 A and B, ARL8A expression levels are similar in all the analyzed cell lines. For ARL8B, we observed that the protein levels increase from non-tumoral MCF10A to tumoral BC cell lines, with a significant increase only being obtained for MCF-7 (Figure 28 A and C). Additionally, an increase in ARL8B protein expression was also observed from non-invasive (MCF10DCIS.com) to invasive BC cell lines (Figure 28 A and C), although less striking when compared with the results obtained for the mRNA analysis (Figure 27).

In summary, mRNA for *ARL8A* and *ARL8B* are increased in BC cells compared with non-tumoral MCF10A cells, while we observed an increase in protein expression only for ARL8B from non-tumoral do BC cell lines.

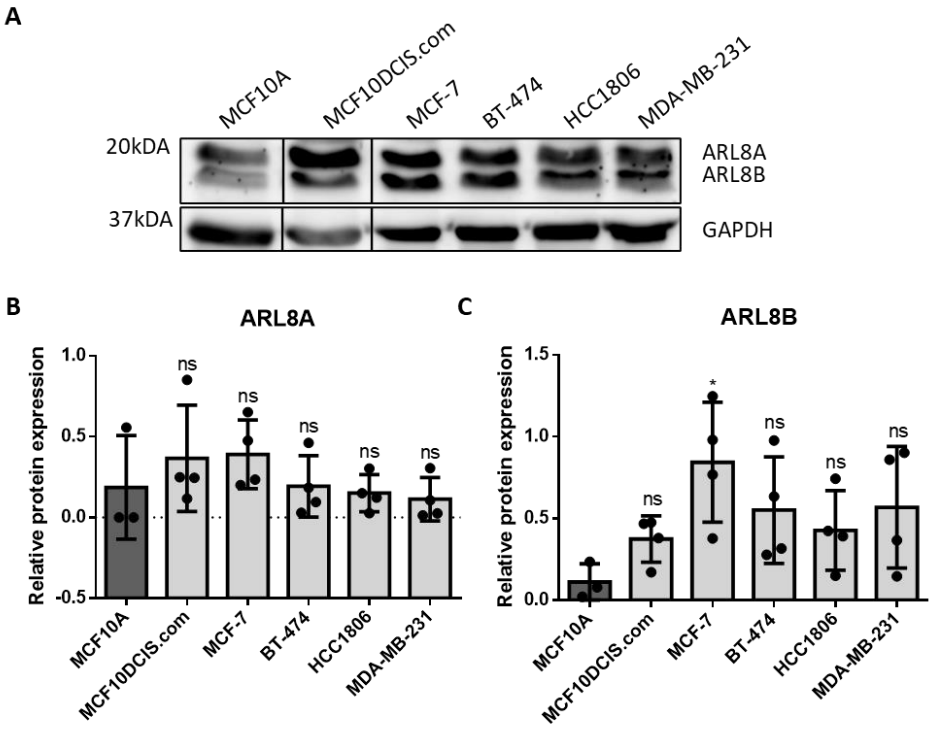

Figure 28 - ARL8A and ARL8B protein expression is increased in breast cancer cell lines. Protein levels were analyzed by immunoblotting using cell lysates from non-tumorigenic MCF10A, non-invasive ductal carcinoma *in situ* MCF10DCIS.com, MCF-7 (luminal A), BT-474 (luminal B), HCC1806 (triple negative), MDA-MB-231 (triple negative) BC cells. **A.** Representative image of ARL8A and ARL8B expression in BC cell lines**. B.** Results show the relative protein levels normalized to GAPDH. Error bars represent the mean ± SD of at least three independent experiments. The statistical analysis was performed applying a One-ANOVA with Dunnett's test. ns – non-significant, * $P<0.05$.

ARL8A and *ARL8B* are efficiently silenced in HCC1806 cells

Given that *ARL8A* and *ARL8B* were shown to be upregulated in HCC1806 cells, we decided to use this cell line to test the modulation of these two proteins has an impact on cells' tumorigenic features. To achieve this, we started by silencing *ARL8A* or *ARL8B* in HCC1806, using lentiviruses encoding for shRNAs 1 (C11) and 2 (C12) to silence *ARL8A*, shRNAs 1 (B7) and 2 (B9) to silence *ARL8B.* Then, silenced HCC1806 cells were used to analyze ARL8A and ARL8B mRNA and protein expression by real-time qPCR and immunoblotting, respectively. As shown in Figure 29 A and B, both *ARL8A* and *ARL8B* were efficiently silenced in HCC1806 cells. In the case of *ARL8A* the silencing efficiencies ranged from 66.7 % to 72.6% silencing efficiencies for shRNA 1 (C11) and from 66.2 % to 71.3 % for shRNA 2 (C12) compared with shRNA control (Mission) (Figure 29 A). For ARL8B, the silencing efficiencies, relative to shRNA control (Mission), ranged from 69.9 % and 82.3 % for shRNA 1 (B7) and from 59.8% and 80% for shRNA 2 (B9) (Figure 29 B).

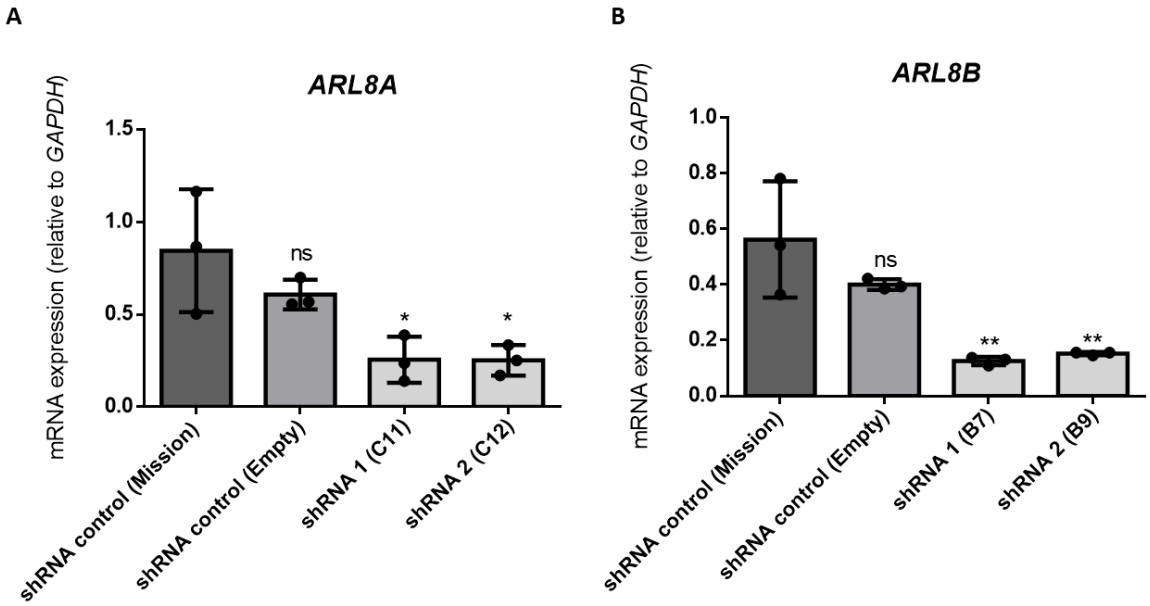

Figure 29 - *ARL8A* and *ARL8B* are efficiently in HCC1806 cells. Lentiviral particles were used to transduce HCC1806 cells with different shRNAs to silence *ARL8A* and *ARL8B*. Transduced cells were selected with puromycin, total RNA was extracted, and cDNA was synthesized. mRNA expression was measured by real-time qPCR, using *GAPDH* as a housekeeping gene. Results show the relative ratios normalized to *GAPDH*. Error bars represent the mean ± SD of *three* independent experiments. The statistical analysis was performed applying a One-ANOVA with Dunnett's test. ns – non-significant, * $P<0.05$, ** $P<0.01$.

ARL8A and *ARL8B* silencing in HCC1806 was also assessed by immunoblotting. As shown in Figure 30, ARL8A protein levels decrease upon silencing with shRNA 1 (C1) and shRNA 2 (C2), since we observed an almost complete disappearance of the upper band under these conditions, when compared to both control shRNAs (Mission and Empty). In the case of ARL8B, we observed a decrease in the corresponding band for both shRNA 1 (B7) and shRNA 2 (B9), compared with both controls. In the case of shRNA 1 (B7), protein levels are lower than the ones corresponding to shRNA 2 (B9), which goes in line with the results obtained from the mRNA analysis. Thus, this analysis allowed us to confirm the efficient silencing of *ARL8A* and *ARL8B* in HCC1806 cells. These cells were further used for the functional assays.

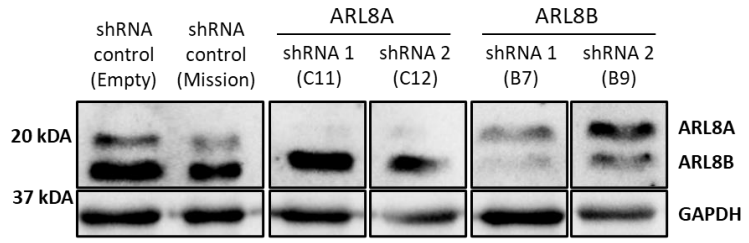

Figure 30 - ARL8A and ARL8B protein levels upon silencing in HCC1806 cells. Lentiviral particles were used to transduce HCC1806 cells with different shRNAs to silence *ARL8A* and *ARL8B*. Transduced cells were selected with puromycin, total protein was extracted, and immunoblotting analysis was performed using an antibody that recognizes both ARL8A and ARL8B isoforms. GAPDH was used as an internal control.

ARL8A and *ARL8B* silencing does not impair HCC1806 cell proliferation

ARL8B was shown to impact tumor volume *in vivo* in prostate cancer [256]. Moreover, the same study showed that ARL8B silencing impairs proliferation in nutrient-deficient conditions [256]. It is also known that lysosome exocytosis is important for membrane repair upon cell division, a process that is crucial for sustained cell proliferation [216]. Additionally, ARL8B was shown to regulate lysosome exocytosis in radiation-resistant BC cells [278]. Therefore, we decided to assess if the depletion of *ARL8A* and *ARL8B* impairs proliferation of HCC1806 cells in nutrient-rich conditions. We used transduced HCC1806 cells to assess cell proliferation, using two methods – MTT assay and trypan blue exclusion test. The results depicted in Figure 31 A showed no difference in metabolic activity between control shRNAs (Mission and Empty) and shRNAs 1 and 2 (C11 and C12) targeting *ARL8A*. The same was observed for shRNAs 1 and 2 (B7 and B9), which target *ARL8B* (Figure 31 B), indicating that ARL8 proteins do not regulate the metabolic activity of BC cells.

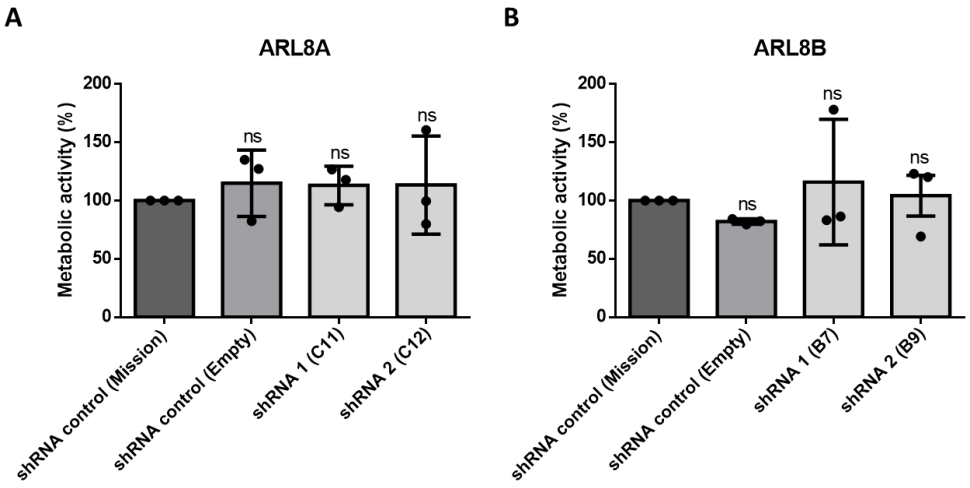

Figure 31 - *ARL8A* or *ARL8B* silencing does not affect the metabolic activity of HCC1806 cells. HCC1806 cells silenced for *ARL8A* and *ARL8B* were seeded in 96-well plates. Afterwards, cells were incubated with MTT, and the formed formazan crystals were dissolved with DMSO. Absorbance was measured at 570 nm and 690 nm (to remove background). Absorbances were calculated as A570nm - A690nm and were normalized to shRNA control (Mission). Results are represented as mean ± SD of three independent experiments. The statistical analysis was performed applying a One-ANOVA with Dunnett's test, ns – non-significant.

To confirm the results obtained through the MTT assay, we also analyzed cell proliferation using the trypan blue exclusion assay. The percentage of viable cells for each condition was calculated by normalizing the number of live cells to shRNA control (Mission) and the results are represented as the percentage of live cells. As shown in Figure 32 A, *ARL8A* silencing with shRNAs 1 and 2 (C11 and C12) leads to no differences in the percentage of viable cells, compared with control

shRNAs (Mission and Empty). In the case of shRNAs 1 and 2 (B7 and B9), which target *ARL8B*, similar results were obtained (Figure 32 B), suggesting that neither ARL8A nor ARL8 regulate cell viability.

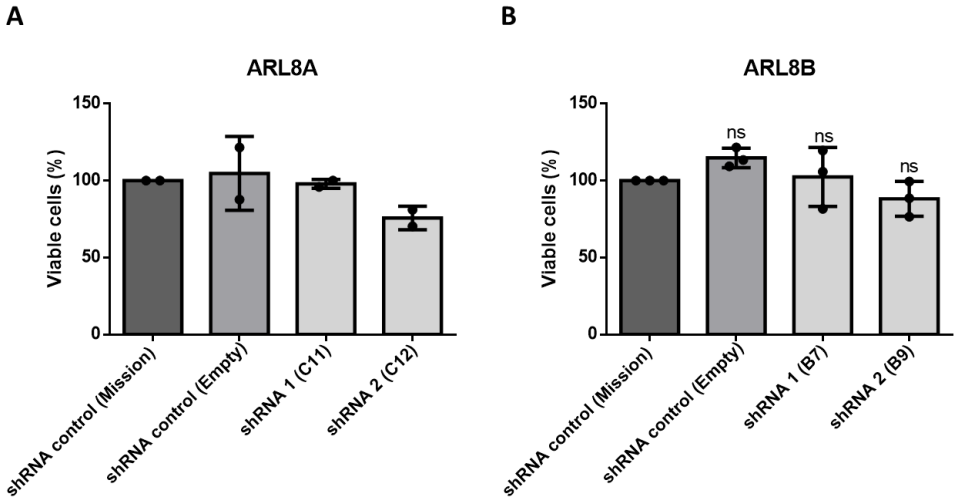

Figure 32 - *ARL8A* or *ARL8B* silencing does not affect cell viability of HCC1806 cells. HCC1806 cells silenced for *ARL8A* ort *ARL8B* were seeded in 96-well plates. Afterwards, cells were detached and stained with trypan blue to exclude dead (blue) cells. Live and dead cells were counted using a Neubauer chamber and the percentage of viable cells was normalized to shRNA control (Mission). **A.** ARL8A. Results are represented as mean ± SD of two independent experiments. **B.** ARL8B. Results are represented as mean ± SD of three independent experiments. The statistical analysis was performed applying a One-ANOVA with Dunnett's test, ns – non-significant.

Taken together, the results obtained with the MTT and trypan blue exclusion methods suggest that, in nutrient-rich conditions, neither ARL8A nor ARL8B regulate cell proliferation of HCC1806 BC cells.

ARL8A and *ARL8B* silencing impairs HCC1806 collective cell migration

As mentioned before, cell migration is an essential feature of cancer cells and it is crucial for successful invasion of the surrounding tissues and colonization of distant organs, and, therefore, metastasis formation [296]. It has been shown that ARL8B silencing reduces the migratory capacity of prostate cancer cells [256]. Moreover, lysosome positioning and exocytosis were shown to promote cancer cell migration [297].

Although we did not observe any differences in migration upon *ARL8B* silencing in MDA-MB-231 cells (Figure 19), we wanted to understand if the depletion of *ARL8A* or *ARL8B* has an impact on the migratory capacity of HCC1806 BC cells. To do this, we used a wound healing "scratch" assay to assess collective migration of HCC1806 silenced for *ARL8A* or *ARL8B*. Wound closure percentages

were calculated for each shRNA and normalized to shRNA control (Mission). As shown in Figure 33, we observed a significant reduction (34.6 %) in the wound closure upon *ARL8A* silencing with shRNA 1 (C11) and (30.7 %) with shRNA 2 (C12), when compared with shRNA control (Mission).

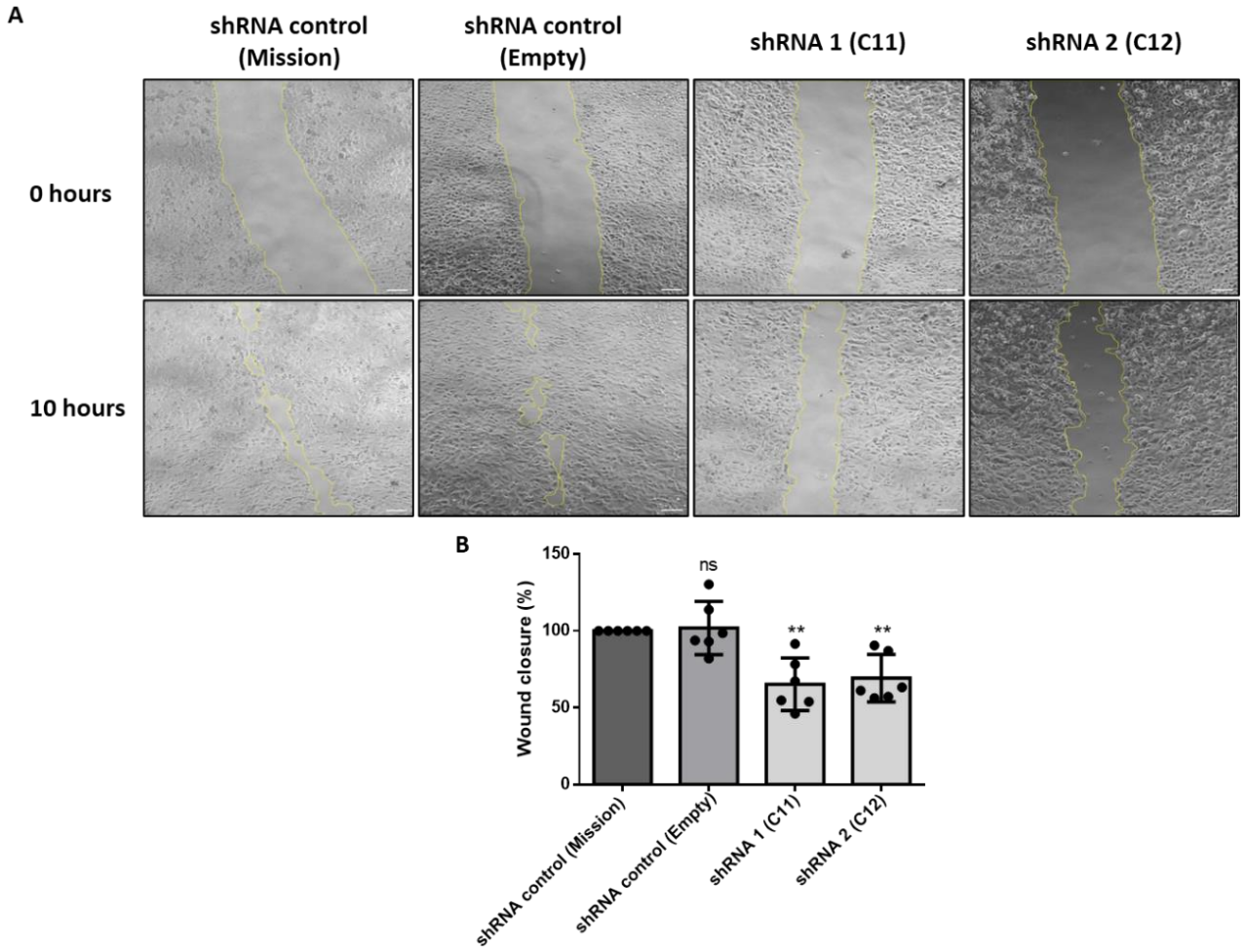

Figure 33 - *ARL8A* silencing decreases collective cell migration in HCC1806 cells. HCC1806 cells silenced for *ARL8A* were allowed to grow until a monolayer was formed. Cells were then starved ON in serum-free media and treated with mitomycin C to inhibit proliferation. Scratches were made using a pipette tip. Cell migration was induced with complete medium, and images were acquired at 0 hours and 10 hours. **A.** Representative images were taken at 0 hours and 10 hours. Yellow lines represent the wound area measured in Fiji. Scale Bar: 100 µm. **B.** Wound closure percentages were measured as follows: [1 - (gap area at t = 10 hours/gap area at t = 0 hours) x 100]. The results were normalized to shRNA control (Mission). Results are represented as mean ± SD of six independent experiments. The statistical analysis was performed applying a One-ANOVA with Dunnett's test, ns – non-significant, **p<0.01.

We also observed a reduction in the wound closure percentage of HCC1806 cells upon *ARL8B* silencing, although only significantly for shRNA 2 (B9) (Figure 34). Specifically, a reduction of 24.7 % in wound closure percentage was obtained with shRNA 1 (B7) and 48.5 % with shRNA 2 (B9), when compared with shRNA control (Mission).

In conclusion, these results suggest that both *ARL8A* or *ARL8B* depletion impairs collective cell migration of HCC1806 BC cells, suggesting a role for these two proteins in the regulation of BC cell migration.

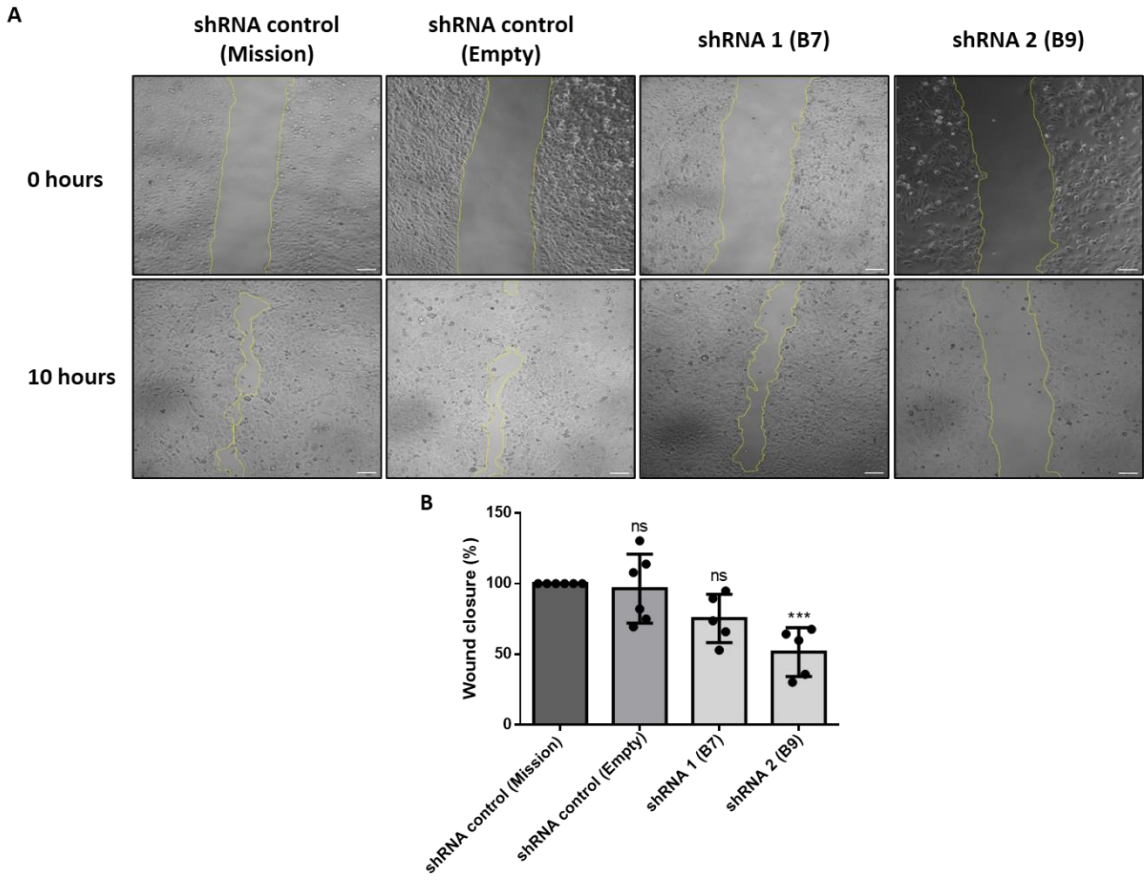

Figure 34 - *ARL8B* silencing decreases collective cell migration in HCC1806 cells. HCC1806 cells silenced for *ARL8B* were allowed to grow until a monolayer was formed. Cells were then starved ON in serum-free media and treated with mitomycin C to inhibit proliferation. Scratches were made using a pipette tip. Cell migration was induced with complete medium, and images were acquired at 0 hours and 10 hours. **A.** Representative images were taken at 0 hours and 10 hours. Yellow lines represent the wound area measured in Fiji. Scale Bar – 100 µm. **B.** Wound closure percentages measured as follows: [1 - (gap area at t = 10 hours/gap area at t = 0 hours) x 100]. The results were normalized to shRNA control (Mission). Results are represented as mean ± SD of at least five independent experiments. The statistical analysis was performed applying a One-ANOVA with Dunnett's test, ns – non-significant, **p<0.01.

ARL8B silencing impairs HCC1806 BC single cell migration

To confirm the role of ARL8B in HCC1806 in cell migration, we also assessed if the silencing of this protein impairs migration at a single-cell level. For this, we used a transwell migration (Boyden chamber) assay. The percentage of migrating cells was normalized to shRNA control (Mission). As depicted in Figure 35, a decrease in the migration of HCC1806 cells upon ARL8B

silencing was observed, although it was only significant for shRNA 2 (B9) (Figure 35 A and B). Specifically, a reduction of 5.5 % in migration was obtained with shRNA 1 (B7) and 42 % with shRNA 2 (B9), when compared with shRNA control (Mission). Taken together these results suggest that ARL8B regulates BC cell migration collectively and at a single-cell level.

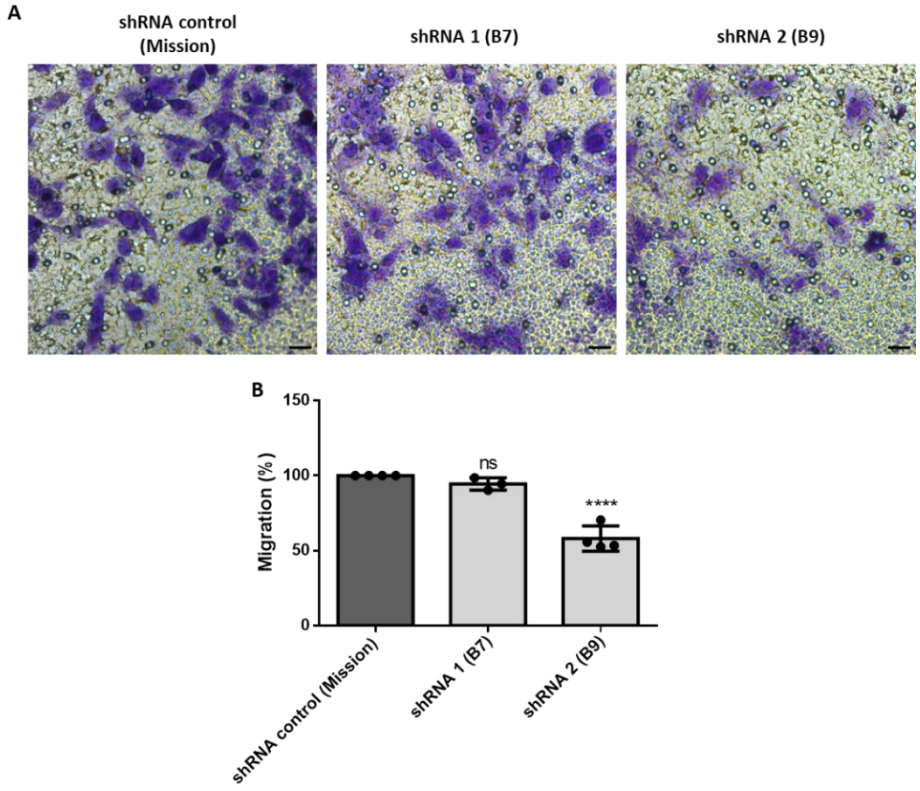

Figure 35 - *ARL8B* silencing decreases single cell migration in HCC1806 cells. HCC1806 cells silenced for ARL8B were seeded on the upper chamber of a transwell and allowed to migrate towards the lower chamber containing a chemoattractant (complete medium with 10% serum). Then, cells that migrated to the lower chamber were stained with crystal violet and counted. **A.** Representative images taken from the lower chambers after staining the nuclei with crystal violet. Scale bar: 50 µm. **B.** The percentage of migrating cells of each condition was normalized to shRNA control (Mission). Results are represented as mean ± SD of at least three independent experiments. The statistical analysis was performed applying a One-ANOVA with Dunnett's test, ns – non-significant, ****p<0.0001.

ARL8B but not *ARL8A* silencing impairs HCC1806 BC cell invasion in 3D

Together with migration, cancer cell invasion is fundamental for metastasis formation. Cancer cells acquire the capacity to remodel and degrade the ECM, to invade surrounding and distant tissues [64]. ARL8B was shown to promote prostate cancer cell invasion in 2D and 3D *in vitro* assays, as well as metastasis formation in mice [256]. Also, in BC radiation-resistant cells, ARL8B depletion leads to a decrease in cell invasion, in a process dependent on lysosome exocytosis [256].

Lysosome exocytosis is known to play a role in cancer cell invasion, through the secretion of proteases that lead to ECM remodeling and degradation [216].

Therefore, we decided to assess if ARL8A and ARL8B regulate HCC1806 cell invasion. To do this, we used spheroids, which better mimic *in vivo* tumors. In this assay, spheroids were formed with HCC1806 cells silenced for *ARL8A* or *ARL8B.* Moreover, fully formed spheroids were embedded in Matrigel, and invasion was monitored for 4 days. The invasion area was quantified by dividing the total spheroid area at 4 days by the total spheroid area at 0 days. As depicted in Figure 36, the invasion area of HCC1806 cells after 4 days is not altered upon silencing of *ARL8A*. Particularly, the fold increase in invasion area was found to be similar for shRNA 1 (C11) and shRNA 2 (C12), when compared with shRNA control Mission (Figure 36 B). Moreover, it is possible to observe that the invasion pattern was found to be different from the one obtained with MDA-MB-231 cells (Figure 24). Indeed, instead of the spindle-like protrusions observed for MDA-MB-231 cells, HCC1806 cells seem to form "bud-like" projections.

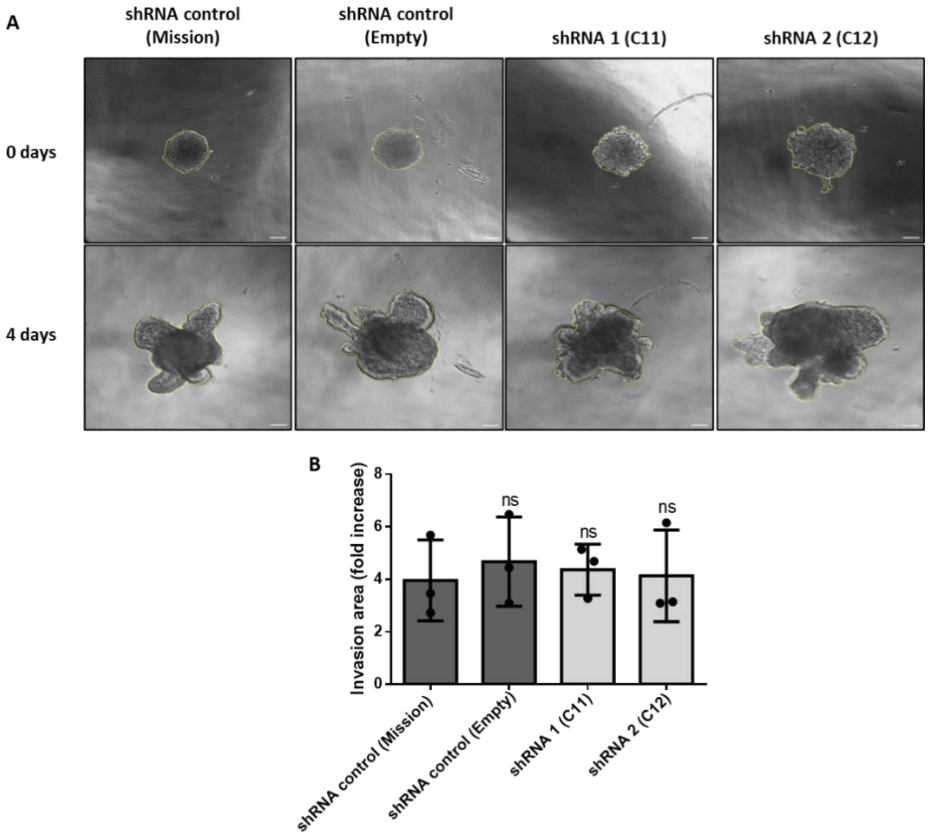

Figure 36 - *ARL8A* silencing does not affect HCC1806 cell invasion into Matrigel. HCC1806 cells silenced for *ARL8A* were used to form spheroids. Then, fully formed spheroids were embedded in Matrigel and invasion was monitored for 4 days. **A.** Representative images were taken at 0 hours and 4 days. Yellow lines represent the spheroid total area. Scale bar: 100 µm. **B.** Invasion area quantification, calculated by dividing the total spheroid area at 4 days by the total spheroid area at 0 days. The results are represented as mean ± SD of at least three independent experiments. The statistical analysis was performed applying a One-ANOVA with Dunnett's test, ns, non-significant.

Curiously, we observed that *ARL8B* silencing leads to a significant decrease in the invasion area of HCC1806 spheroids after 4 days (Figure 37). Specifically, the invasion area (fold increase) was found to be 1.7 x lower for shRNA 1 (B7) and 1.8 x lower for shRNA 2 (B9), when compared with shRNA control (Mission) (Figure 37 B). Taken together, these results suggest that ARL8B but not ARL8A regulates 3D cell invasion of HCC1806 in Matrigel.

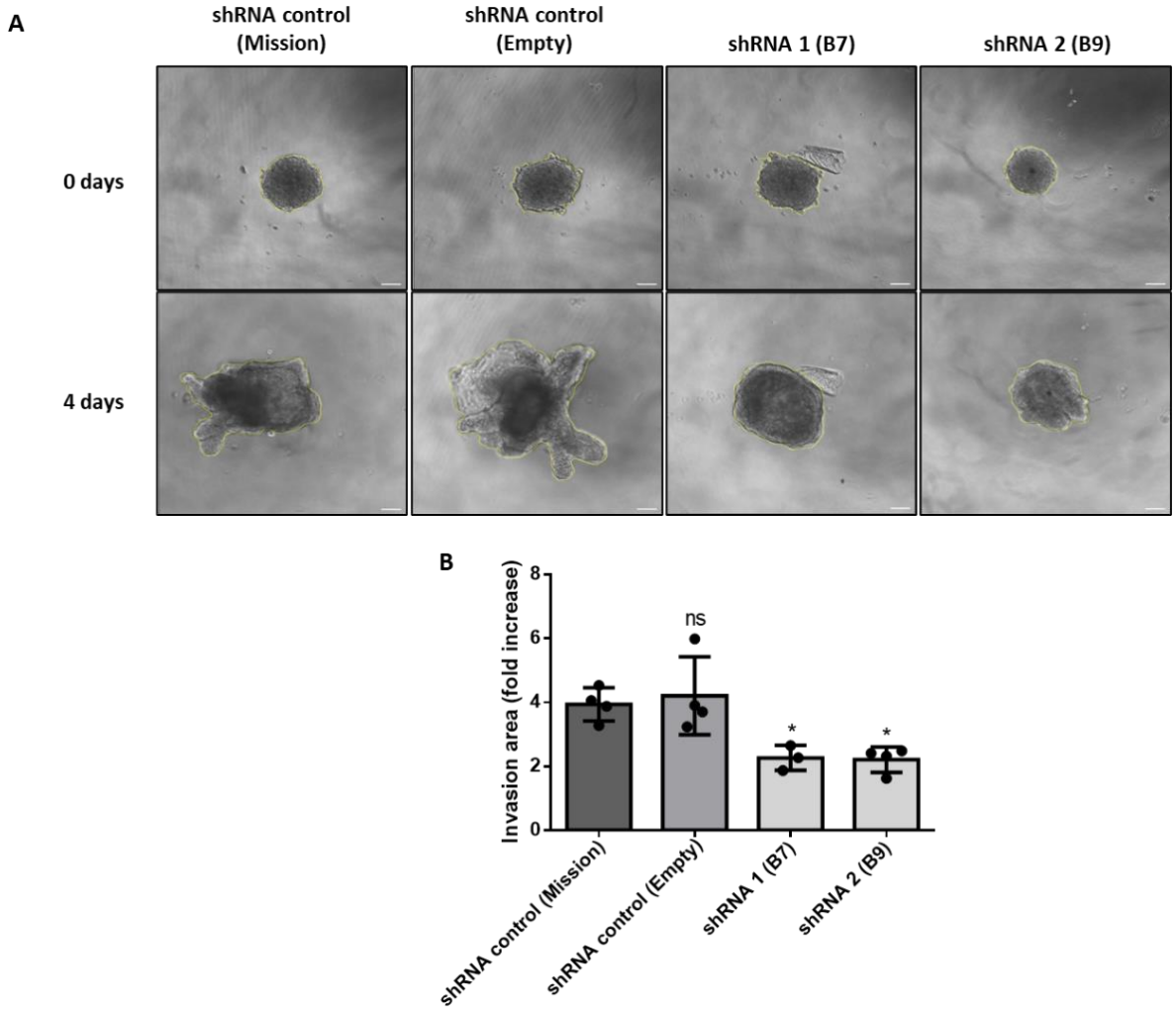

Figure 37 - *ARL8B* silencing reduces HCC1806 cell invasion into Matrigel. HCC1806 cells silenced for *ARL8B* were used to form spheroids. Then, fully formed spheroids were embedded in Matrigel and invasion was monitored for 4 days. **A.** Representative images were taken at 0 hours and 4 days. Yellow lines represent the spheroid total area. Scale bar: 100 µm. **B.** Invasion area quantification, calculated by dividing the total spheroid area at 4 days by the total spheroid area at 0 days. The results are represented as mean ± SD of at least three independent experiments. The statistical analysis was performed applying a One-ANOVA with Dunnett's test, ns, non-significant, *p<0.05.

To confirm that these observations were mainly due to ECM remodeling/degradation and not because of differences in cell proliferation, we decided to evaluate if 3D cell growth is impaired upon ARL8B silencing in HCC1086 cells. For this, we used a commercially available kit to assess

cellular ATP levels as a measure of cell viability. Briefly, cell spheroids were incubated with CellTiterGlo ® 3D Reagent and the luminescence measured in a spectrofluorometer. As shown in Figure 38, no differences in cell viability were found for shRNA 2 (B7), when compared with shRNA control (Mission). On the other hand, *ARL8B* silencing leads to a significant decrease (43.4 %) in cell viability for shRNA 2 (B9). Indeed, it is possible to observe a decrease in spheroid area at day 0 for shRNA 2 (B9) (Figure 37 A), suggesting that, in fact, cell proliferation is impaired in this condition and that ARL8B may regulate cell viability on a 3D setting.

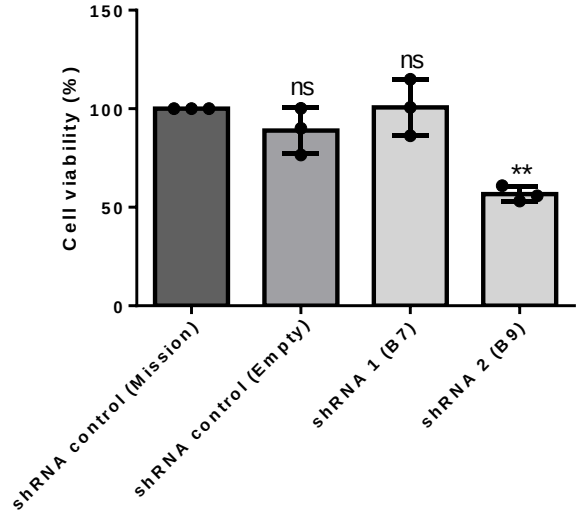

Figure 38 - 3D cell viability upon *ARL8B* silencing in HCC1806 cells. HCC1806 cells silenced for *ARL8B* were used to form spheroids. Then, fully formed spheroids were incubated with CellTiterGlo® 3D reagent, and luminescence was acquired on a spectrophotometer. The cell viability percentage was calculated by normalizing luminescence values for each condition to shRNA control (Mission). Results are represented as mean ± SD of three independent experiments. The statistical analysis was performed applying a One-ANOVA with Dunnett's test, ns – non-significant, **p<0.01.

In order to confirm that the impairment in cell invasion upon ARL8B depletion is not due to the obtained differences in cell proliferation, we decided to evaluate 3D cell invasion in serum-free conditions. First, we confirmed the feasibility of the assay by assessing the cell viability of HCC1806 spheroids after 7 days in serum-free medium. For this, we stained spheroids with FDA, which labels viable cells and produces green fluorescein. We also used the nucleic acid red dye PI to label dead cells. In Figure 39 it is possible to observe that upon FDA/PI staining, HCC1806 spheroids presented an outer layer of viable green cells, while red dead cells were more concentrated in the core area (inner layer). Moreover, even in serum-free conditions, the spheroid area for shRNA 2 (B9) was found to be smaller, when compared with shRNA control (Mission) and shRNA 1 (B7). Nonetheless, this analysis allowed us to conclude that the spheroids presented the desired features of a 3D

culture, where the outer layer is enriched in proliferating/viable cells and the inner layer presents dead cells characteristic of the necrotic core.

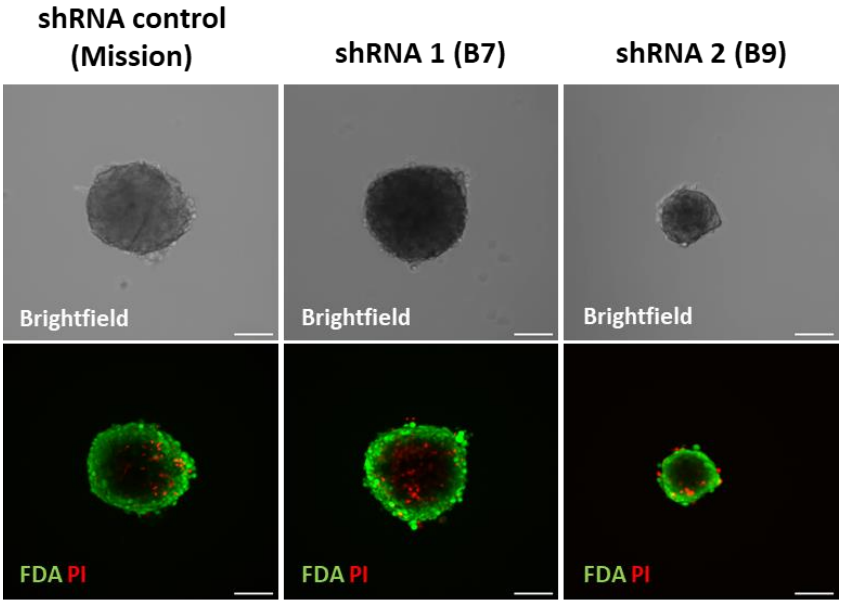

Figure 39 - Viability of HCC1806 cell spheroids in serum-free conditions. HCC1806 cells silenced for ARL8B were used to form spheroids. Then, fully formed spheroids were incubated in serum-free medium for 7 days. Afterwards, spheroids were stained with FDA (green) and PI (red) to label live and dead cells, respectively. Confocal images were acquired and are represented as z-projections of the spheroid center area. Scale bars: 100 µm.

For the invasion assay in serum-free medium, we mixed Matrigel with a fluorogenic substrate for proteases, namely DQ™ Red BSA. In this case, Matrigel proteins are labelled with BODIPY dyes, which confers a strong fluorescence quenching effect. Upon degradation of the Matrigel by the proteases secreted by spheroids, the quenching is relieved, and the resulting fluorescence is acquired by fluorescent microscopy [298]. The invasion was measured using the fluorescent red signal resulting from DQ™ Red BSA degradation at 7 days, divided by the total spheroid area at 0 days. As shown in Figure 40, *ARL8B* depletion leads to a decrease in invasion area of 1.9 x for shRNA 1 (B7) and 1.7 x for shRNA 2 (B9), comparing with shRNA control (Mission). Thus, the obtained results suggest that ARL8B also regulates 3D cell invasion of HCC1806 cells in Matrigel in serum-free conditions, where cell proliferation is diminished.

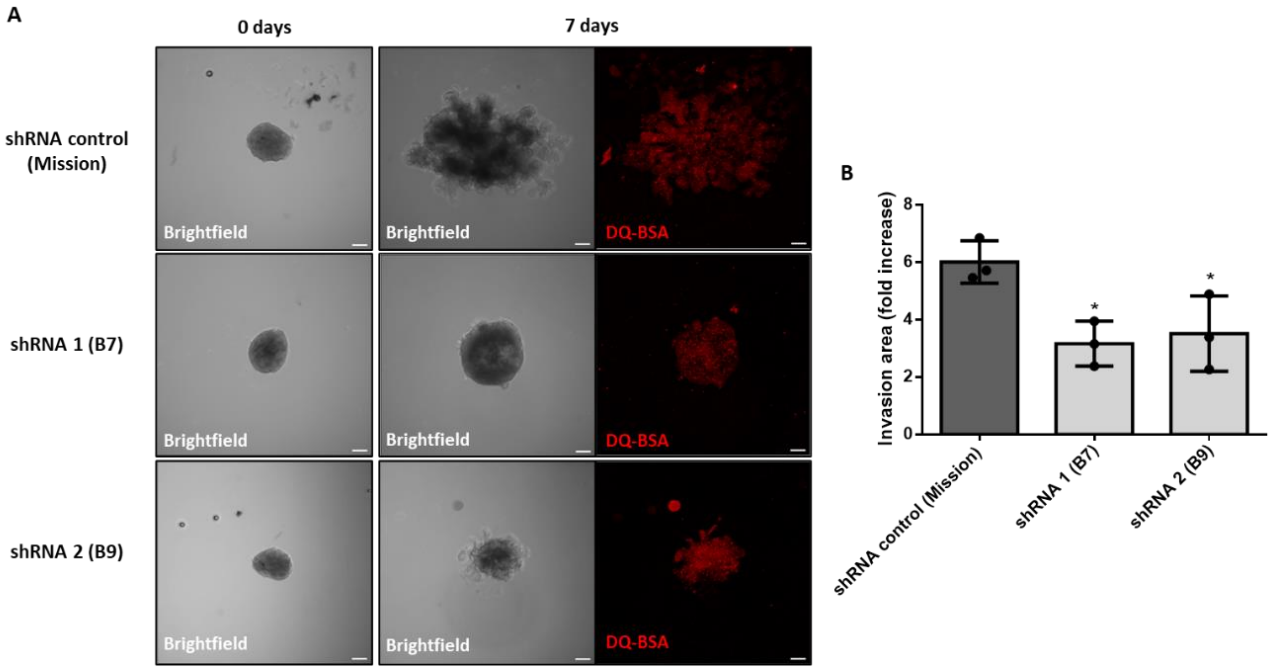

Figure 40 - *ARL8B* silencing reduces HCC1806 cell invasion into Matrigel in serum-free conditions. HCC1806 cells silenced for *ARL8B* were used to form spheroids. Then, fully formed spheroids were embedded in Matrigel, mixed with DQ™ Red BSA in serum-free medium, and invasion was monitored for 7 days. **A.** Representative confocal images taken at 0 hours and 7 days. Scale bar: 100 µm. **B.** Invasion area quantification, calculated by dividing the total spheroid area at 7 days by the total spheroid area at 0 days. The results are represented as mean ± SD of three independent experiments. The statistical analysis was performed applying a One-ANOVA with Dunnett's test, *p<0.05.

Role of ARL8B overexpression in MCF10DCIS.com 3D cell invasion

An important feature of BC progression is the transition from a non-invasive confined DCIS to an invasive IDC. In this switch, BC cells acquire invasive properties, breach the BM, and invade the surrounding tissues, ultimately leading to the formation of metastases [299,300].

Our previous results suggested that ARL8B depletion leads to a decrease in the invasion capacity of HCC1806 cells. Therefore, we decided to assess if ARL8B can also play a role in the switch from DCIS to IDC. Namely, we wanted to verify if the overexpression of ARL8B leads to the acquisition of an invasive behavior by MCF10DCIS.com cells, which mimic the *in situ* non-invasive BC tumors. To achieve this, we transduced MCF10DCIS.com cells with lentiviruses encoding ARL8B-Flag or GST-Flag. GST-Flag control was added in this experiment to account for the possible effects of cell transduction/overexpression in MCF10DCIS.com cell behavior. Then, both non-transduced MCF10DCIS.com cells and overexpressing ARL8B-Flag/GST-Flag were used to form spheroids, which were embedded in Matrigel, and the invasion was monitored for 8 days. The invasion area was

calculated by dividing the total spheroid area at 8 days by the total spheroid area at 0 days. As expected, we observed that non-transduced MCF10DCIS.com cells do not invade after 8 days in Matrigel. On the other hand, transduced MCF10DCIS.com cells overexpressing GST-Flag or ARL8B-Flag show an increase in invasion area after 8 days in Matrigel (Figure 41). These results suggest that the induced stress from cell transduction is enough to alter the cell behavior of MCF10DCIS.com cells, precluding the extraction of any conclusions from this experiment.

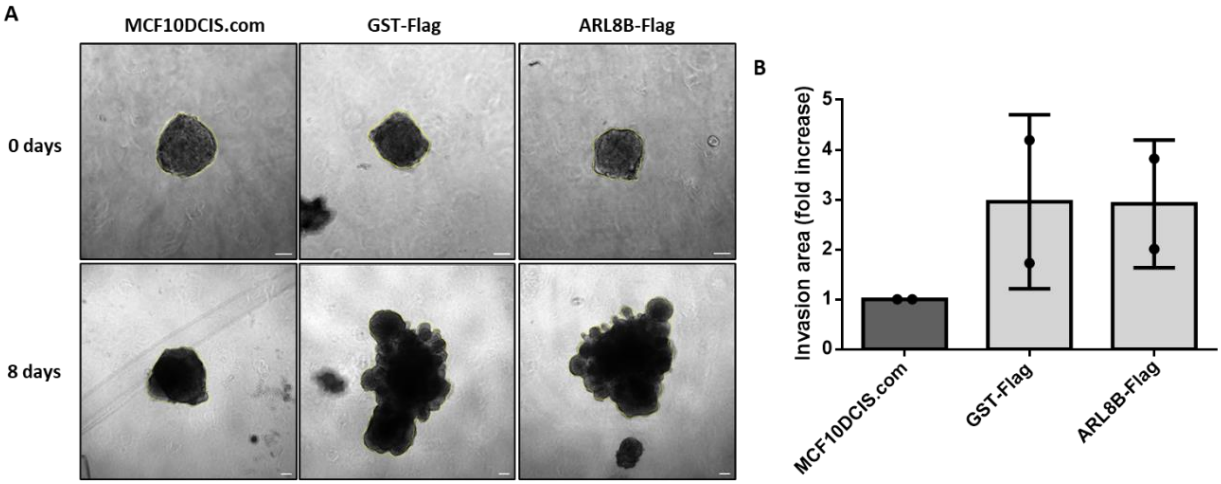

Figure 41 - ARL8B-flag overexpression in MCF10DCIS.com cell invasion in 3D. Non-transduced MCF10DCIS.com cells, MCF10DCIS.com cells overexpressing ARL8-Flag, and MCF10DCIS.com cells overexpressing GST-Flag were used to form spheroids. Then, fully formed spheroids were embedded in Matrigel and invasion was monitored for 8 days. **A.** Representative images were taken at 0 hours and 8 days. Yellow lines represent the spheroid total area. Scale bar: 100 µm. **B.** Invasion area quantification, calculated by dividing the total spheroid area at 8 days by the total spheroid area at 0 days. The results are represented as mean ± SD of at two independent experiments.

ARL8B silencing impairs lysosome exocytosis in HCC19806 cells

Lysosome exocytosis is one of the processes subverted by cancer cells to promote cell proliferation, migration, and invasion [216,297]. When lysosomes reach the cell periphery and fuse with the PM, they release their content, including proteases, which can promote ECM remodeling and degradation and, consequently, cell invasion [216]. As mentioned before, ARL8B was shown to regulate invasion in radiation-resistant BC cells, though a mechanism dependent on lysosome exocytosis. Specifically, it was shown that ARL8B silencing leads to a decrease in ionizing radiation-induced lysosomal exocytosis and cell invasion [278].

We observed that ARL8B silencing leads to a decrease in 3D invasion of invasive HCC1806 BC cells. So, we asked whether this decrease could be due to a reduction in lysosome exocytosis. To

answer this question, we first analyzed the localization of ARL8B in HCC1806 cells. For this, we transfected ARL8B-GFP or GFP alone in HCC1806 cells and stained them with LAMP1, a frequently used marker of LEs and lysosomes. As expected, confocal microscopy analysis showed that ARL8B-GFP co-localizes with LAMP1 in HCC1806 BC cells. On the other hand, no co-localization between GFP and LAMP1 was observed. Moreover, we found that HCC1806 cells transfected with GFP showed mostly clustered lysosomes near the nucleus, which is not so clear in cells transfected with ARL8B-GFP (Figure 42). This is probably due to the increased lysosomal anterograde movement towards the cell periphery, which is known to be regulated by ARL8B [206]. Thus, our results confirm that Arl8B is present in HCC1806 lysosomes and that, when overexpressed, it leads to a redistribution of the lysosomes to the cell periphery.

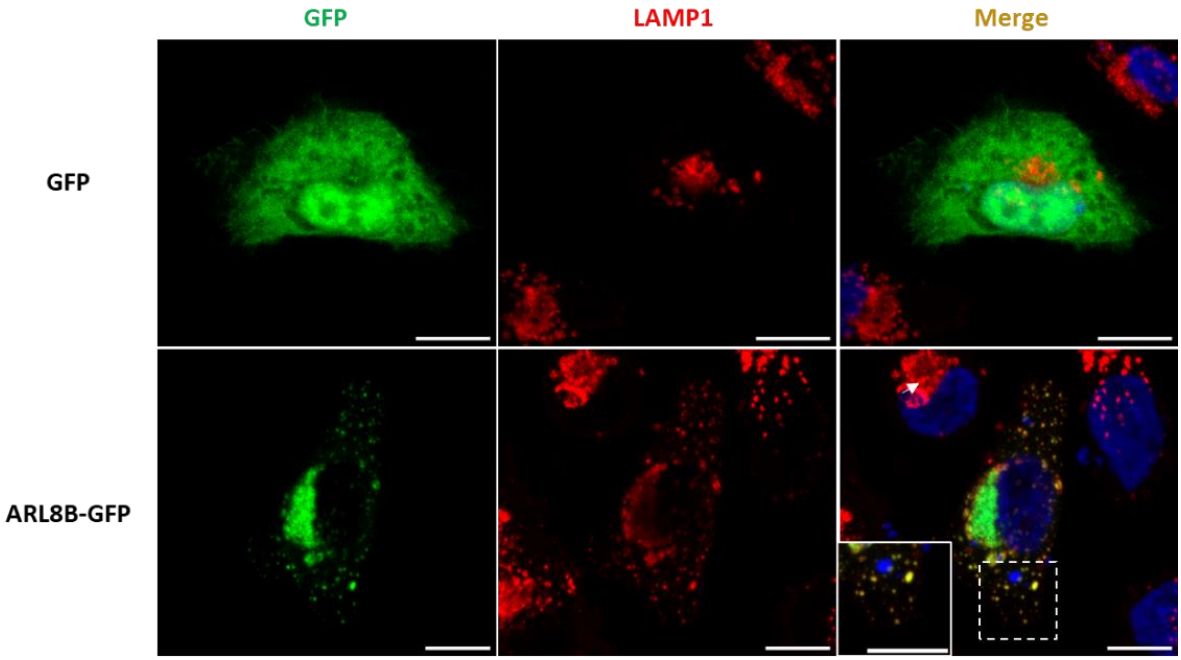

Figure 42 - ARL8B localizes to lysosomes in HCC1806 cells. HCC1806 cells were transfected with GFP or ARL8B-GFP. Afterwards, fixed cells were incubated with LAMP1-647 antibody to stain LE/lysosomes and DAPI to stain nuclei. Confocal images were acquired and are represented as z-projections. GFP (green), LAMP1 (red), nuclei (blue). The inset is a magnified image of the dashed region and ARL8B-GFP co-localization with LAMP1 is indicated by a white arrow. Scale bars, 10 µm.

After confirming that ARL8B localizes to lysosomes in HCC1806 BC cells, we analyzed the effect of silencing ARL8B on lysosome exocytosis in the same cell line. To achieve this, we used cells silenced for ARL8B and assessed Ca^{2+}- dependent lysosome exocytosis using two methods. First, we used flow cytometry to assess the presence of LAMP1 staining at the cell surface. Briefly, lysosome exocytosis was stimulated with ionomycin, a known Ca^{2+} ionophore. Cells were then stained a

LAMP1 antibody that detects the luminal domain of the protein, expressed at the cell surface upon lysosome fusion with the PM. Finally, dead cells were labeled with PI, and LAMP1/PI signals were measured by flow cytometry (Figure 43 A). The results are represented as the percentage of LAMP1 positive/PI negative cells and normalized to shRNA control (Mission). We were not able to detect any differences in Ca^{2+}- dependent lysosome exocytosis, using this methodology (Figure 43 B). However, some technical drawbacks that will be discussed later may help explain these results.

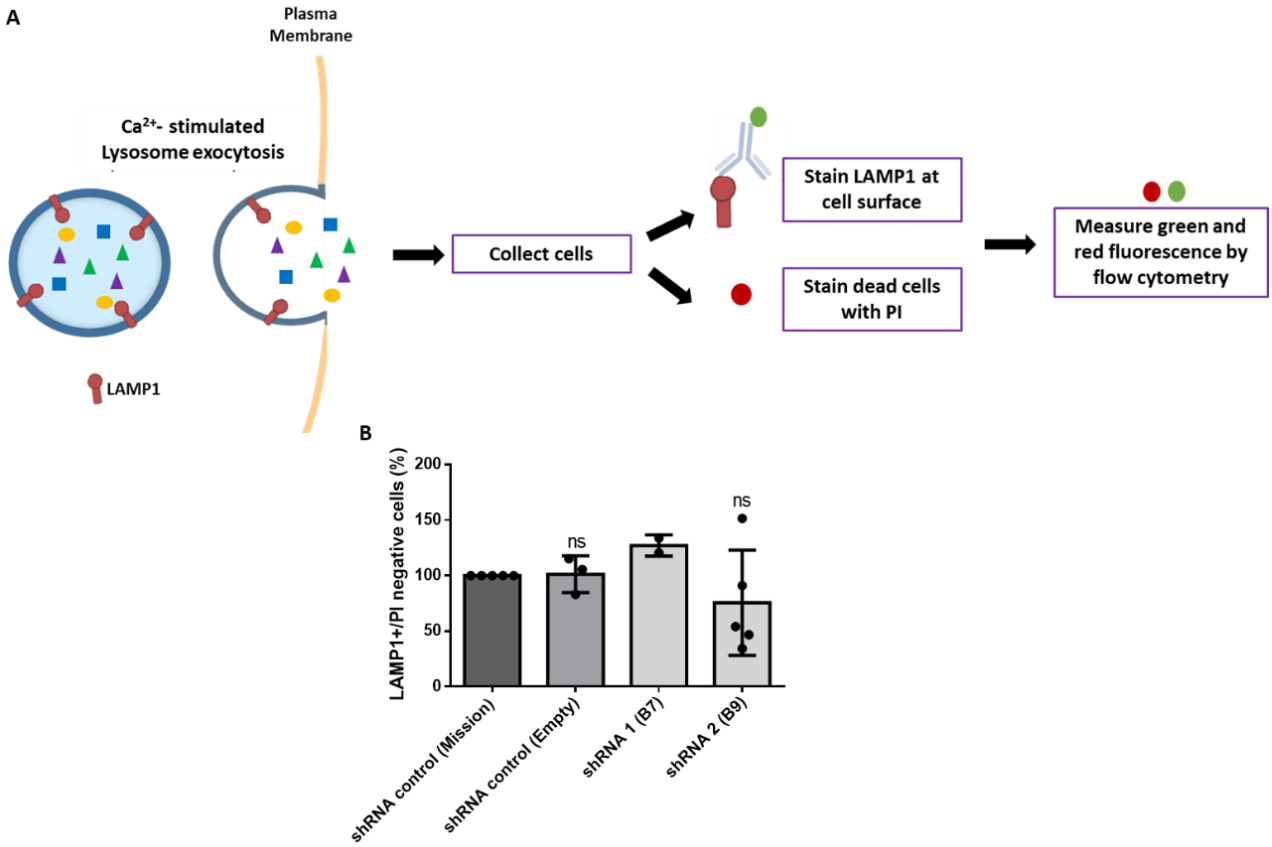

Figure 43 - *ARL8B* silencing does not affect LAMP1 cell-surface levels in HCC1806 cells HCC1806 cells were transduced with lentiviruses encoding different shRNAs targeting ARL8B. After seeding, cells were incubated with 10 µM ionomycin and 4 mM $CaCl_2$ to stimulate lysosome exocytosis. Cells were collected, stained with anti-LAMP1 antibody and PI (to label dead cells), and analyzed by flow cytometry. **A.** Schematic representation of the methodology used to measure LAMP1 at levels at the cell surface. **A.** The results represent the percentage of LAMP1-positive (LAMP1+) cells and PI-negative (PI−) cells for each condition, normalized to the shRNA control (Mission). Results are represented as mean ± SD of at least two independent experiments. The statistical analysis was performed applying a One-ANOVA with Dunnett's test. ns, non-significant, *P<0.05, **** P<0.0001.

Given that LAMP1 is not specific of lysosomes and is also present in the membrane of LEs, we used a second approach to assess Ca^{2+}- dependent lysosome exocytosis through the release of the lysosomal enzyme β-hexosaminidase. In this assay, HCC1806 silenced for *ARL8B* were seeded and lysosome exocytosis was stimulated with ionomycin. Afterwards, cells and supernatants were

collected and β-hexosaminidase release was measured by adding a fluorogenic substrate that is hydrolyzed by hexosaminidases and emits fluorescence, which can be measured on a spectrofluorometer (Figure 44 A). Results for each condition are represented as the percentage of β-hexosaminidase release, normalized to shRNA control (Mission). As shown in Figure 44 B, *ARL8B* silencing leads to a decrease in CA^{2+}- dependent lysosome exocytosis. Moreover, we observed a reduction in β-hexosaminidase release of 40.2% and 87% for shRNA 1 (B7) and shRNA 2 (B9), respectively, when compared to shRNA control (Mission). Taken together, these results suggest that ARL8B regulates lysosome exocytosis in HCC1806 cells.

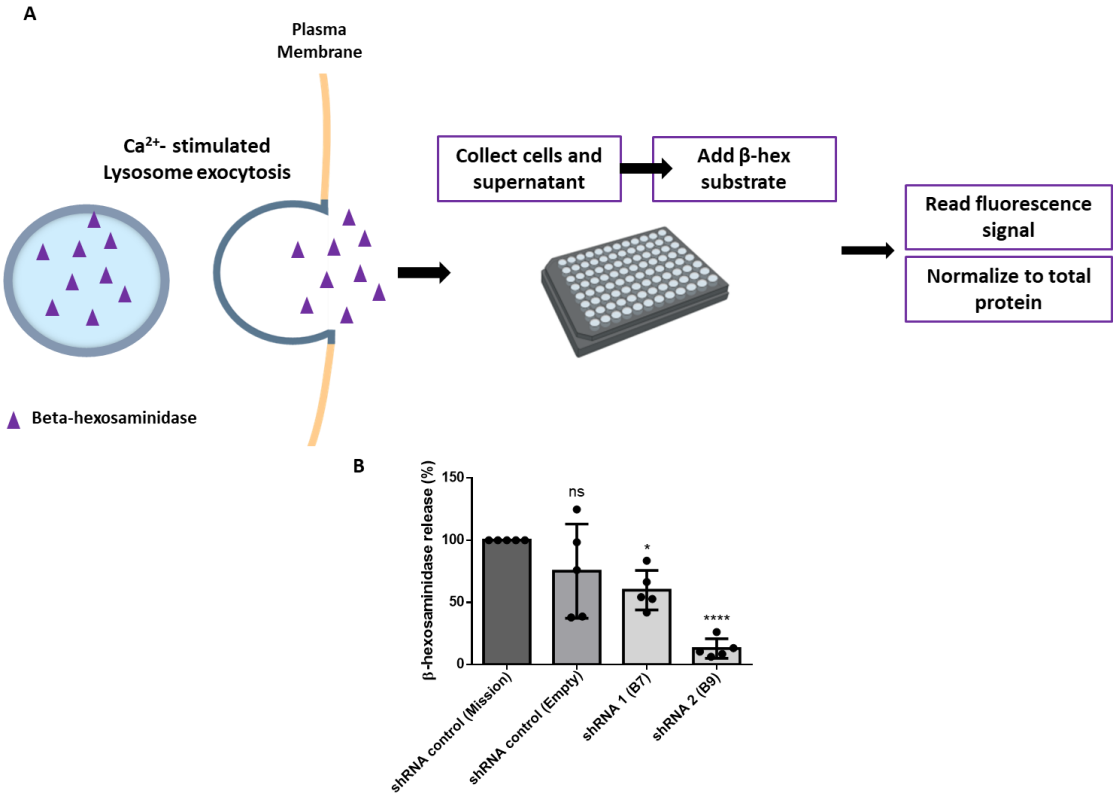

Figure 44 - *ARL8B* silencing impairs β-hexosaminidase release in HCC1806. HCC1806 cells were transduced with lentiviruses encoding different shRNAs targeting ARL8B. After seeding, cells were incubated with 10 µM ionomycin and 4 mM $CaCl_2$ to stimulate lysosome exocytosis. Cell extracts and supernatants were collected and β-hexosaminidase release was measured by spectrophotometry, upon addition of 4-MU-β-D-GlcNAc. **A**. Schematic representation of the methodology used to measure β-hexosaminidase (β-hex) release. **B.** The results represent the percentage of β-hexosaminidase release (activity), normalized to the shRNA control (Mission). Results are represented as mean ± S of five independent experiments. The statistical analysis was performed applying a One-ANOVA with Dunnett's test. ns, non-significant, **P*<0.05, **** *P*<0.0001.

ARL8B silencing does not affect the expression of EMT markers in HCC1806 cells

EMT is a process frequently used by cancer cells to promote migration and invasion and it is associated with the several steps of the metastatic cascade [62]. During this transition, epithelial cells acquire mesenchymal features losing their cell-to-cell adhesions and polarity, leading to higher motility and increased invasive properties [75]. EMT is regulated by several TFs, such as SNAIL and SLUG, which control the expression of genes that promote mesenchymal features and inhibit the expression of genes that confer epithelial characteristics (*e.g.,* E-cadherin) [73].

To assess if the depletion of ARL8B in HCC1806 cells impacts on EMT, we decided to measure the protein levels of SLUG and E-cadherin by immunoblotting. As depicted in Figure 45, no alterations were observed in SLUG and E-cadherin protein expression, upon silencing of ARL8B in HCC1806 cells. Moreover, we also included MCF-7 cells as a control, since they exhibit more epithelial-like features [301]. As expected, E-cadherin expression is higher in this cell line, when compared with the HCC1806 samples. Likewise, the low expression of SLUG also highlights the more epithelial characteristics of MCF-7. Thus, these results suggest that ARL8B does not affect the regulation of EMT in HCC1806 BC cells.

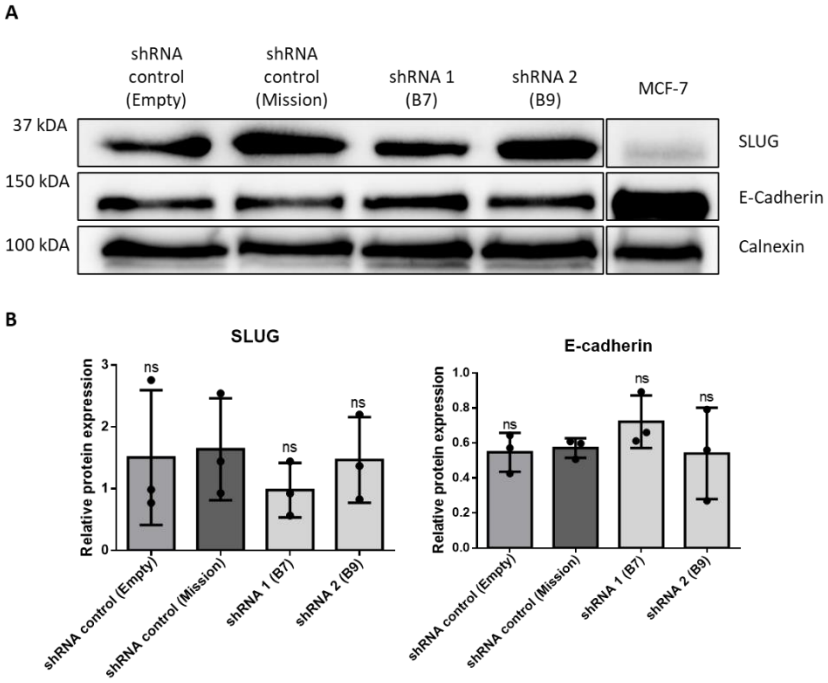

Figure 45 - Legend on the next page.

Figure 45 - *ARL8B* silencing does not affect SLUG and E-cadherin protein levels. HCC1806 cells were transduced with lentiviruses encoding different shRNAs targeting ARL8B. Then, total protein extracts were used to detect SLUG and E-cadherin protein levels. **A**. Representative image of SLUG and E-cadherin protein expression in HCC1806 cells silenced for *ARL8B* and in MCF-7. Calnexin was used as an internal control. **B.** Results show the relative protein levels normalized to GAPDH. Error bars represent the mean ± SD of at least three independent experiments. The statistical analysis was performed applying a One-ANOVA with Dunnett's test, ns – non-significant.

Chapter 4. Discussion, conclusions, and future perspectives

Discussion

BC therapies and diagnosis methods have improved considerably over the years. However, BC remains the type of cancer with the highest number of deaths in women [1]. Moreover, as with other cancers, the formation of metastasis remains by far the major cause of mortality in these patients [62]. So, it is essential to find new strategies and therapeutic targets to impair the progression of BC. This can only be achieved by increasing the knowledge about the molecular mechanisms that cancer cells subvert to survive and disseminate. In this work, we evaluated the expression profile of the ARL subfamily members in BC samples, which allowed us to identify dysregulated genes in this disease. Moreover, we gained insights on the role of ARFRP1, ARL13B and ARL8A/B on BC progression, showing that these proteins can be further explored as potential therapeutic targets for the treatment of breast tumors.

Differential expression of *ARL* genes in breast cancer samples

Several studies have highlighted the importance of membrane traffic regulators in the progression of cancer. Specifically, it was shown that these proteins are subverted by cancer cells to overcome the barriers imposed by the microenvironment, acquire resistance to apoptosis, increase proliferation, migration, and invasion, among other features [283,284]. Members of the Rab and Arf families of small GTPases are regulators of membrane traffic and have been linked to the progression of different types of cancers, including BC [227,286].

In this work, we discovered that different *ARLs* are differentially expressed at the mRNA level, between non-tumorigenic and tumorigenic cell lines. Specifically, we found that *ARL1*, *ARL2*, *ARL5A, ARL5B*, *ARL6, ARL8B*, *ARL11*, *ARL13B*, and *ARFRP1* mRNA levels are higher in highly invasive MDA-MB-231 cell lines, when compared with non-tumorigenic MCF10A cells and non-invasive MCF10DCIS.com cells. Moreover, we performed a bioinformatic analysis for some of the genes, to assess their expression in breast tumor samples and normal adjacent breast tissues from the TCGA database. We observed that *ARL1*, *ARL8B, ARL11,* and *ARFRP1* are upregulated in tumor samples, while *ARL2* and *ARL6* are downregulated in tumor samples, compared with normal adjacent breast samples. The results obtained for ARL2 in the bioinformatic analysis are in line with what is published in the literature, *i.e.*, low *ARL2* expression is associated with more aggressive tumors[274].

On the other hand, these results show an opposite trend to that observed in cell lines, where *ARL2* mRNA expression is higher in highly invasive MDA-MB-231 cells. This could be explained by multiple factors. First, cell lines have been widely used for cancer research, due to their relatively low cost, easy handling, and lower variability among assays and, hence more reproducible results. However, there are several drawbacks to the use of cell lines. In continuous and long periods in culture, cell lines adapt and are prone to genotypic and phenotypic drifts, especially those that are widely used like MCF-7 and MDA-MB-231. These drifts can result in the selection of cell subpopulations that display different growth rates, and different hormone receptor levels, among other discrepancies including the karyotype. So, although the cell line morphology may be identical, the phenotypic and genetic characteristics may be substantially different in cell lines from different sources [302]. Secondly, cell lines do not recapitulate the high heterogeneity of BC, which can lead to different results when analyzing the expression of a given target in cell lines and patient samples. Third, and perhaps of utmost importance, small GTPases like ARLs are regulated through their activity to modulate different cellular responses. For example, ARL4D was shown to localize to the PM in its active GTP-bound state and to the mitochondria in its inactive GDP-bound state, regulating different cellular processes depending on its activity status. Likewise, although the differential expression of ARLs can be representative of their role in cancer progression, we cannot exclude that the activity of these proteins can have a higher impact on a specific phenotype than their expression. We also found that *ARL13B* is overexpressed in highly invasive MDA-MB-231 cells, which corroborates the findings previously reported by us, namely that *ARL13B* is upregulated in breast tumor cell lines and BC samples from grade II, and promotes BC cell migration and invasion[280].

In this study, we also analyzed the mRNA expression of *ARL1*, *ARL2*, *ARL8B* and *ARFRP1* in normal adjacent tissues and BC tumor samples. However, we did not observe any significant differences between normal adjacent tissues and breast cancer samples. The most plausible explanation for this is the low number of samples analyzed. Since patient samples exhibit a considerable heterogeneity among them, the statistical power of a low number of samples can be highly affected. So, it would be important to increase the number of samples to better characterize the expression of *ARL* genes in BC patient samples. mRNA and protein levels do not always correlate, which can be due to differences in mRNA and protein stability, as well as their rate of degradation [303]. Therefore, it would be important to address the protein expression of the most promising candidates in cell lines and patient samples, by immunoblotting and immunohistochemistry and verify if they show the same trend observed for mRNA levels.

ARFRP1 as a regulator of breast cancer cell migration and invasion

The mRNA expression screen and the bioinformatic analysis allowed us to select candidates to perform a functional screen, where we assessed the migratory capacity of highly invasive cancer cells after silencing *ARL1*, *ARL8B*, and *ARFRP1*. From this analysis, we found that the silencing of *ARFRP1* impairs the migratory capacity of highly invasive MDA-MB-231 cells. *Arfrp1* depletion in intestinal cells of mice was found to displace E-cadherin from the PM and promote its accumulation at the TGN, suggesting that ARFRP1 regulates the traffic of E-cadherin to the PM [176]. Although the relationship between E-cadherin expression and collective cell migration has been established in several types of tumors[304], MDA-MB-231 cells were found to lack the expression of E-cadherin[305], which suggests that the mechanism by which ARFRP1 regulates cell migration is not through the regulation of this adhesion molecule. The study conducted by Zahn and colleagues also found that Arfrp1 co-immunoprecipitated with E-cadherin binding partners, namely α-catenin, β-catenin, γ-catenin, and $p120^{ctn}$ and *Arfrp1* depletion leads to the misplacement of β-catenin, with partial localization in intracellular membranes[176]. It is well established that Wnt prevents the degradation of β-catenin and allows its translocation to the nucleus to promote the transcription of Wnt target gene expression. When the E-cadherin/β-catenin complex is disrupted, β-catenin is free to be translocated to the nucleus and activate several target genes that promote tumorigenesis[306]. Additionally, β-catenin levels were found to be increased in the cytoplasm and nucleus in 40% of primary BCs, which correlates with poor prognosis[307–309]. So, it would be important to evaluate β-catenin localization by microscopy in cells that express very low amounts of E-cadherin, like MDA-MB-231 and assess if this localization is changed upon *ARFRP1* depletion. Also, it would be important to understand if the modulation of ARFRP1 in epithelial-like BC cells that express E-cadherin, influences migration. ARFRP1 was also shown to regulate the export of Van-Gogh-like 2 (Vangl2) from the TGN, through its effector AP-1[310]. Vangl2 is a core protein of the planar cell polarity non-canonical Wnt pathway, which is essential for the cellular organization along the perpendicular axis across the plane of the tissue. Analysis of the TCGA data revealed that Vangl2 is upregulated in BC [311]. Moreover, a study found that Vangl2 regulates migration, anchorage-dependent and independent cell proliferation of basal BC cell lines, as well as tumor growth in mice [312]. So, it would also be important to evaluate if the transport of Vangl2 is impaired in BC cells depleted for ARFRP1, by assessing the localization of Vangl2 by microscopy. Moreover, we could assess if the silencing of Vangl2 also impairs migration of MDA-MB-231 cells using wound-healing assays. We would expect

that Vangl2 localization at the PM is impaired in cells silenced for ARFRP1 and that collective cell migration would be decreased upon Vangl2 silencing. Moreover, we found that the silencing of *ARFRP1* does not impair the metabolic activity of BC cells, suggesting that this protein does not regulate cell proliferation in BC.

We also found that *ARFRP1* silencing impairs 3D cell invasion in collagen I. However, although preliminary, our experiments with Matrigel suggest that *ARFRP1* silencing does not impair cell invasion in this type of matrix. Nothing is known about the role of ARFRP1 in BC, but it is plausible that differences found between the two types of matrices (collagen I and Matrigel) can help explain the results obtained. The ECM can be divided into two types - BM and interstitial matrix (IM). The BM can be found beneath the epithelial and endothelial cell layers. On the other hand, the IM forms porous 3D networks around cells to interconnect stromal cells and it is connected to the BM [295]. The main components of the BM are collagen type IV, laminin, entactin/nidogen, and proteoglycans, while the IM is mainly composed of fibrillar collagens (*e.g.,* I, III, and V) fibronectin and elastins[8]. Moreover, Matrigel is a mixture of collagen IV, laminin, entactin, and proteoglycans and it is normally used in cancer cell invasion assays to mimic the BM. So, it is possible that the silencing of *ARFRP1* does not impair the degradation and remodeling of Matrigel components, pointing towards a role for this protein in cancer invasion after BM breakdown. Also, because of its structure, collagen I degradation relies on the activity of specific MMPs, including MMP -1, -8, -13, and -14. Likewise, future experiments to analyze the MMP secretion profile upon ARFRP1 modulation would be necessary to clarify the differences between Matrigel and collagen I matrix invasion. For this, we could use gelatin zymography and MPP activity kits. Moreover, ARFRP1 was shown to function upstream of ARL1 in the recruitment of tethering factors to the TGN [177]. Curiously, Eiseler and colleagues found that ARL1 is involved in the secretion of MMPs [166]. Therefore, it would be important to verify if the silencing of *ARFRP1* in invasive BC cells affects the recruitment of ARL1 to the TGN and consequently MMP secretion.

Since we found that ARFRP1 regulates the invasion of BC cells in collagen I, we assessed if this small GTPase also has a role in invadopodia function. These actin-rich structures are formed in cancer cells and allow ECM remodeling/degradation required for cell invasion [115]. Furthermore, the formation of invadopodia has been implicated in several steps of the metastasis cascade [114]. In 2D *in vitro* experiments, invadopodia are formed on the ventral surface of invasive cancer cells and allow the focal degradation of the underlying ECM. When cells are plated on gelatin, invadopodia appear as dot-like structures which mainly localize to the perinuclear region. In our experiments,

we were able to detect the formation of these structures in MDA-MB-231 cells, but we did not find any significant differences in invadopodia activity upon *ARFRP1* silencing. One factor that could help to explain these results is the structural difference between collagen I and gelatin. Gelatin is produced from insoluble collagen thermal denaturation or disintegration (mostly collagen I). As mentioned before, specialized collagenases are required for collagen I degradation. On the other hand, gelatin is susceptible to degradation by many proteases [313]. So, we can speculate that ARFRP1 regulates the expression/secretion of specialized collagenases like MMP-1, 8, 13 and 14 that are able to degrade fibrillar collagen like collagen I, but not gelatinases. 3D invasion assays using DQ™ collagen type I and DQ™ gelatin upon modulation of ARFRP1 expression would be important to monitor the degradation of these two types of substrates. In this case, we would expect that in 3D, the fluorescence produced from the degradation of DQ™ collagen type I would be decreased in cells silenced for *ARFRP1* compared to non-silenced cells, while the fluorescence levels would be the same as in the control, in cells embedded in DQ™ gelatin.

Proposed models for the role of ARFRP1 in breast cancer cell migration and invasion

We have shown that ARFRP1 regulates BC cell migration and invasion. We speculate that ARFRP1 regulates migration through the transport of Vangl2 to the PM. Also, we propose that ARFRP1 regulates invasion by recruiting ARL1 and mediating MMP secretion. Finally, ARFRP1 may be a regulator of β-catenin localization within the cell, whose nuclear translocation mediates migration and invasion of BC cells (Figure 46).

ARL13B as a regulator of breast cancer cell invasion

Our group has established that ARL13B regulates migration and invasion in BC cells, through the regulation of integrin turnover, in highly invasive BC cell lines [280]. So, we wanted to assess if ARL13B also promotes invasion of MCF10DCIS.com cells, suggesting a role for this protein in the transition from *in situ* to invasive BC. First, and in complement to what we previously found, we checked if ARL13B silencing impairs invasion, using 3D spheroids embedded in Matrigel. These experiments allowed us to confirm that ARL13B also modulates BC cell invasion in a 3D setting of

highly invasive BC cells. Following these experiments, we overexpressed ARL13B in MCF10DCIS.com, which presents the features of DCIS and monitored spheroid invasion in Matrigel. Although we observed an increased spheroid area upon ARL13B overexpression, when compared with the control, the differences were not statistically significant.

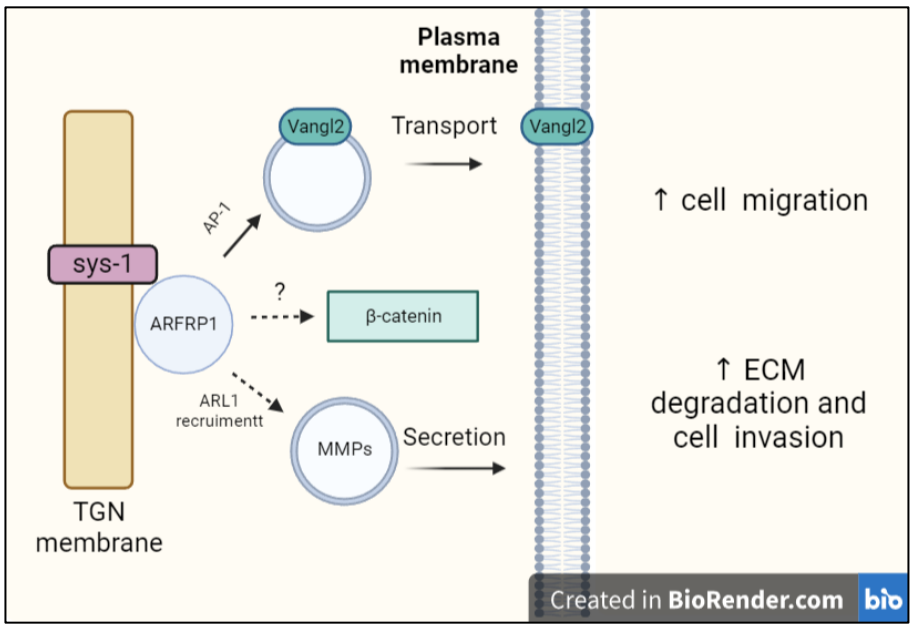

Figure 46 - ARFRP1 as a regulator of breast cancer cell migration and invasion. A. ARFRP1 promotes cell migration in BC cells. A putative mechanism to explain this is the regulation of Vangl2 transport to the PM, mediated by ARFRP1 effector AP-1. ARFRP1 also regulates BC cell invasion, and we propose that this GTPase mediates MMP secretion, through the recruitment of ARL1, leading to ECM degradation. Finally, BC migration and invasion could be mediated by ARFRP1 regulation of β-catenin localization and availability for nuclear transport. Created with BioRender.

ARL13B overexpression was previously shown to promote the growth of BC tumors in mice, suggesting the role of this protein in BC cell proliferation [280]. Furthermore, ARL13B was shown to be a positive regulator of proliferation in both gastric and medulloblastoma cancer cells [264,265]. Likewise, it is possible that the results that we obtained with the 3D spheroids are a result of increased cell proliferation promoted by ARL13B and not necessarily cell invasion, since the two processes cannot be separated in 3D and can both contribute to the observed increase in spheroid area. Therefore, it would be important to measure MCF10DCIS.com cell proliferation on a 3D setting, upon ARL13B overexpression, using commercial kits that measure cell viability. Moreover, addressing the levels of matrix degradation using DQ™ collagen type I and DQ™ gelatin would allow to conclude if ARL13B promotes ECM remodeling of MCF10DCIS.com cells. Furthermore, we could perform the experiment in serum-free medium to minimize the effect of cell proliferation. If ARL13B can indeed

promote invasion of MCF10DCIS.com cells, we would expect more fluorescence resulting from the matrix degradation, in cells overexpressing ARL13B.

We also found that the expression levels of ARL13B-mCherry appeared to be much lower than the ones displayed by the control mCherry. This could be a result of an overall reduced expression of ARL13B. In the future, we could enrich our population of cells expressing higher levels of ARL13B using fluorescence-activated cell sorting (FACS) and the mCherry tag to sort the cells. Also, we cannot exclude the possibility that decreased fluorescent levels observed for ARL13B-mCherry are a result of its cellular localization. ARL13B is established as a ciliary protein that regulates the function and stability of primary cilia [188]. On the other hand, our group reported that ARL13B can regulate cellular functions outside the cilia, like the stability of FAs or the regulation of the actin cytoskeleton in CDRs [191,280]. Furthermore, ARL13B was reported to regulate the progression of gastric carcinomas and medulloblastomas, probably through a mechanism dependent on cilia and the canonical Shh signaling pathway [264,265]. However, it was shown that contrary to gastric cancer cells or medulloblastoma cells, BC cells display a decreased or complete loss of primary cilia [314–316]. Indeed, an analysis of primary cilia frequency in BC cell lines was performed where the isogenic cell lines MCF10A, MCF10AT, MCF10AT3B, MCF10DCIS.com, and MCF10CA1 were used [316]. These cell lines represent the progression from normal/hyperplastic breast tissue (MCF10A) to premalignant breast disease (MCF10AT and MCF10AT3B), to non-invasive DCIS (MCF10DCIS.com), and invasive and metastatic BC (MCF10CA1). The authors found that the primary cilia incidence is significantly higher in normal and premalignant cells (MCF10A, MCF10AT, and MCF10AT3B), when compared to tumoral MCF10DCIS.com and MCF10CA1 cells, where the frequency of primary cilia is much lower [316]. Likewise, the mechanisms underlying the role of ARL13 in BC cancer progression may be different from those observed for gastric cancer and medulloblastoma. So, it would be important to address and clarify what is the localization of ARL13B in MCF10DCIS.com. Unpublished results obtained in our lab showed that besides FAs and stress fibers, ARL13B co-localizes with E-cadherin at AJs, in MCF-7 cells. Therefore, we can speculate that since MCF10DCIS.com cells display fewer cilia, ARL13B localizes to actin-rich structures like AJs and FAs in these cells. Finally, studies should be conducted to establish if the role of ARL13B in BC progression is dependent on the non-canonical Shh signaling since this pathway has been reported in cells without cilia [317–319].

ARL8A and ARL8B mRNA and protein expression are increased in breast cancer cell lines

ARL8A and ARL8B are known regulators of lysosome motility, namely the anterograde movement of these organelles [208]. Moreover, the lysosomal movement towards the cell periphery is essential for lysosome exocytosis, which has been extensively associated with cancer progression, including BC [297]. Therefore, we aimed to assess the role of ARL8A and ARL8B in BC progression. First, we evaluated the mRNA and protein levels of ARL8A and AR8B in non-tumoral cells and distinct BC cell lines with different invasive capacities. At the mRNA level, both *ARL8A* and *ARL8B* were shown to be upregulated in invasive BC cell lines, when compared with the non-tumorigenic MCF10A cells, with the higher expression obtained for the TNBC HCC1806 cell line. In terms of protein levels, ARL8A displayed similar expression in all the cell lines analyzed and ARL8B was found overexpressed in BC cell lines. Curiously, we observed different expression profiles when comparing mRNA and protein levels. As mentioned before, the mRNA and protein levels do not correlate perfectly in all tissues and differences have been observed when comparing non-tumoral and tumoral samples. Also, using antibodies that recognize specifically ARL8A or ARL8B, could lead to more clear results. Nevertheless, the results obtained suggest that the expression levels of ARL8A and ARL8B are increased in BC cell lines, pointing to a possible role of these two proteins in BC progression.

The role of ARL8A and ARL8B in cell proliferation, migration, and invasion of breast cancer cells

Sustained proliferation is one of cancer hallmarks and it is essential for tumor growth and progression[60]. Therefore, we wanted to understand if ARL8A and ARL8B would regulate BC cell proliferation. We did not observe a significant difference in cell proliferation upon silencing of *ARL8A* and *ARL8B*, suggesting that ARL8A and ARL8B do not play a role in BC cell growth. These observations are in line with previous studies performed on prostate cancer cells [256]. Indeed, Dykes and his colleagues reported that, when grown in nutrient-rich media (the same conditions used by us), prostate cancer cells silenced for *ARL8B* display the same proliferation rate as control cells. On the other hand, cells grown under nutrient-deprived conditions displayed a reduction to almost half in the proliferation rate in cells silenced for ARL8B. Thus, the authors proposed that ARL8B regulates

prostate cancer cell proliferation in nutrient-deprived conditions through the modulation of lipid hydrolysis. It has been shown that lysosomes fuse with inclusion bodies and regulate the hydrolysis of internalized and stored lipids, which is mediated by lysosomal acid lipase (LAL). So, the authors suggest that ARL8B regulates the hydrolysis of internalized/stored lipids, by mediating the movement of lysosomes and consequent fusion with inclusion bodies. This allows a continuous and adequate ATP production to sustain the proliferative capacity of cancer cells in nutrient-deprived conditions [256]. During cancer progression, cells face low-nutrient environments in which they must maintain their proliferative capacity to survive. Therefore, in the future, it would be important to analyze if lipid hydrolysis is impaired upon silencing of *ARL8A* and *ARL8B* in BC cells that grow in nutrient-deprived conditions and if this results in decreased cell proliferation.

Multicellular movements are promoted by collective cell migration, and this has been observed in both physiological and pathological conditions, including the formation of cancer metastasis [101]. So, we also wanted to understand if ARL8A and ARL8B regulate collective BC cell migration. We have shown that either *ARL8A* or *ARL8B* silencing led to a decrease in the collective migratory capacity of HCC1806 cells. Moreover, we confirmed that ARL8B has a role in migration by assessing the single-cell migratory capacity of HCC1806 cells, using transwells. Curiously, we did not find differences in the collective migratory capacity of MDA-MB-31 cells upon silencing ARL8B, suggesting that this protein does not regulate motility of these cells. Even though HCC1806 and MDA-MB-231 are both TNBC cell lines and do not express ER, PR, or HER2 receptors, they present distinct characteristics [289]. HCC1806 were shown to express basal cytokeratins 5, 6, 14, and 17, which are characteristic of the basal TNBC subtype. On the other hand, the expression of these cytokeratins was not detected in MDA-MB-231. Moreover, MDA-MB-231 express vimentin which is absent in HCC1806 and is characteristic of mesenchymal cells [320]. The origin of each cell line is also very distinct. While MDA-MB-231 cells were obtained from a pleural infusion of a patient with metastatic breast adenocarcinoma, HCC1806 was obtained from a primary acantholytic squamous cell carcinoma [289]. So, it possible that ARL8A and ARL8B only regulate tumor progression in primary tumors and not metastases. In the future, it would be important to use other cell lines that derive from both primary tumors and metastases to assess their migratory capacity upon ARL8A and ARL8B modulation and confirm this hypothesis.

Cells require the coordinated action of several mechanisms to migrate. Namely, the formation and turnover of FAs, regulation of actin dynamics, and the spatial distribution of specific molecules [97]. In a study performed with mouse fibroblasts, FA dynamics was shown to be dependent

on LEs carrying the p14-MP1 (LAMTOR2/3) complex, which are transported to the cell periphery through a kinesin-1 and Arl8b-dependent mechanism [321]. The delivery of these LEs to FAs promotes the removal of IQ motif-containing GTPase-activating protein 1 (IQGAP1), allowing the efficient turnover of FAs and consequent migration. On the other hand, when p14-MP1 or Arl8b are absent, IQGAP1 is not removed and accumulates in FAs, leading to decreased FA dynamics and consequently, impaired cell migration [321]. Also, in prostate cancer cells, ARL8B was shown to regulate cell motility. In this study, the authors suggested that the impaired cell movement observed upon ARL8B silencing is a consequence of restricted lysosome traffic towards the cell periphery [256]. Indeed, it was shown that integrins that mediate cell adhesion and migration such as α5β1, can be delivered to the PM by LEs/lysosome-dependent transport [322]. However, these mechanisms are still not fully understood, and more studies must be performed to elucidate the role of lysosomal transport in cell adhesion and migration. Nevertheless, we can speculate that ARL8A and ARL8B may regulate cell migration by acting on FA turnover or integrin traffic within the cell. So, in the future, it would be important to evaluate if ARL8A/ARL8B modulation affects the dynamic of FAs in BC cells and/or if the transport of integrins in LEs/lysosomes is dependent on these two small GTPases.

Cancer cells need to acquire invasive capacity to remodel/degrade the surrounding ECM and be able to move to the surrounding tissues and distant locations [62]. Since our results suggested that ARL8A and ARL8B promote BC cell migration, we also evaluated whether these two proteins regulate 3D cell invasion. Curiously, we observed that ARL8B but not ARL8A silencing impairs 3D cell invasion of HCC1806 BC cells, suggesting a distinct role for both proteins in this process. Moreover, we observed a distinct pattern of invasion in Matrigel with HCC1806 spheroids, compared with what was observed in the experiments with MDA-MB-231 cells. Specifically, we observed that when embedded in Matrigel, MDA-MB-231 spheroids form invasive spike-like protrusions, while HCC1806 spheroids present a bud-like cell invasion. This is consistent with a previous study showing that HCC1608 spheroids display amoeboid migration and a bud-like invasion phenotype [323]. Once again, this highlights that these cells behave differently and can subvert different machinery to promote tumorigenesis. It is important to mention that the distinction between cell invasion and cell proliferation can be challenging, when using HCC1806 spheroids, since we cannot clearly distinguish the cells from the spheroid core from the ones that are invading. Likewise, we assessed if cell proliferation is impaired in 3D upon *ARL8B* silencing. We found that there is a reduction in cell proliferation when the expression of ARL8B was decreased for shRNA 2 (B9) but not for shRNA 1 (B7). This could be the result of an off-target effect of this shRNA. Nevertheless, we are confident to

conclude that cell invasion is regulated by ARL8B, given that, after 4 days, the spheroids formed with ARL8B-silenced cells maintained their round shape with almost no bud-like protrusions. These results were confirmed using serum-free conditions to minimize the effect of cell proliferation and embedding the spheroids in Matrigel labeled with DQ-BSA™, which allows the monitorization of matrix degradation. We also assessed if ARL8B regulates the acquisition of invasive properties by non-invasive DCIS cells, which is characterized as non-invasive BC. Although we observed an increase in spheroid growth in Matrigel upon ARL8B overexpression, when compared with non-transduced MCF10DCIS.com, we also observed the same phenotype in GST-overexpressing cells. These results suggest that the transduction and/or selection steps alter the behavior of MCF10DCIS.com cells, therefore masking any differences in invasion. Moreover, as observed for ARL13B, we cannot exclude the contribution of proliferation in these experiments. Thus, future assays using substrates that emit fluorescence upon degradation (*e.g.*, DQ BSA, or DQ Collagen) would help to clarify the role of ARL8B in the progression from non-invasive to invasive BC.

It was interesting to find that ARL8B but not ARL8A regulates cell invasion of BC cells in 3D, but both proteins regulate migration. Although both proteins localize to lysosomes, much less is known about the mechanisms by which ARL8A regulates lysosome motility. It has been established that ARL8B regulates the anterograde movement of lysosomes by being recruited by BORC and mediating the binding of its effector SKIP to kinesin-1 or through binding to kinesin-3 [206]. Moreover, it was found that BORC also functions upstream of ARL8A in the regulation of kinesin-mediated transport [210]. Furthermore, in *C. elegans,* it was shown the BORC subunit SAM-4 interacts directly with ARL-8-GDP, suggesting that it acts as a GEF [324]. Whether this direct interaction is also established between BORC subunits and ARL8A/ARL8B in mammalian cells is still unknown. Moreover, because most of the studies were performed with ARL8B, no effectors have been identified for ARL8A-mediated anterograde movement. Likewise, it is possible that ARL8A and ARL8B may regulate lysosome movement towards the cell periphery through binding to different effectors and regulators, promoting different cell phenotypes when silenced. On the other hand, it was very recently revealed that ARL8A and ARL8B may also regulate the retrograde traffic of endolysosomes through binding to effectors RUFY3 and RUFY4 [213]. These recent findings suggest that ARL8 proteins can regulate both retrograde and anterograde lysosome movement. This is not exclusive of ARL8 proteins since RAB7, which also regulates the movement of LEs/lysosomes has been associated with the regulation of anterograde and retrograde movement, by binding to FYCO1 or RILP, respectively [325,326]. So, in future experiments, it would be important to define which

RAB7/ARL8-mediated molecular mechanisms are at play in the regulation of lysosome motility in BC cells. For example, one could evaluate the expression and localization at LEs/lysosomes of the different molecular players that regulate both retrograde and anterograde lysosomal movements, by microscopy and immunoblotting analysis, in BC cells. Also, it should be evaluated if the silencing of these proteins in BC cells, leads to the modulation of BC cell migration and invasion. We would expect that the mechanisms regulating LE/lysosome anterograde movement are increased in BC and therefore, silencing of SKIP and FYCO3 would lead to an impaired migration and invasion of these cells.

ARL8B regulates breast cancer cell invasion through lysosome exocytosis

Lysosome exocytosis has been associated with multiple diseases, including cancer, regulating ECM degradation/remodeling through the release of proteases. Also, lysosome exocytosis was shown to be important for membrane repair, which is involved in cancer cell growth and survival [216,297]. In this study, we have shown that ARL8B regulates 3D invasion of HCC1806 cells. Given that this small GTPase regulates the transport of lysosomes to the cell periphery, thus regulating the positioning of these organelles for exocytosis, we assessed if ARL8B also modulates lysosome exocytosis in HCC1806 BC cells. Indeed, we found that ARL8B silencing in HCC1806 cells impairs the release of the lysosomal β-hexosaminidase to the extracellular medium. However, the LAMP1 levels at the cell surface measured by flow cytometry are not affected by ARL8B silencing. This is probably due to the high adherence of HCC1806 cells to the surface of the plate, which leads to a need of incubating for a long time with the dissociation reagent to detach the cells. Indeed, in previous experiments performed at our lab, we observed that cell scraping and the use of dissociation agents for long periods increase the levels of PI-positive cells, suggesting under these conditions, cells suffer membrane damage in these conditions and become non-viable or die. So, it is possible that we are inducing damage to the cell membrane and increasing the levels of LAMP1 at the cell surface, which could mask any differences. Moreover, LAMP1 is also present in LEs, and these can also be exocytosed. Likewise, the measurement of the release of lysosomal enzymes to the media represents a more accurate and specific method to assess lysosome exocytosis. In the future, the activity of other secreted lysosomal enzymes like cathepsins should also be performed to confirm these obtained results. Nevertheless, the impairment of β-hexosaminidase release from HCC1806 upon ARL8B silencing suggests that lysosome exocytosis is impaired in these conditions.

Furthermore, as lysosome exocytosis has been linked to tumor invasion, we propose that this is one of the mechanisms by which ARL8B regulates HCC1806 cell invasion. Indeed, in prostate cancer cells, ARL8B was shown to regulate lysosomal protease release, which are required for ECM degradation, and consequent cell invasion [256]. Additionally, in radiation-resistant BC cells, lysosome exocytosis was impaired by ARL8B or BORC silencing, and these observations were linked to the reduced ECM degradation observed by the authors [278]. Curiously, in this study, the co-localization of different proteases, including MMP-3, MMP-14, cathepsin B, and cathepsin D and ARL8B-positive lysosomes was observed. Indeed, cathepsins can degrade ECM directly, but they can also activate other MMPs to promote ECM remodeling. The association of these proteases with tumor progression and metastasis has been widely studied. So, an important experiment to perform in the future is the analysis of protease expression and release upon ARL8B modulation in BC cells, using immunoblotting, zymography and enzymatic activity kits.

Proposed model for ARL8A and ARL8B regulation of BC progression

We have shown that ARL8A and ARL8B regulate BC cell migration and speculate that this may be mediated by the modulation of FA dynamics. Also, our results and the results obtained by other researchers [256,278] highlight the importance of ARL8B in regulating lysosome exocytosis and consequent protease release that remodels the ECM and allows cancer cells to invade (Figure 47).

ARL8B is not a regulator of epithelial-to-mesenchymal transition in invasive breast cancer cells

EMT is a process that cancer cells adopt to change their morphology and transition from an epithelial to a mesenchymal state, where they exhibit higher motility and invasiveness [75]. It has been shown that cancer cells can activate autophagy upon stimulation by stressful factors such as hypoxia [327]. Also, the degradation of epithelial molecules such as E-cadherin through autophagy was observed. The reduced levels of E-cadherin can induce EMT and lead to cancer cell invasion and metastasis [328]. Marwaha *et al.*, described that the Rab7 effector PLEKHM1 also binds to ARL8B in lysosomes and that these two small GTPases regulate lysosomal degradation of internalized cargo through endocytic and autophagic pathways [329]. Although these mechanisms still need further

clarification, we assessed if ARL8B regulates the levels of EMT markers in BC cells. We found that ARL8B silencing does not alter the levels of SLUG and E-cadherin in HCC1806 cells, suggesting that EMT is not being regulated by ARL8B-dependent mechanisms. Moreover, the levels of SLUG and E-cadherin in HCC1806 cells point to a hybrid EMT state in these cells since we observed that both proteins are expressed. These intermediate EMT states were shown to confer more plasticity to cancer cells and to be relevant for collective cell migration and invasion, as well as metastases formation [330]. Our observations were reinforced when we observed that the expression of SLUG is almost absent in MCF-7 cells, while the expression of E-cadherin is higher in this cell line, which typically presents a more epithelial and less aggressive phenotype.

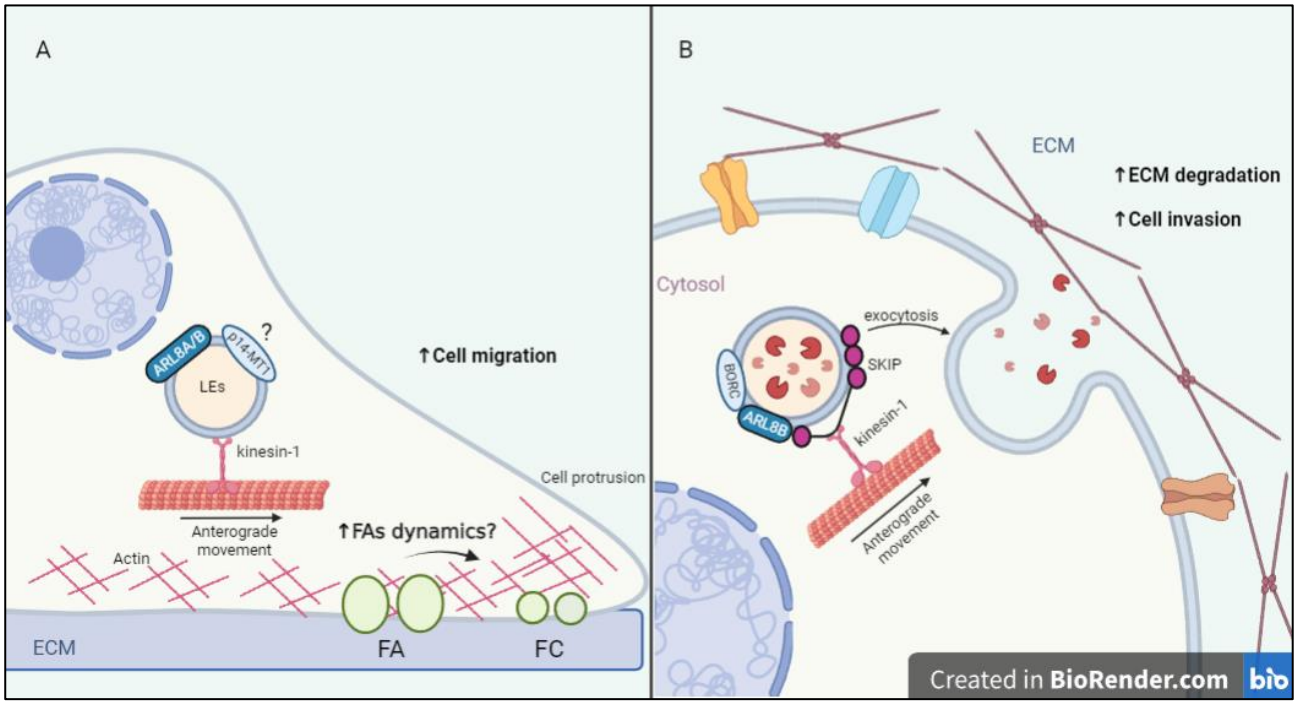

Figure 47 - ARL8 proteins as regulators of breast cancer cell migration and invasion. A. ARL8A and ARL8B promote cell migration of BC cells. A putative mechanism for this would be the regulation of focal adhesion (FA) dynamics and focal complex (FC) formation that were shown to be dependent on late endosomes (LEs) carrying p14-MP1 complex. These are transported to the cell periphery through a kinesin-1 and Arl8b-dependent mechanism. **B.** ARL8B also promotes BC cell invasion. ARL8B is recruited to lysosomes by BORC and mediates the interaction of its effector SKIP with kinesin-1. We propose that in BC cells, ARL8B regulates the transport of lysosomes to the cell periphery where they are exocytosed and release proteases that result in ECM degradation. Created with BioRender.

Targeting ARLs for breast cancer treatment

As observed by us and other researchers, different members of the ARL subfamily of small GTPases have been associated with cancer progression, including BC. So, the development of small

GTPase inhibitors could be a promising new strategy for cancer treatment. However, it remains a major challenge to find such molecules, especially because small GTPases have highly conserved regulatory roles and are expressed in many tissues. Nonetheless, there are several mechanisms by which it is possible to target small GTPases, including ARLs. One way to do this could be to inhibit the expression of overexpressed ARLs. Furthermore, it is also a possibility to design inhibitors that can block GTP binding or GTPase binding to membranes. Activity regulators like GAPs and GEFs can also be targeted. Specifically, one can inhibit GEF activity or the ARF-GEF interaction, stimulate GAP activity/expression and inhibit the binding of ARLs to downstream effectors. Finally, one can also target these effectors by inhibiting their function or changing the expression levels (Figure 48) [227]. Although there are not inhibitors of ARLs to this date, there are already inhibitors for known effectors. For example, the ARL13B effector NMIIA was found to be differentially expressed and/or activated in various malignancies, which can lead to alterations in the migratory and invasive capacities of cancer cells [331]. Moreover, blebbistatin blocks the ATPase activity of NMIIA and it was found to impair BC cell and pancreatic adenocarcinoma cell invasion [332,333].

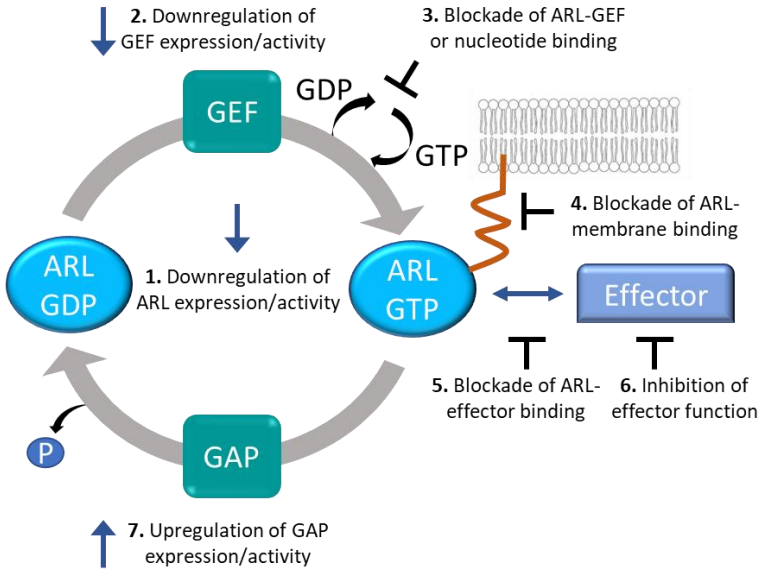

Figure 48 - Potential strategies to use ARL proteins regulation cycle as targets for cancer treatment. A. Strategies to target ARL family members that act as oncogenes include downregulation of ARL expression and/or activity (1); downregulation of GEF expression and/or activity (2); blockade of ARL-GEF binding or ARL-GTP binding (3); Blockade of active ARL binding to membranes (4) or effectors (5); inhibition of effectors function (6); Upregulation of GAP expression and/ or activity (7). Adapted from [227].

So, it is essential to unravel the signaling pathways regulated by ARL small GTPases that are involved in BC progression to find the most suitable approach for an efficient treatment of this

disease. Also, increasing the knowledge on effectors/binding partners, as well as specific GAPs/GEFs that can mediate the activity of ARL proteins, is necessary.

Conclusions and future perspectives

Unraveling the mechanisms that underly the acquisition of invasive phenotypes and the consequent formation of metastases by BC cells is essential to find new treatments for this malignancy. The work presented in this PhD thesis shows that several *ARL* genes, namely *ARL1, ARL8B, ARL11 and ARFRP1*, are upregulated in highly invasive BC cell lines and patient samples. This highlights the importance of studying these membrane traffic regulators in the context of BC progression. Our results suggest that ARFRP1 regulates BC cell migration and invasion. Indeed, this is the first report showing the role of ARFRP1 in cancer progression, which can also be relevant in other types of malignancies besides BC. We also confirmed that ARL13B is required for BC cell invasion, although it does not seem to mediate the transition from non-invasive DCIS to invasive BC. This work also established a role for lysosome-positioning regulators in BC progression. We found that ARL8A and ARL8B regulate BC cell migration, suggesting a role for these small GTPases in the cell adhesion and motility processes. Moreover, our results indicate that ARL8B regulates BC cell invasion, possibly through the modulation of lysosome exocytosis. The results obtained with this study also suggest that targeting cellular processes that are regulated by members of the ARL subfamily, like lysosome exocytosis, could serve as new strategies to impair the progression of BC. Thus, this study strongly suggests that ARFRP1, ARL13B, and ARL8, could be potential therapeutic targets to impair BC progression and reduce the high mortality that is associated with this disease.

Our work highlights the importance of investigating membrane traffic regulators, including those of the ARL subfamily of proteins, as potential regulators of BC. However, it is important to mention that this study represents the beginning of a promising field in BC research and future experiments are essential to validate our candidates as targets for the treatment of BC. As discussed before, targeting of ARL GTPases represents a major challenge, since many of these proteins are ubiquitously expressed and are essential for several physiological processes. Therefore, in future experiments, the molecular mechanisms by which ARFRP1, ARL13B and ARL8 proteins regulate BC progression, should be dissected. Specifically, the signaling pathways that are involved in this regulation should be characterized. It would be interesting to evaluate whether the regulation of

migration and invasion by ARFRP1 is mediated by Wnt/β-cathenin signaling pathway and/or MMP traffic and secretion. Also, we have previously proposed that the role of ARL13B in BC progression is likely mediated by a cilium-independent mechanism and non-canonical Shh signaling. Likewise, it would be important to evaluate if this non-canonical signaling pathway is altered in BC and if it is regulated by ARL13B. Finally, it is important to evaluate if FA turnover is impaired upon ARL8A/ARL8B silencing in BC cells and whether this influences the role of ARL8A and ARL8B in BC cell migration. Moreover, it would be important to dissect the proteins involved in the regulation of lysosome exocytosis by ARL8B in BC. This could be done by assessing which of the known effectors and regulators of ARL8B are involved in BC cell invasion. The results from these experiments could lead to the discovery of other potential targets, including effectors/binding partners and regulators of ARL activity (GAPs and GEFs) that could be used to design more specific and more efficient BC therapies. Also, our experiments were mainly done using BC cell lines, which can be seen as a limitation. Although cell lines have been widely used for BC research, they do not recapitulate the heterogeneity of BC and present several drawbacks that were already described. Therefore, our results should be validated using a model that more closely represents the genetic and phenotypic variety of BC in patients. For this, the expression of ARFRP1, ARL13B and ARL8 should be modulated in patient-derived cells and in vivo models (*e.g.,* mouse). This would allow the validation of the role of these small GTPases in a more representative model of BC and to be one step closer to an application to the clinics.

In conclusion, the results obtained with this study reinforce the notion that membrane traffic regulators can be subverted by cancer cells, including BC cells, to promote migration and invasion. This highlights the importance of considering these proteins as targets for the design of future therapies for BC treatment.

References

1. Sung H, Ferlay J, Siegel RL, et al. Global Cancer Statistics 2020: GLOBOCAN Estimates of Incidence and Mortality Worldwide for 36 Cancers in 185 Countries. CA Cancer J Clin 2021;71(3):209–49.
2. Harbeck N, Penault-Llorca F, Cortes J, et al. Breast cancer. 2019.
3. Globocan.Portugal. Available from: https://gco.iarc.fr/today/data/factsheets/populations/620-portugal-fact-sheets.pdf
4. Loibl S, Poortmans P, Morrow M, Denkert C, Curigliano G. Breast cancer. Lancet 2021;397(10286):1750–69.
5. Darkwah WK, Aidoo G, Akoto D, Alhassan K, Adormaa BB, Puplampu JB. Proliferative activity of various grades and types of breast carcinoma using AgNOR (Argyrophilic Nuclear Organizer Region) expression and its prognostic significance. All Life 2021;14(1):375–91.
6. McGuire KP. Breast Anatomy and Physiology. In: Breast Disease. Cham: Springer International Publishing; 2016. p. 1–14.
7. Garrod D. Cell Adhesion and the Extracellular Matrix. Med Cell Biol Third Ed 2007;191–225.
8. Lepucki A, Orlińska K, Mielczarek-Palacz A, Kabut J, Olczyk P, Komosińska-Vassev K. The Role of Extracellular Matrix Proteins in Breast Cancer. J Clin Med 2022;11(5):1–30.
9. Nowell P. C. The clonal evolution of tumor cell populations. Science (80-) 1976;194:23–8.
10. Reya T, Morrison SJ, Clarke MF, Weissman IL. Stem cells, cancer, and cancer stem cells. Nature 2001;414(6859):105–11.
11. Bombonati A, Sgroi DC. The molecular pathology of breast cancer progression. J Pathol 2011;223(2):308–18.
12. Zubair M, Wang S, Ali N. Advanced Approaches to Breast Cancer Classification and Diagnosis. Front Pharmacol 2021;11(February):1–24.
13. Makki J. Diversity of breast carcinoma: Histological subtypes and clinical relevance. Clin Med Insights Pathol 2015;8(1):23–31.
14. Shea EKH, Koh VCY, Tan PH. Invasive breast cancer: Current perspectives and emerging views. Pathol Int 2020;70(5):242–52.
15. Kozłowski J, Kozłowska A, Kocki J. Breast cancer metastasis – insight into selected molecular mechanisms of the phenomenon. Postepy Hig Med Dosw 2015;69:447–51.
16. Smolarz B, Zadrożna Nowak A, Romanowicz H. Breast Cancer—Epidemiology, Classification,

Pathogenesis and Treatment (Review of Literature). Cancers (Basel) 2022;14(10):1–27.

17. van Seijen M, Lips EH, Thompson AM, et al. Ductal carcinoma in situ: to treat or not to treat, that is the question. Br J Cancer 2019;121(4):285–92.
18. Hophan SL, Odnokoz O, Liu H, et al. Ductal Carcinoma In Situ of Breast: From Molecular Etiology to Therapeutic Management. Endocrinol (United States) 2022;163(4):1–9.
19. Cserni G, Sejben A. Grading Ductal Carcinoma In Situ (DCIS) of the Breast – What's Wrong with It? Pathol Oncol Res 2020;26(2):665–71.
20. Thompson AM, Clements K, Cheung S, et al. Management and 5-year outcomes in 9938 women with screen-detected ductal carcinoma in situ: the UK Sloane Project. Eur J Cancer 2018;101:210–9.
21. Elshof LE, Schaapveld M, Schmidt MK, Rutgers EJ, van Leeuwen FE, Wesseling J. Subsequent risk of ipsilateral and contralateral invasive breast cancer after treatment for ductal carcinoma in situ: incidence and the effect of radiotherapy in a population-based cohort of 10,090 women. Breast Cancer Res Treat 2016;159(3):553–63.
22. Bijker N, Peterse JL, Duchateau L, et al. Risk factors for recurrence and metastasis after breast-conserving therapy for ductal carcinoma-in-situ: Analysis of European Organization for Research and Treatment of Cancer Trial 10853. J Clin Oncol 2001;19(8):2263–71.
23. Bane A. Ductal Carcinoma In Situ : What the Pathologist Needs to Know and Why . Int J Breast Cancer 2013;2013:1–7.
24. Champion CD, Ren Y, Thomas SM, et al. DCIS with Microinvasion: Is It In Situ or Invasive Disease? Ann Surg Oncol 2019;26(10):3124–32.
25. Lambert K, Patani N, Mokbel K. Ductal carcinoma in situ: Recent advances and future prospects. Int J Surg Oncol 2012;2012.
26. Pinder SE. Ductal carcinoma in situ (DCIS): Pathological features, differential diagnosis, prognostic factors and specimen evaluation. Mod Pathol 2010;23(SUPPL. 2):8–13.
27. Tsang JYS, Tse GM. Molecular Classification of Breast Cancer. Adv Anat Pathol 2020;27(1):27–35.
28. Elston CW, Ellis IO. Pathological prognostic factors in breast cancer. I. The value of histological grade in breast cancer: experience from a large study with long-term follow-up. Histopathology 1991;19(5):403–10.
29. Cserni G, Chmielik E, Cserni B, Tot T. The new TNM-based staging of breast cancer. Virchows Arch 2018;472(5):697–703.

30. Turner KM, Yeo SK, Holm TM, Shaughnessy E, Guan JL. Heterogeneity within molecular subtypes of breast cancer. Am J Physiol - Cell Physiol 2021;321(2):C343–54.
31. Perou CM, Sørlie T, Eisen MB, et al. Molecular portraits of human breast tumours. Nature 2000;406(6797):747–52.
32. Yersal O, Barutca S. Biological subtypes of breast cancer: Prognostic and therapeutic implications. World J Clin Oncol 2014;5(3):412–24.
33. Lehmann BD, Jovanović B, Chen X, et al. Refinement of triple-negative breast cancer molecular subtypes: Implications for neoadjuvant chemotherapy selection. PLoS One 2016;11(6):1–22.
34. Derakhshan F, Reis-Filho JS. Pathogenesis of Triple-Negative Breast Cancer. Annu Rev Pathol Mech Dis 2021;17:181–204.
35. Łukasiewicz S, Czeczelewski M, Forma A, Baj J, Sitarz R, Stanisławek A. Breast cancer—epidemiology, risk factors, classification, prognostic markers, and current treatment strategies—An updated review. Cancers (Basel) 2021;13(17):1–30.
36. Buzdar AU. Breast cancer in men. Oncology 2003;17(10):1361–4.
37. Shiovitz S, Korde LA. Genetics of breast cancer: A topic in evolution. Ann Oncol 2015;26(7):1291–9.
38. Corso G, Intra M, Trentin C, Veronesi P, Galimberti V. CDH1 germline mutations and hereditary lobular breast cancer. Fam Cancer 2016;15(2):215–9.
39. Kechagioglou, Papi RM, Provatopoulou X, Kalogera E, Papadimitriou E, Grigoropoulos P, et al. Tumor suppressor PTEN in breast cancer: heterozygosity, mutations and protein expression. Anticancer Res 2014;34(3):1387–400.
40. Shahbandi A, Nguyen HD, Jackson JG. TP53 Mutations and Outcomes in Breast Cancer: Reading beyond the Headlines. Trends in Cancer 2020;6(2):98–110.
41. Chen J, Lindblom A. Germline mutation screening of the STK11/LKB1 gene in familial breast cancer with LOH on 19p. Clin Genet 2000;57(5):394–7.
42. Ng J, Shuryak I. Minimizing second cancer risk following radiotherapy: Current perspectives. Cancer Manag Res 2014;7:1–11.
43. Kim EY, Chang Y, Ahn J, et al. Mammographic breast density, its changes, and breast cancer risk in premenopausal and postmenopausal women. Cancer 2020;126(21):4687–96.
44. Hill DA, Prossnitz ER, Royce M, Nibbe A. Temporal trends in breast cancer survival by race and ethnicity: A population-based cohort study. PLoS One 2019;14(10):1–14.

45. Ursin G, Bernstein L, Lord SJ, et al. Reproductive factors and subtypes of breast cancer defined by hormone receptor and histology. Br J Cancer 2005;93(3):364–71.
46. James FR, Wootton S, Jackson A, Wiseman M, Copson ER, Cutress RI. Obesity in breast cancer - What is the risk factor? Eur J Cancer 2015;51(6):705–20.
47. Kotepui M. Diet and risk of breast cancer. Wspolczesna Onkol 2016;20(1):13–9.
48. Mørch LS, Skovlund CW, Hannaford PC, Iversen L, Fielding S, Lidegaard Ø. Contemporary Hormonal Contraception and the Risk of Breast Cancer. N Engl J Med 2017;377(23):2228–39.
49. Vinogradova Y, Coupland C, Hippisley-Cox J. Use of hormone replacement therapy and risk of breast cancer: Nested case-control studies using the QResearch and CPRD databases. BMJ 2020;371.
50. Chen X, Wang Q, Zhang Y, Xie Q, Tan X. Physical Activity and Risk of Breast Cancer: A Meta-Analysis of 38 Cohort Studies in 45 Study Reports. Value Heal 2019;22(1):104–28.
51. Liu Y, Nguyen N, Colditz GA. Links between alcohol consumption and breast cancer: A look at the evidence. Women's Heal 2015;11(1):65–77.
52. Catsburg C, Miller AB, Rohan TE. Active cigarette smoking and risk of breast cancer. Int J Cancer 2015;136(9):2204–9.
53. Irwig L, Macaskill P, Houssami N. Evidence relevant to the investigation of breast symptoms: The triple test. Breast 2002;11(3):215–20.
54. Alvarado M, Ozanne E, Esserman L. Overdiagnosis and Overtreatment of Breast Cancer. Am Soc Clin Oncol Educ B 2016;32:e40–5.
55. Abe O, Abe R, Enomoto K, et al. Effects of chemotherapy and hormonal therapy for early breast cancer on recurrence and 15-year survival: An overview of the randomised trials. Lancet 2005;365(9472):1687–717.
56. Jonathan Yang T, Ho AY. Radiation Therapy in the Management of Breast Cancer. Surg Clin North Am 2013;93(2):455–71.
57. Hanahan D, Weinberg RA. The Hallmarks of Cancer. Cell 2000;100(1):57–70.
58. Hanahan D, Weinberg RA. Hallmarks of cancer: The next generation. Cell 2011;144(5):646–74.
59. Hanahan D. Hallmarks of Cancer: New Dimensions. Cancer Discov 2022;12(1):31–46.
60. Ravi S, Alencar AM, Arakelyan J, et al. An Update to Hallmarks of Cancer. Cureus 2022;2011(5):1–16.
61. Lazebnik Y. What are the hallmarks of cancer? Nat Rev Cancer 2010;10(4):232–3.

62. Majidpoor J, Mortezaee K. Steps in metastasis: an updated review. Med Oncol 2021;38(1):1–17.
63. Bui S, Mejia I, Díaz B, Wang Y. Adaptation of the Golgi Apparatus in Cancer Cell Invasion and Metastasis. Front Cell Dev Biol 2021;9(December):1–20.
64. Pachmayr E, Treese C, Stein U. Underlying Mechanisms for Distant Metastasis - Molecular Biology. Visc Med 2017;33(1):11–20.
65. Lambert AW, Pattabiraman DR, Weinberg RA. Emerging Biological Principles of Metastasis. Cell 2017;168(4):670–91.
66. Paget S. The distribution of secondary growths in cancer of the breast. 1889. Cancer Metastasis Rev 1989;8(2):98–101.
67. Fidler IJ. The pathogenesis of cancer metastasis: the “seed and soil” hypothesis revisited. Nat Rev Cancer 2003;3(6):453–8.
68. Chen W, Hoffmann AD, Liu H, Liu X. Organotropism: new insights into molecular mechanisms of breast cancer metastasis. npj Precis Oncol 2018;2(1).
69. Yang J, Antin P, Berx G, et al. Guidelines and definitions for research on epithelial–mesenchymal transition. Nat Rev Mol Cell Biol 2020;21(6):341–52.
70. Hay ED. An overview of epithelio-mesenchymal transformation. Acta Anat. (Basel). 1995;154(1):8–20.
71. Pastushenko I, Blanpain C. EMT Transition States during Tumor Progression and Metastasis. Trends Cell Biol 2019;29(3):212–26.
72. Puisieux A, Brabletz T, Caramel J. Oncogenic roles of EMT-inducing transcription factors. Nat Cell Biol 2014;16(6):488–94.
73. Nieto MA, Huang RYYJ, Jackson RAA, Thiery JPP. Emt: 2016. Cell 2016;166(1):21–45.
74. Brabletz T. To differentiate or not-routes towards metastasis. Nat Rev Cancer 2012;12(6):425–36.
75. Dongre A, Weinberg RA. New insights into the mechanisms of epithelial–mesenchymal transition and implications for cancer. Nat Rev Mol Cell Biol 2019;20(2):69–84.
76. Batlle E, Sancho E, Francí C, et al. The transcription factor Snail is a repressor of E-cadherin gene expression in epithelial tumour cells. Nat Cell Biol 2000;2(2):84–9.
77. Nieto MA, Sargent MG, Wilkinson DG, Cooke J. Control of cell behavior during vertebrate development by Slug, a zinc finger gene. Science (80-) 1994;264(5160):835–9.
78. Hajra KM, Chen DYS, Fearon ER. The SLUG zinc-finger protein represses E-cadherin in breast

cancer. Cancer Res 2002;62(6):1613–8.

79. Yang MH, Hsu DSS, Wang HW, et al. Bmi1 is essential in Twist1-induced epithelial-mesenchymal transition. Nat Cell Biol 2010;12(10):982–92.

80. Fang X, Cai Y, Liu J, et al. Twist2 contributes to breast cancer progression by promoting an epithelial-mesenchymal transition and cancer stem-like cell self-renewal. Oncogene 2011;30(47):4707–20.

81. Sánchez-Tilló E, Lázaro A, Torrent R, et al. ZEB1 represses E-cadherin and induces an EMT by recruiting the SWI/SNF chromatin-remodeling protein BRG1. Oncogene 2010;29(24):3490–500.

82. Comijn J, Comijn J, Berx G, et al. The two-handed E box binding zinc finger protein SIP1 downregulates E-cadherin and induces invasion. Mol Cell 2001;7(6):1267–78.

83. Wu Y, Ginther C, Kim J, et al. Expression of Wnt3 Activates Wnt/β-Catenin Pathway and Promotes EMT-like Phenotype in Trastuzumab-Resistant HER2-Overexpressing Breast Cancer Cells. Mol Cancer Res 2012;10(12):1597–606.

84. Choi J, Sun YP, Joo CK. Transforming growth factor-β1 represses E-cadherin production via Slug expression in lens epithelial cells. Investig Ophthalmol Vis Sci 2007;48(6):2708–18.

85. Peinado H, Quintanilla M, Cano A. Transforming growth factor β-1 induces Snail transcription factor in epithelial cell lines. Mechanisms for epithelial mesenchymal transitions. J Biol Chem 2003;278(23):21113–23.

86. Shintani Y, Fujiwara A, Kimura T, et al. IL-6 secreted from Cancer-Associated fibroblasts mediates chemoresistance in NSCLC by increasing epithelial-mesenchymal transition signaling. J Thorac Oncol 2016;11(9):1482–92.

87. Yu Y, Xiao CH, Tan LD, Wang QS, Li XQ, Feng YM. Cancer-associated fibroblasts induce epithelial-mesenchymal transition of breast cancer cells through paracrine TGF-β signalling. Br J Cancer 2014;110(3):724–32.

88. Lai X, Li Q, Wu F, et al. Epithelial-Mesenchymal Transition and Metabolic Switching in Cancer: Lessons From Somatic Cell Reprogramming. Front Cell Dev Biol 2020;8(August):1–13.

89. Pastushenko I, Brisebarre A, Sifrim A, et al. Identification of the tumour transition states occurring during EMT. Nature 2018;556(7702).

90. Yu M, Bardia A, Wittner BS, et al. Circulating Breast Tumor Cells Exhibit Dynamic Changes in Epithelial and Mesenchymal Composition. Science 2013;339(6119):580–4.

91. Yamada KM, Sixt M. Mechanisms of 3D cell migration. Nat Rev Mol Cell Biol 2019;20(12):738–

52.

92. Seetharaman S, Etienne-Manneville S. Cytoskeletal Crosstalk in Cell Migration. Trends Cell Biol 2020;30(9):720–35.
93. Paňková K, Rösel D, Novotný M, Brábek J. The molecular mechanisms of transition between mesenchymal and amoeboid invasiveness in tumor cells. Cell Mol Life Sci 2010;67(1):63–71.
94. Wu J shun, Jiang J, Chen B jun, Wang K, Tang Y ling, Liang X hua. Plasticity of cancer cell invasion: Patterns and mechanisms. Transl Oncol 2021;14(1):100899.
95. Mierke CT. The matrix environmental and cell mechanical properties regulate cell migration and contribute to the invasive phenotype of cancer cells. Reports Prog Phys 2019;82(6):064602.
96. Khalil AA, Ilina O, Gritsenko PG, Bult P, Span PN, Friedl P. Collective invasion in ductal and lobular breast cancer associates with distant metastasis. Clin Exp Metastasis 2017;34(6–7):421–9.
97. Nagai T, Ishikawa T, Minami Y, Nishita M. Tactics of cancer invasion: Solitary and collective invasion. J Biochem 2021;167(4):347–55.
98. Campbell K, Casanova J. A common framework for EMT and collective cell migration. Dev 2016;143(23):4291–300.
99. Yang Y, Zheng H, Zhan Y, Fan S. An emerging tumor invasion mechanism about the collective cell migration. Am J Transl Res 2019;11(9):5301–12.
100. Mayor R, Etienne-Manneville S. The front and rear of collective cell migration. Nat Rev Mol Cell Biol 2016;17(2):97–109.
101. Qin L, Yang D, Yi W, Cao H, Xiao G. Roles of leader and follower cells in collective cell migration. Mol Biol Cell 2021;32(14):1267–72.
102. Gaggioli C, Hooper S, Hidalgo-Carcedo C, et al. Fibroblast-led collective invasion of carcinoma cells with differing roles for RhoGTPases in leading and following cells. Nat Cell Biol 2007;9(12):1392–400.
103. Pollard TD. Actin and actin-binding proteins. Cold Spring Harb Perspect Biol 2016;8(8):1–17.
104. Svitkina T. The actin cytoskeleton and actin-based motility. Cold Spring Harb Perspect Biol 2018;10(1):1–21.
105. Rottner K, Schaks M. Assembling actin filaments for protrusion. Curr Opin Cell Biol 2019;56:53–63.
106. Welch MD, Mullins RD. Cellular control of actin nucleation. Annu Rev Cell Dev Biol

2002;18:247–88.

107. Edwards M, Zwolak A, Schafer DA, Sept D, Dominguez R, Cooper JA. Capping protein regulators fine-tune actin assembly dynamics. Nat Rev Mol Cell Biol 2014;15(10):677–89.
108. Ono S. Mechanism of Depolymerization and Severing of Actin Filaments and Its Significance in Cytoskeletal Dynamics. Int Rev Cytol 2007;258(07):1–82.
109. Chan KT, Creed SJ, Bear JE. Unraveling the enigma: Progress towards understanding the coronin family of actin regulators. Trends Cell Biol 2011;21(8):481–8.
110. Goode BL, Sweeney MO, Eskin JA. GMF as an Actin Network Remodeling Factor. Trends Cell Biol 2018;28(9):749–60.
111. Chen M, Zhu W, Liang Z, Yao S, Zhang X, Zheng Y. Effect of F-Actin Organization in Lamellipodium on Viscoelasticity and Migration of Huh-7 Cells Under pH Microenvironments Using AM-FM Atomic Force Microscopy. Front Phys 2021;9(May):1–12.
112. Murphy DA, Courtneidge SA. The “ins” and “outs” of podosomes and invadopodia: Characteristics, formation and function. Nat Rev Mol Cell Biol 2011;12(7):413–26.
113. Peláez R, Pariente A, Pérez-Sala Á, Larrayoz IM. Integrins: Moonlighting Proteins in Invadosome Formation. Cancers (Basel) 2019;11(5):615.
114. Eddy RJ, Weidmann MD, Sharma VP, Condeelis JS. Tumor Cell Invadopodia: Invasive Protrusions that Orchestrate Metastasis. Trends Cell Biol 2017;27(8):595–607.
115. Beaty BT, Condeelis J. Digging a little deeper: The stages of invadopodium formation and maturation. Eur J Cell Biol 2014;93(10–12):438–44.
116. Augoff K, Hryniewicz-Jankowska A, Tabola R. Invadopodia: clearing the way for cancer cell invasion. Ann Transl Med 2020;8(14):902–902.
117. Saha T, Gil-Henn H. Invadopodia, a Kingdom of non-receptor tyrosine kinases. Cells 2021;10(8).
118. Sharma VP, Eddy R, Entenberg D, Kai M, Gertler FB, Condeelis J. Tks5 and SHIP2 regulate invadopodium maturation, but not initiation, in breast carcinoma cells. Curr Biol 2013;23(21):2079–89.
119. Carmona G, Perera U, Gillett C, et al. Lamellipodin promotes invasive 3D cancer cell migration via regulated interactions with Ena/VASP and SCAR/WAVE. Oncogene 2016;35(39):5155–69.
120. Bravo-Cordero JJ, Magalhaes MAO, Eddy RJ, Hodgson L, Condeelis J. Functions of cofilin in cell locomotion and invasion. Nat Rev Mol Cell Biol 2013;14(7):405–17.
121. Helgeson LA, Nolen BJ. Mechanism of synergistic activation of Arp2/3 complex by cortactin

and N-WASP. Elife 2013;2013(2):1–26.

122. Beaty BT, Sharma VP, Bravo-Cordero JJ, et al. β1 integrin regulates Arg to promote invadopodial maturation and matrix degradation. Mol Biol Cell 2013;24(11):1661–75.
123. Jeannot P, Besson A. Cortactin function in invadopodia. Small GTPases 2020;11(4):256–70.
124. Oser M, Mader CC, Gil-Henn H, et al. Specific tyrosine phosphorylation sites on cortactin regulate Nck1-dependent actin polymerization in invadopodia. J Cell Sci 2010;123(21):3662–73.
125. Mgrditchian T, Sakalauskaite G, Müller T, Hoffmann C, Thomas C. The multiple roles of actin-binding proteins at invadopodia. Int Rev Cell Mol Biol 2021;360:99–132.
126. Oser M, Yamaguchi H, Mader CC, et al. Cortactin regulates cofilin and N-WASp activities to control the stages of invadopodium assembly and maturation. J Cell Biol 2009;186(4):571–87.
127. Parekh A, Weaver AM. Regulation of invadopodia by mechanical signaling. Exp Cell Res 2016;343(1):89–95.
128. Quintero-Fabián S, Arreola R, Becerril-Villanueva E, et al. Role of Matrix Metalloproteinases in Angiogenesis and Cancer. Front Oncol 2019;9(December):1–21.
129. Jacob A, Prekeris R. The regulation of MMP targeting to invadopodia during cancer metastasis. Front Cell Dev Biol 2015;3(FEB):1–9.
130. Monsky WL, Kelly T, Lin CY, et al. Binding and localization of M(r) 72,000 matrix metalloproteinase at cell surface invadopodia. Cancer Res 1993;53(13):3159–64.
131. Bourguignon LYW, Gunja-Smith Z, Iida N, et al. CD44v3,8-10 is involved in cytoskeleton-mediated tumor cell migration and matrix metalloproteinase (MMP-9) association in metastatic breast cancer cells. J Cell Physiol 1998;176(1):206–15.
132. Poincioux R, Lizárraga F, Chavrier P. Matrix invasion by tumour cells: A focus on MT1-MMP trafficking to invadopodia. J Cell Sci 2009;122(17):3015–24.
133. Niland S, Riscanevo AX, Eble JA. Matrix metalloproteinases shape the tumor microenvironment in cancer progression. Int J Mol Sci 2022;23(1).
134. Cui N, Hu M, Khalil RA. Biochemical and Biological Attributes of Matrix Metalloproteinases. In: Gene. 2017. p. 1–73.
135. Winer A, Adams S, Mignatti P. Matrix Metalloproteinase Inhibitors in Cancer Therapy: Turning Past Failures Into Future Successes. Mol Cancer Ther 2018;17(6):1147–55.
136. Martins LM, de Melo Escorcio Dourado CS, Campos-Verdes LM, et al. Expression of matrix

metalloproteinase 2 and 9 in breast cancer and breast fibroadenoma: A randomized, double-blind study. Oncotarget 2019;10(64):6879–84.

137. Jiang H, Li H. Prognostic values of tumoral MMP2 and MMP9 overexpression in breast cancer: a systematic review and meta-analysis. BMC Cancer 2021;21(1):1–13.
138. Yana I, Weiss SJ. Regulation of membrane type-1 matrix metalloproteinase activity by proprotein convertases. Mol Biol Cell 2000;11(7):2387–401.
139. Li Z, Takino T, Endo Y, Sato H. Activation of MMP-9 by membrane type-1 MMP/MMP-2 axis stimulates tumor metastasis. Cancer Sci 2017;108(3):347–53.
140. Szabova L, Chrysovergis K, Yamada SS, Holmbeck K. MT1-MMP is required for efficient tumor dissemination in experimental metastatic disease. Oncogene 2008;27(23):3274–81.
141. Kumar A, Ahmad A, Vyawahare A, Khan R. Membrane Trafficking and Subcellular Drug Targeting Pathways. Front Pharmacol 2020;11(May):1–17.
142. Derby MC, Gleeson PA. New Insights into Membrane Trafficking and Protein Sorting. Int Rev Cytol 2007;261(07):47–116.
143. Yarwood R, Hellicar J, Woodman PG, Lowe M. Membrane trafficking in health and disease. Dis Model Mech 2020;13(4).
144. Pantazopoulou A, Glick BS. A kinetic view of membrane traffic pathways can transcend the classical view of Golgi compartments. Front Cell Dev Biol 2019;7(JULY):1–12.
145. Brandizzi F, Barlowe C. Organization of the ER–Golgi interface for membrane traffic control. Nat Rev Mol Cell Biol 2013;14(6):382–92.
146. Anantharam A, Kreutzberger AJB. Unraveling the mechanisms of calcium-dependent secretion. J Gen Physiol 2019;151(4):417–34.
147. McMahon HT, Boucrot E. Molecular mechanism and physiological functions of clathrin-mediated endocytosis. Nat Rev Mol Cell Biol 2011;12(8):517–33.
148. Wandinger-Ness A, Zerial M. Rab proteins and the compartmentalization of the endosomal system. Cold Spring Harb Perspect Biol 2014;6(11):a022616.
149. Wartosch L, Bright NA, Luzio JP. Lysosomes. Curr Biol 2015;25(8):R315–6.
150. Cullen PJ, Steinberg F. To degrade or not to degrade: mechanisms and significance of endocytic recycling. Nat Rev Mol Cell Biol 2018;19(11):679–96.
151. Reiner DJ, Lundquist EA. Small GTPases. WormBook 2018;2018:1–65.
152. Gray JL, von Delft F, Brennan PE. Targeting the Small GTPase Superfamily through Their Regulatory Proteins. Angew Chemie - Int Ed 2020;59(16):6342–66.

153. Tetlow AL, Tamanoi F. The ras superfamily g-proteins. 1st ed. Elsevier Inc.; 2013.
154. Cherfils J, Zeghouf M. Regulation of small GTPases by GEFs, GAPs, and GDIs. Physiol Rev 2013;93(1):269–309.
155. Carlos Amor J, Harrison DH, Kahn RA, Ringe D. Structure of the human ADP-ribosylation factor 1 complexed with GDP. Nature 1994;372(6507):704–8.
156. Sztul E, Chen P, Casanova JE, et al. ARF GTPases and their GEFs and GAPs: concepts and challenges. Mol Biol Cell 2019;30(11):1249–71.
157. Li T, Guo Y. ADP-Ribosylation Factor Family of Small GTP-Binding Proteins: Their Membrane Recruitment, Activation, Crosstalk and Functions. Front Cell Dev Biol 2022;10(February):1–9.
158. Adarska P, Wong-Dilworth L, Bottanelli F. ARF GTPases and Their Ubiquitous Role in Intracellular Trafficking Beyond the Golgi. Front Cell Dev Biol 2021;9(July):1–7.
159. Li Y, Kelly WG, Logsdon JM, et al. Functional genomic analysis of the ADP-ribosylation factor family of GTPases: Phylogeny among diverse eukaryotes and function in C. elegans. FASEB J 2004;18(15):1834–50.
160. Kahn RA, Cherfils J, Elias M, Lovering RC, Munro S, Schurmann A. Nomenclature for the human Arf family of GTP-binding proteins: ARF, ARL, and SAR proteins. J Cell Biol 2006;172(5):645–50.
161. Donaldson JG. Multiple Roles for Arf6: Sorting, Structuring, and Signaling at the Plasma Membrane. J Biol Chem 2003;278(43):41573–6.
162. Saito K, Maeda M, Katada T. Regulation of the Sar1 GTPase cycle is necessary for large cargo secretion from the endoplasmic reticulum. Front Cell Dev Biol 2017;5(AUG):1–8.
163. Arimoto KI, Funami K, Saeki Y, et al. Polyubiquitin conjugation to NEMO by triparite motif protein 23 (TRIM23) is critical in antiviral defense. Proc Natl Acad Sci USA 2010;107(36): 15856–61.
164. Watanabe M, Takahashi H, Saeki Y, et al. The E3 ubiquitin ligase TRIM23 regulates adipocyte differentiation via stabilization of the adipogenic activator PPARγ. Elife 2015;4:e05615.
165. Yu CJ, Lee FJS. Multiple activities of Arl1 GTPase in the trans-Golgi network. J Cell Sci 2017;130(10):1691–9.
166. Eiseler T, Wille C, Koehler C, Illing A, Seufferlein T. Protein kinase D2 assembles a multiprotein complex at the trans-Golgi network to regulate matrix metalloproteinase secretion. J Biol Chem 2016;291(1):462–77.
167. Cruz-Garcia D, Ortega-Bellido M, Scarpa M, et al. Recruitment of arfaptins to the trans-Golgi

network by PI(4)P and their involvement in cargo export. EMBO J 2013;32(12):1717–29.

168. Gehart H, Goginashvili A, Beck R, et al. The BAR Domain Protein Arfaptin-1 Controls Secretory Granule Biogenesis at the trans-Golgi Network. Dev Cell 2012;23(4):756–68.
169. D'Souza RS, Semus R, Billings EA, Meyer CB, Conger K, Casanova JE. Rab4 Orchestrates a Small GTPase Cascade for Recruitment of Adaptor Proteins to Early Endosomes. Curr Biol 2014;24(11):1187–98.
170. Houghton FJ, Bellingham SA, Hill AF, et al. Arl5b is a Golgi-localised small G protein involved in the regulation of retrograde transport. Exp Cell Res 2012;318(5):464–77.
171. Rosa-Ferreira C, Christis C, Torres IL, Munro S. The small G protein Arl5 contributes to endosome-to-Golgi traffic by aiding the recruitment of the GARP complex to the Golgi. Biol Open 2015;4(4):474–81.
172. Marwaha R, Dwivedi D, Sharma M. Emerging Roles of Arf-Like GTP-Binding Proteins : From Membrane Trafficking to Cytoskeleton Dynamics and Beyond. Proc Indian Natl Sci Acad 2019;85(1):189–212.
173. Zhao J, Wang M, Deng W, et al. ADP-ribosylation factor-like GTPase 15 enhances insulin-induced AKT phosphorylation in the IR/IRS1/AKT pathway by interacting with ASAP2 and regulating PDPK1 activity. Biochem Biophys Res Commun 2017;486(4):865–71.
174. Wu Y, Bai Y, McEwan DG, Bentley L, Aravani D, Cox RD. Palmitoylated small GTPase ARL15 is translocated within Golgi network during adipogenesis. Biol Open 2021;10(12).
175. Hesse D, Hommel A, Jaschke A, et al. Altered GLUT4 trafficking in adipocytes in the absence of the GTPase Arfrp1. Biochem Biophys Res Commun 2010;394(4):896–903.
176. Zahn C, Jaschke A, Weiske J, et al. ADP-ribosylation factor-like GTPase ARFRP1 is required for trans-Golgi to plasma membrane trafficking of E-cadherin. J Biol Chem 2008;283(40):27179–88.
177. Ishida M, Bonifacino JS. ARFRP1 functions upstream of ARL1 and ARL5 to coordinate recruitment of distinct tethering factors to the trans-Golgi network. J Cell Biol 2019;218(11):3681–96.
178. Schrick JJ, Vogel P, Abuin A, Hampton B, Rice DS. ADP-ribosylation factor-like 3 is involved in kidney and photoreceptor development. Am J Pathol 2006;168(4):1288–98.
179. Grayson C, Bartolini F, Chapple JP, et al. Localization in the human retina of the X-linked retinitis pigmentosa protein RP2, its homologue cofactor C and the RP2 interacting protein ARl3. Hum Mol Genet 2002;11(24):3065–74.

180. Dewees SI, Vargová R, Hardin KR, et al. Phylogenetic profiling and cellular analyses of ARL16 reveal roles in traffic of IFT140 and INPP5E. Mol Biol Cell 2022;33(4):ar33.
181. Chiang AP, Nishimura D, Searby C, et al. Comparative genomic analysis identifies an ADP-ribosylation factor-like gene as the cause of Bardet-Biedl syndrome (BBS3). Am J Hum Genet 2004;75(3):475–84.
182. Zhang Q, Nishimura D, Seo S, et al. Bardet-Biedl syndrome 3 (Bbs3) knockout mouse model reveals common BBS-associated phenotypes and Bbs3 unique phenotypes. Proc Natl Acad Sci U S A 2011;108(51):20678–83.
183. Wiens CJ, Tong Y, Esmail MA, et al. Bardet-biedl syndrome-associated small GTPase ARL6 (BBS3) functions at or near the ciliary gate and modulates Wnt signaling. J Biol Chem 2010;285(21):16218–30.
184. Liew GM, Ye F, Nager AR, et al. The Intraflagellar Transport Protein IFT27 Promotes BBSome Exit from Cilia through the GTPase ARL6/BBS3. Dev Cell 2014;31(3):265–78.
185. Gotthardt K, Lokaj M, Koerner C, Falk N, Gießl A, Wittinghofer A. A G-protein activation cascade from Arl13B to Arl3 and implications for ciliary targeting of lipidated proteins. Elife 2015;4:1–16.
186. Ivanova AA, Caspary T, Seyfried NT, et al. Biochemical characterization of purified mammalian ARL13B protein indicates that it is an atypical GTPase and ARL3 guanine nucleotide exchange factor (GEF). J Biol Chem 2017;292(26):11091–108.
187. Duldulao NA, Lee S, Sun Z. Cilia localization is essential for in vivo functions of the Joubert syndrome protein Arl13b/Scorpion. Development 2009;136(23):4033–42.
188. Larkins CE, Aviles GDG, East MP, Kahn RA, Caspary T. Arl13b regulates ciliogenesis and the dynamic localization of Shh signaling proteins. Mol Biol Cell 2011;22(23):4694–703.
189. Seixas C, Choi SY, Polgar N, et al. Arl13b and the exocyst interact synergistically in ciliogenesis. Mol Biol Cell 2016;27(2):308–20.
190. Revenkova E, Liu Q, Luca Gusella G, Iomini C. The Joubert syndrome protein ARL13B binds tubulin to maintain uniform distribution of proteins along the ciliary membrane. J Cell Sci 2018;131(9).
191. Casalou C, Seixas C, Portelinha A, et al. Arl13b and the non-muscle myosin heavy chain IIA are required for circular dorsal ruffle formation and cell migration. J Cell Sci 2014;127(12):2709–22.
192. Higginbotham H, Eom T-Y, Mariani LE, et al. Arl13b in Primary Cilia Regulates the Migration

and Placement of Interneurons in the Developing Cerebral Cortex. Dev Cell 2012;23(5):925–38.

193. Pruski M, Rajnicek A, Yang Z, et al. The ciliary GTPase Arl13b regulates cell migration and cell cycle progression. Cell Adhes Migr 2016;10(4):393–405.
194. Bhamidipati A, Lewis SA, Cowan NJ. ADP ribosylation factor-like protein 2 (Arl2) regulates the interaction of tubulin-folding cofactor D with native tubulin. J Cell Biol 2000;149(5):1087–96.
195. Francis JW, Newman LE, Cunningham LA, Kahn RA. A trimer consisting of the Tubulin-specific Chaperone D (TBCD), regulatory GTPase ARL2, and β-tubulin is required for maintaining the microtubule network. J Biol Chem 2017;292(10):4336–49.
196. Newman LE, Zhou CJ, Mudigonda S, et al. The ARL2 GTPase is required for mitochondrial morphology, motility, and maintenance of ATP levels. PLoS One 2014;9(6):1–15.
197. Newman LE, Schiavon CR, Zhou C, Kahn RA. The abundance of the ARL2 GTPase and its GAP, ELMOD2, at mitochondria are modulated by the fusogenic activity of mitofusins and stressors. PLoS One 2017;12(4):1–29.
198. Jacobs S, Schilf C, Fliegert F, et al. ADP-ribosylation factor (ARF)-like 4, 6, and 7 represent a subgroup of the ARF family characterized by rapid nucleotide exchange and a nuclear localization signal. FEBS Lett 1999;456(3):384–8.
199. Hofmann I, Thompson A, Sanderson CMM, Munro S. The Arl4 Family of Small G Proteins Can Recruit the Cytohesin Arf6 Exchange Factors to the Plasma Membrane. Curr Biol 2007;17(8):711–6.
200. Patel M, Chiang TC, Tran V, Lee FJS, Coŝeś JF. The Arf family GTPase Arl4A complexes with ELMO proteins to promote actin cytoskeleton remodeling and reveals a versatile ras-binding domain in the ELMO proteins family. J Biol Chem 2011;286(45):38969–79.
201. Hong C, Walczak R, Dhamko H, et al. Constitutive activation of LXR in macrophages regulates metabolic and inflammatory gene expression: Identification of ARL7 as a direct target. J Lipid Res 2011;52(3):531–9.
202. Wei S mei, Xie C gao, Abe Y, Cai J ting. ADP-ribosylation factor like 7 (ARL7) interacts with α-tubulin and modulates intracellular vesicular transport. Biochem Biophys Res Commun 2009;384(3):352–6.
203. Li CC, Wu TS, Huang CF, et al. GTP-binding-defective ARL4D alters mitochondrial morphology and membrane potential. PLoS One 2012;7(8).
204. Calin GA, Trapasso F, Shimizu M, et al. Familial Cancer Associated with a Polymorphism in

ARLTS1. New Englang J Med 2005;352:1667–76.

205. Arya SB, Kumar G, Kaur H, Kaur A, Tuli A. ARL11 regulates lipopolysaccharide-stimulated macrophage activation by promoting mitogen-activated protein kinase (MAPK) signaling. J Biol Chem 2018;293(25):9892–909.

206. Khatter D, Sindhwani A, Sharma M. Arf-like GTPase Arl8: Moving from the periphery to the center of lysosomal biology. Cell Logist 2015;5(3):1–8.

207. Starheim KK, Gromyko D, Evjenth R, et al. Knockdown of Human N α -Terminal Acetyltransferase Complex C Leads to p53-Dependent Apoptosis and Aberrant Human Arl8b Localization . Mol Cell Biol 2009;29(13):3569–81.

208. Khatter D, Sindhwani A, Sharma M. Arf-like GTPase Arl8: Moving from the periphery to the center of lysosomal biology. Cell Logist 2015;5(3):1–8.

209. Rosa-Ferreira C, Munro S. Arl8 and SKIP Act Together to Link Lysosomes to Kinesin-1. Dev Cell 2011;21(6):1171–8.

210. Guardia CM, Farías GG, Jia R, Pu J, Bonifacino JS. BORC Functions Upstream of Kinesins 1 and 3 to Coordinate Regional Movement of Lysosomes along Different Microtubule Tracks. Cell Rep 2016;17(8):1950–61.

211. Khatter D, Raina VB, Dwivedi D, Sindhwani A, Bahl S, Sharma M. The small GTPase Arl8b regulates assembly of the mammalian HOPS complex on lysosomes. J Cell Sci 2015;128(9):1746–61.

212. Lin X, Yang T, Wang S, et al. RILP interacts with HOPS complex via VPS41 subunit to regulate endocytic trafficking. Sci Rep 2014;4:1–12.

213. Keren-Kaplan T, Sarić A, Ghosh S, et al. RUFY3 and RUFY4 are ARL8 effectors that promote coupling of endolysosomes to dynein-dynactin. Nat Commun 2022;13(1).

214. Kumar G, Chawla P, Dhiman N, et al. RUFY3 links Arl8b and JIP4-Dynein complex to regulate lysosome size and positioning. Nat Commun 2022;13(1).

215. Tancini B, Buratta S, Delo F, et al. Lysosomal exocytosis: The extracellular role of an intracellular organelle. Membranes (Basel) 2020;10(12):1–21.

216. Buratta S, Tancini B, Sagini K, et al. Lysosomal exocytosis, exosome release and secretory autophagy. Int J Mol Sci 2020;21(2576):1–20.

217. Reddy A, Caler E V, Andrews NW. Plasma Membrane Repair Is Mediated by Ca2+-Regulated Exocytosis of Lysosomes. Cell 2001;106(2):157–69.

218. Castro-Gomes T, Corrotte M, Tam C, Andrews NW. Plasma membrane repair is regulated

extracellularly by proteases released from lysosomes. PLoS One 2016;11(3):1–26.

219. Lacombe J, Karsenty G, Ferron M. Regulation of lysosome biogenesis and functions in osteoclasts. Cell Cycle 2013;12(17):2744–52.
220. Bossi G, Griffiths GM. CTL secretory lysosomes: Biogenesis and secretion of a harmful organelle. Semin Immunol 2005;17(1):87–94.
221. Naegeli KM, Hastie E, Garde A, et al. Cell Invasion In Vivo via Rapid Exocytosis of a Transient Lysosome-Derived Membrane Domain. Dev Cell 2017;43(4):403-417.e10.
222. Geisslinger F, Müller M, Vollmar AM, Bartel K. Targeting Lysosomes in Cancer as Promising Strategy to Overcome Chemoresistance—A Mini Review. Front Oncol 2020;10(July):1–7.
223. Bestman JE, Huang L, Lee-Osbourne J, Cheung P, Cline HT. An in vivo screen to identify candidate neurogenic genes in the developing Xenopus visual system. Dev Biol 2015;408(2):269–91.
224. Derakhshani A, Mollaei H, Parsamanesh N, et al. Gene co-expression network analysis for identifying modules and functionally enriched pathways in vitiligo disease: A systems biology study. Iran J Allergy, Asthma Immunol 2020;19(5):517–28.
225. Paul P, Van Den Hoorn T, Jongsma MLM, et al. A genome-wide multidimensional RNAi screen reveals pathways controlling MHC class II antigen presentation. Cell 2011;145(2):268–83.
226. Casalou C, Faustino A, Barral DC. Arf proteins in cancer cell migration. Small GTPases 2016;7(4):270–82.
227. Casalou C, Ferreira A, Barral DC. The Role of ARF Family Proteins and Their Regulators and Effectors in Cancer Progression : A Therapeutic Perspective. Front Cell Dev Biol 2020;8(April):1–13.
228. Brito C, Costa-silva B, Barral DC, Pojo M. Unraveling the relevance of arl gtpases in cutaneous melanoma prognosis through integrated bioinformatics analysis. Int J Mol Sci 2021;22(17).
229. Taniuchi K, Iwasaki S, Saibara T. BART inhibits pancreatic cancer cell invasion by inhibiting ARL2-mediated RhoA inactivation. Int J Oncol 2011;39:1243–52.
230. Lee H, Choi SG, Ha S, Yoon S, Kim WY. ARL2 is required for homologous recombination repair and colon cancer stem cell survival. FEBS Open Bio 2022;12(8):1523–33.
231. Li Z, Jiang M, Zhang T, Liu S. GAS6-AS2 Promotes Hepatocellular Carcinoma via miR-3619-5p/ARL2 Axis under Insufficient Radiofrequency Ablation Condition. Cancer Biother Radiopharm 2021;36(10):879–87.
232. Liu W, Yao D, Huang B. LncRNA PVT1 promotes cervical cancer progression by sponging miR-

503 to upregulate ARL2 expression. Open Life Sci 2021;16(1):1–13.

233. Wu X, Yan L, Liu Y, Shang L. Circ_0000527 promotes osteosarcoma cell progression through modulating miR-646/ARL2 axis. Aging (Albany NY) 2021;13(4):6091–102.
234. Li H-J, Sun X-M, Li Z-K, et al. LncRNA UCA1 Promotes Mitochondrial Function of Bladder Cancer via the MiR- 195 / ARL2 Signaling Pathway. Cell Physiol Biochem 2017;43:2548–61.
235. Pang X, Wang Y, Miao B, Fei S, Chen W. Regulation of ARL2 in colorectal cancer cell proliferation and tumorigenicity, and its negative association with AXL. Oncol Lett 2021;21(3):196.
236. Wang Y, Guan G, Cheng W, et al. ARL2 overexpression inhibits glioma proliferation and tumorigenicity via down-regulating AXL. BMC Cancer 2018;18:1–13.
237. Wang Y, Zhao W, Liu X, Guan G, Zhuang M. ARL3 is downregulated and acts as a prognostic biomarker in glioma. J Transl Med 2019;17(1):210.
238. Fujii S, Matsumoto S, Nojima S, Morii E, Kikuchi A. Arl4c expression in colorectal and lung cancers promotes tumorigenesis and may represent a novel therapeutic target. Oncogene 2014;34(October):1–11.
239. Fujii S, Shinjo K, Matsumoto S, Harada T. Epigenetic upregulation of ARL4C , due to DNA hypomethylation in the 3 ’ -untranslated region , promotes tumorigenesis of lung squamous cell carcinoma. Oncotarget 2016;7(49):81571–87.
240. Hu Q, Masuda T, Sato K, Tobo T, Nambara S. Identification of ARL4C as a Peritoneal Dissemination-Associated Gene and Its Clinical Significance in Gastric Cancer. Ann Surg Oncol 2018;25(3):745–53.
241. Harada T, Matsumoto S, Hirota S, Kimura H, Fujii S. Chemically modified antisense oligonucleotide against ARL4C inhibits primary and metastatic liver tumor growth. Mol Cancer Ther 2019;18(3):602–12.
242. Harada A, Matsumoto S, Yasumizu Y, Akama T, Eguchi H, Kikuchi A. Localization of kras downstream target arl4c to invasive pseudopods accelerates pancreatic cancer cell invasion. Elife 2021;10:1–34.
243. Isono T, Chano T, Yoshida T, et al. ADP-ribosylation factor-like 4C is a predictive biomarker of poor prognosis in patients with renal cell carcinoma. Am J Cancer Res 2019;9(2):415–23.
244. Guo X, Jo VY, Mills AM, et al. Clinically relevant molecular subtypes in leiomyosarcoma. Clin Cancer Res 2015;21(15):3501–11.
245. Wakinoue S, Chano T, Amano T, Isono T, Kimura F. ADP-ribosylation factor-like 4C predicts

worse prognosis in endometriosis-associated ovarian cancers. Cancer Biomarkers 2018;1:1–7.

246. Chen Q, Weng H, Tang X, et al. ARL4C stabilized by AKT / mTOR pathway promotes the invasion of PTEN-deficient primary human glioblastoma. J Pathol 2019;247(December 2018):266–78.
247. Zhang P, Xu Y, Chen S, et al. ARL4C Regulates the Progression of Clear Cell Renal Cell Carcinoma by Affecting the Wnt/ β -Catenin Signaling Pathway. J Oncol 2022;2022.
248. Chen X, Zhang Y, Qian W, et al. Arl4c promotes the growth and drug resistance of pancreatic cancer by regulating tumor-stromal interactions. iScience 2021;24(12):103400.
249. Su D, Katsaros D, Xu S, et al. ADP-ribosylation factor-like 4C (ARL4C), a novel ovarian cancer metastasis suppressor, identified by integrated genomics. Am J Transl Res 2015;7(2):242–56.
250. Nonaka Y, Tsuda N, Shichijo S, et al. Recognition of ADP-ribosylation factor 4-like by HLA-A2-restricted and tumor-reactive cytotoxic T lymphocytes from patients with brain tumors. Tissue Antigens 2002;60(2):319–27.
251. Chi JH, Panner A, Cachola K, et al. Increased expression of the glioma-associated antigen ARF4L after loss of the tumor suppressor PTEN. J Neurosurg 2008;108(February):299–303.
252. Huang Z, Lan T, Wang J, Chen Z, Zhang X. Identification and validation of seven RNA binding protein genes as a prognostic signature in oral cavity squamous cell carcinoma. Bioengineered 2021;12(1):7248–62.
253. Wang Q, Huang Z, Guo W, et al. MicroRNA-202-3p Inhibits Cell Proliferation by Targeting ADP-Ribosylation Factor-like 5A in Human Colorectal Carcinoma. Hum Cancer Biol 2014;20(10):1146–58.
254. Zhao S, Zhang Y, Pei M, Wu L, Li J. miR-145 inhibits mitochondrial function of ovarian cancer by targeting ARL5B. J Ovarian Res 2021;14(1):1–9.
255. Liu X, Shen Q, Yu T, et al. Small GTPase Arl6 controls RH30 rhabdomyosarcoma cell growth through ciliogenesis and Hedgehog signaling. Cell Biosci 2016;6:1–11.
256. Dykes SS, Gray AL, Coleman DT, et al. The Arf-like GTPase Arl8b is essential for three-dimensional invasive growth of prostate cancer in vitro and xenograft formation and growth in vivo. Oncotarget 2016;7(21).
257. Yendamuri S, Trapasso F, Calin GA. ARLTS1 – a novel tumor suppressor gene. Cancer Lett 2008;264:11–20.
258. Petrocca F, Iliopoulos D, Qin HR, et al. Alterations of the Tumor Suppressor Gene ARLTS1 in

Ovarian Cancer. Cancer Res 2006;66(21):10287–92.

259. Hamadou WS, Besbes S, Mani R, et al. ARLTS1, potential candidate gene in familial aggregation of hematological malignancies. Bull Cancer 2017;104(2):123–7.
260. Frank B, Meyer P, Boettger MB, et al. ARLTS1 variants and melanoma risk. Int J Cancer 2006;119(7):1736–7.
261. Castellví-Bel S, Castells A, de Cid R, et al. Association of the ARLTS1 Cys148Arg variant with sporadic and familial colorectal cancer. Carcinogenesis 2007;28(8):1687–91.
262. Siltanen S, Fischer D, Rantapero T, et al. ARLTS1 and Prostate Cancer Risk - Analysis of Expression and Regulation. PLoS One 2013;8(8):1–10.
263. Yang XY, Yu H, Peng ZL. Involvement of ARLTS1 in chemotherapy and apoptosis in ovarian cancer cell line. Arch Gynecol Obstet 2011;284(5):1241–6.
264. Bay SN, Long AB, Caspary T. Disruption of the ciliary GTPase Arl13b suppresses Sonic hedgehog overactivation and inhibits medulloblastoma formation. Proc Natl Acad Sci 2018;115(7):1570–5.
265. Shao J, Xu L, Chen L, et al. Arl13b Promotes Gastric Tumorigenesis by Regulating Smo Trafficking and Activation of the Hedgehog Signaling Pathway. Cancer Res 2017;77(15):4000–13.
266. Shireman JM, Atashi F, Lee G, et al. De novo purine biosynthesis is a major driver of chemoresistance in glioblastoma. Brain 2021;144(4):1230–46.
267. Guo F, Yuan D, Zhang J, Zhang H, Wang C, Zhu L. Silencing of ARL14 Gene Induces Lung Adenocarcinoma Cells to a Dormant State. Front Cell Dev Biol 2019;7(October):1–9.
268. Zhang B, Xu A, Wu D, et al. Arl14 as a prognostic biomarker in non-small cell lung cancer. J Inflamm Res 2021;14(September):6557–74.
269. Wang L, Shi J, Huang Y, et al. A six - gene prognostic model predicts overall survival in bladder cancer patients. Cancer Cell Int 2019;19:1–15.
270. Mao Y, Zhao Q, Yin S, Ding X, Wang H. Genome-wide expression profiling and bioinformatics analysis of deregulated genes in human gastric cancer tissue after gastroscopy. Asia Pac J Clin Oncol 2018;14(February 2017):29–36.
271. Ong CHC, Lee DY, Lee B, et al. Hypoxia-regulated carbonic anhydrase IX (CAIX) protein is an independent prognostic indicator in triple negative breast cancer. Breast Cancer Res 2022;24(1):38.
272. Beghin A, Honore S, Messana C, et al. ADP ribosylation factor like 2 (Arl2) protein influences

microtubule dynamics in breast cancer cells. Exp Cell Res 2007;13.

273. Beghin A, Matera E, Brunet-manquat S. Expression of Arl2 is associated with p53 localization and chemosensitivity in a breast cancer cell line. Cell Cycle 2008;7(19):3074–82.
274. Beghin A, Belin S, Sleiman RH, et al. ADP Ribosylation Factor Like 2 (Arl2) Regulates Breast Tumor Aggressivity in Immunodeficient Mice. PLoS One 2009;4(10).
275. Li L, Sun RM, Jiang GQ. ATF3 demethylation promotes the transcription of ARL4C, which acts as a tumor suppressor in human breast cancer. Onco Targets Ther 2020;13:3467–76.
276. Kothari C, Clemenceau A, Ouellette G, et al. Tbc1d9: An important modulator of tumorigenesis in breast cancer. Cancers (Basel) 2021;13(14).
277. Kothari C, Osseni MA, Agbo L, et al. Machine learning analysis identifies genes differentiating triple negative breast cancers. Sci Rep 2020;10(1):1–15.
278. Wu PH, Onodera Y, Giaccia AJ, et al. Lysosomal trafficking mediated by Arl8b and BORC promotes invasion of cancer cells that survive radiation. Commun Biol 2020;3(1):1–15.
279. Frank B, Hemminki K, Meindl A, et al. Association of the ARLTS1 Cys148Arg variant with familial breast cancer risk. Int J Cancer 2006;118(10):2505–8.
280. Casalou C, Faustino A, Silva F, et al. Arl13b regulates breast cancer cell migration and invasion by controlling integrin-mediated signaling. Cancers (Basel) 2019;11(10):1461.
281. Li T, Fu J, Zeng Z, et al. TIMER2.0 for analysis of tumor-infiltrating immune cells. Nucleic Acids Res 2020;48(W1):W509–14.
282. Garg S, Sharma M, Ung C, et al. Lysosomal Trafficking, Antigen Presentation, and Microbial Killing Are Controlled by the Arf-like GTPase Arl8b. Immunity 2011;35(2):182–93.
283. Goldenring JR. A central role for vesicle trafficking in epithelial neoplasia: Intracellular highways to carcinogenesis. Nat. Rev. Cancer. 2013;13(11):813–20.
284. Parachoniak CA, Park M. Dynamics of receptor trafficking in tumorigenicity. Trends Cell Biol 2012;22(5):231–40.
285. Colicelli J. Human RAS Superfamily Proteins and Related GTPases. Sci Signal 2004;2004(250):re13–re13.
286. Tzeng HT, Wang YC. Rab-mediated vesicle trafficking in cancer. J Biomed Sci 2016;23(1):1–7.
287. Soule HD, Maloney TM, Wolman SR, et al. Isolation and Characterization of a Spontaneously Immortalized Human Breast Epithelial Cell Line, MCF-10. Cancer Res 1990;50(18):6075–86.
288. Miller F, Santner S, Tait L, Dawson P, Adjuvant NS. Model of Human Comedo Ductal Carcinoma In Situ. Jounral Natl Cancer Inst 2000;92(14):1185–6.

289. Dai X, Cheng H, Bai Z, Li J. Breast cancer cell line classification and Its relevance with breast tumor subtyping. J Cancer 2017;8(16):3131–41.
290. Mester J, Redeuilh G. Proliferation of Breast Cancer Cells: Regulation, Mediators, Targets for Therapy. Anticancer Agents Med Chem 2012;8(8):872–85.
291. Mosmann T. Rapid colorimetric assay for cellular growth and survival: Application to proliferation and cytotoxicity assays. J Immunol Methods 1983;65(1–2):55–63.
292. Pinto B, Henriques AC, Silva PMA, Bousbaa H. Three-dimensional spheroids as in vitro preclinical models for cancer research. Pharmaceutics 2020;12(12):1–38.
293. Saraiva DP, Matias AT, Braga S, Jacinto A, Cabral MG. Establishment of a 3D Co-culture With MDA-MB-231 Breast Cancer Cell Line and Patient-Derived Immune Cells for Application in the Development of Immunotherapies. Front Oncol 2020;10(August):1–13.
294. Leung BM, Lesher-Perez SC, Matsuoka T, Moraes C, Takayama S. Media additives to promote spheroid circularity and compactness in hanging drop platform. Biomater Sci 2015;3(2):336–44.
295. Popova N V., Jücker M. The Functional Role of Extracellular Matrix Proteins in Cancer. Cancers (Basel) 2022;14(1):238.
296. De la Fuente IM, López JI. Cell motility and cancer. Cancers (Basel) 2020;12(8):1–15.
297. Machado ER, Annunziata I, van de Vlekkert D, Grosveld GC, d'Azzo A. Lysosomes and Cancer Progression: A Malignant Liaison. Front Cell Dev Biol 2021;9(February).
298. Goertzen C, Eymael D, Magalhaes M. Three-Dimensional Quantification of Spheroid Degradation-Dependent Invasion and Invadopodia Formation 06 Biological Sciences 0601 Biochemistry and Cell Biology 11 Medical and Health Sciences 1112 Oncology and Carcinogenesis. Biol Proced Online 2018;20(1):1–11.
299. Cowell CF, Weigelt B, Sakr RA, et al. Progression from ductal carcinoma in situ to invasive breast cancer: Revisited. Mol Oncol 2013;7(5):859–69.
300. Yeong J, Thike AA, Tan PH, Iqbal J. Identifying progression predictors of breast ductal carcinoma in situ. J Clin Pathol 2017;70(2):102–8.
301. Comşa Ş, Cîmpean AM, Raica M. The story of MCF-7 breast cancer cell line: 40 Years of experience in research. Anticancer Res 2015;35(6):3147–54.
302. Burdall SE, Hanby AM, Lansdown MRJ, Speirs V. Breast cancer cell lines: Friend or foe? Breast Cancer Res 2003;5(2):89–95.
303. Kosti I, Jain N, Aran D, Butte AJ, Sirota M. Cross-tissue Analysis of Gene and Protein Expression

in Normal and Cancer Tissues. Sci Rep 2016;6(March):1–16.

304. Lintz M, Muñoz A, Reinhart-King CA. The Mechanics of Single Cell and Collective Migration of Tumor Cells. J Biomech Eng 2017;139(2):1–9.
305. Chu K, Boley KM, Moraes R, Barsky SH, Robertson FM. The paradox of E-cadherin: Role in response to hypoxia in the tumor microenvironment and regulation of energy metabolism. Oncotarget 2013;4(3):446–62.
306. Jung YS, Park J Il. Wnt signaling in cancer: therapeutic targeting of Wnt signaling beyond β-catenin and the destruction complex. Exp Mol Med 2020;52(2):183–91.
307. Karayiannakis AJ, Nakopoulou L, Gakiopoulou H, Keramopoulos A, Davaris PS, Pignatelli M. Expression patterns of β-catenin in in situ and invasive breast cancer. Eur J Surg Oncol 2001;27(1):31–6.
308. Sormunen RT, Leong ASY, Vääräniemi JP, Fernando SSE, Eskelinen SM. Immunolocalization of the fodrin, E-cadherin, and β-catenin adhesion complex in infiltrating ductal carcinoma of the breast - Comparison with an in vitro model. J Pathol 1999;187(4):416–23.
309. Tian X, Liu Z, Niu B, et al. E-Cadherin/β-catenin complex and the epithelial barrier. J Biomed Biotechnol 2011;2011.
310. Guo Y, Zanetti G, Schekman R. A novel GTP-binding protein-adaptor protein complex responsible for export of Vangl2 from the trans Golgi network. Elife 2013;2013(2):1–21.
311. Hatakeyama J, Wald JH, Printsev I, Ho H-YH, Carraway KL. Vangl1 and Vangl2: planar cell polarity components with a developing role in cancer. Endocr Relat Cancer 2014;21(5):R345–56.
312. Puvirajesinghe TM, Bertucci F, Jain A, et al. Identification of p62/SQSTM1 as a component of non-canonical Wnt VANGL2-JNK signalling in breast cancer. Nat Commun 2016;7.
313. Gorgieva S, Kokol V. Collagen- vs. Gelatine-Based Biomaterials and Their Biocompatibility: Review and Perspectives. Biomater Appl Nanomedicine 2011;(May 2014).
314. Menzl I, Lebeau L, Pandey R, et al. Loss of primary cilia occurs early in breast cancer development. Cilia 2014;3(1).
315. Nobutani K, Shimono Y, Yoshida M, et al. Absence of primary cilia in cell cycle-arrested human breast cancer cells. Genes to Cells 2014;19(2):141–52.
316. Yuan K, Frolova N, Xie Y, et al. Primary cilia are decreased in breast cancer: Analysis of a collection of human breast cancer cell lines and tissues. J Histochem Cytochem 2010;58(10):857–70.

317. Mariani LE, Bijlsma MF, Ivanova AI, Suciu SK, Kahn RA, Caspary T. Arl13b regulates Shh signaling from both inside and outside the cilium. Mol Biol Cell 2016;27(23):3780–90.
318. Bijlsma MF, Damhofer H, Roelink H. Hedgehog-Stimulated Chemotaxis Is Mediated by Smoothened Located Outside the Primary Cilium. Sci Signal 2012;5(238):139–48.
319. Gigante ED, Taylor MR, Ivanova AA, Kahn RA, Caspary T. Arl13b regulates sonic hedgehog signaling from outside primary cilia. Elife 2020;9:1–23.
320. Volk-Draper LD, Rajput S, Hall KL, Wilber A, Ran S. Novel model for basaloid triple-negative breast cancer: Behavior in vivo and response to therapy. Neoplasia (United States) 2012;14(10):926–42.
321. Schiefermeier N, Scheffler JM, de Araujo MEG, et al. The late endosomal p14-MP1 (LAMTOR2/3) complex regulates focal adhesion dynamics during cell migration. J Cell Biol 2014;205(4):525–40.
322. Dozynkiewicz MA, Jamieson NB, MacPherson I, et al. Rab25 and CLIC3 Collaborate to Promote Integrin Recycling from Late Endosomes/Lysosomes and Drive Cancer Progression. Dev Cell 2012;22(1):131–45.
323. Bano J Del, Florès-Florès R, Josselin E, et al. A bispecific antibody-based approach for targeting mesothelin in triple negative breast cancer. Front Immunol 2019;10(JULY):1–13.
324. Niwa S, Tao L, Lu SY, et al. BORC Regulates the Axonal Transport of Synaptic Vesicle Precursors by Activating ARL-8. Curr Biol 2017;27(17):2569-2578.e4.
325. Jordens I, Fernandez-Borja M, Marsman M, et al. The Rab7 effector protein RILP controls lysosomal transport by inducing the recruitment of dynein-dynactin motors. Curr Biol 2001;11(21):1680–5.
326. Wijdeven RH, Jongsma MLM, Neefjes J, Berlin I. ER contact sites direct late endosome transport. BioEssays 2015;37(12):1298–302.
327. Zhang W, Yuan W, Song J, Wang S, Gu X. LncRNA CPS1-IT1 suppresses EMT and metastasis of colorectal cancer by inhibiting hypoxia-induced autophagy through inactivation of HIF-1α. Biochimie 2018;144:21–7.
328. Liu H, Ma Y, He HW, Zhao WL, Shao RG. SPHK1 (sphingosine kinase 1) induces epithelial-mesenchymal transition by promoting the autophagy-linked lysosomal degradation of CDH1/E-cadherin in hepatoma cells. Autophagy 2017;13(5):900–13.
329. Marwaha R, Arya SB, Jagga D, Kaur H, Tuli A, Sharma M. The Rab7 effector PLE KHM1 binds Arl8b to promote cargo traffic to lysosomes. J Cell Biol 2017;216(4):1051–70.

330. Tsai-Tsen Liao. Hybrid Epithelial / Mesenchymal State in Cancer Metastasis : Clinical Significance and. 2020;
331. Newell-Litwa KA, Horwitz R, Lamers ML. Non-Muscle myosin II in disease: Mechanisms and therapeutic opportunities. DMM Dis Model Mech 2015;8(12):1495–515.
332. Derycke L, Stove C, Wever ODE, et al. The role of non-muscle myosin IIA in aggregation and invasion of human MCF-7 breast cancer cells. Int J Dev Biol 2011;55(November):835–40.
333. Duxbury MS, Ashley SW, Whang EE. Inhibition of pancreatic adenocarcinoma cellular invasiveness by blebbistatin: A novel myosin II inhibitor. Biochem Biophys Res Commun 2004;313(4):992–7.